LNAPL Volume in the Petroleum-Contaminated Groundwater System-A Modeling and Experimental Study

Zhi Hong Zhang

A Thesis

in

The Department

of

Building, Civil and Environmental Engineering

Presented in Partial Fulfillment of the Requirements

for the Degree of Master of Applied Science (Civil Engineering) at

Concordia University

Montreal, Quebec, Canada

December 2007

Your file Votre référence
ISBN: 978-0-494-40875-9
Our file Notre référence
ISBN: 978-0-494-40875-9

ABSTRACT

LNAPL Volume in a Petroleum-Contaminated Groundwater System – A Modeling and Experimental Study

Zhi Hong Zhang

LNAPLs, or light non-aqueous phase liquids, are less dense than water. They can co-exist with water in the aquifer, which are hydrocarbons presenting potential health, resource, and environmental risks. Examples of LNAPL are gasoline, diesel, motor oils, and similar materials.

For many decades, the oil production industry has recognized that LNAPLs accidentally released to the subsurface remain in porous media. The study of the distribution of LNAPL in contaminated soil began in the 1930s. At that time, LNAPL was considered like "pancakes" over groundwater table. In the past two decades, several methods have been studied to analyze the actual LNAPL thickness present in wells or groundwater and the LNAPL volume in petroleum-contaminated sites. However, previous studies were lack of consideration of the heterogeneous characteristics of the soil. Also few model validations could be found.

A new oil volume computation method is developed in the present study, based on an integrated analysis of oil properties, the characteristics of subsurface porous media, and the interactions between oil, soil, and groundwater. Quantitative analyses and tools are thus provided to quantify LNAPL volumes residing in the petroleum-contaminated groundwater system.

Importantly, a pilot-scale experiment was set up and conducted in the Environmental Engineering laboratory at Concordia University with actual oil spills and measurements. The developed model has been tested and validated through the pilot-scale experiment and applied to a real petroleum-contaminated site. In addition, a user-friendly modeling system has been developed in the present study.

The developed modeling tool can be used to identify the field distribution of LNAPL and its volume present in the soil and groundwater system. The approach can support effective LNAPL recovery action at the contaminated site and thus help solving oil spill contamination problems for the management of groundwater resources.

ACKNOWLEGMENTS

I would like to express my sincere gratitude to my supervisor, Dr. Zhi Chen, for his generous guidance during the whole of my graduate studies. I especially wish to extend my thanks to him for his generous suggestions for and contributions to my thesis study.

Dr. Chen has constantly given me so much good advice and has revised my mistakes with much patience and encouragement during my study. His guidance and advice will continue to be helpful for my future study and work. I will continue to benefit from them for the rest of my life.

Special thanks are also due to my team members. They have given me much valuable and helpful assistance in my research and studies.

TABLE OF CONTENTS

List of Figures

List of Tables

List of Symbols

T = apparent oil thickness in monitoring well (m)

ρ_o, ρ_w = oil and water densities, respectively (kg/m^3)

D_w^{ao} = depth of interface of air-oil in monitoring well (m)

D_s^{ao} = depth of oil capillary fringe in soil (m)

P_d^{ao} = air-oil displacement pressure (N/m^2)

L_w = apparent thickness in monitoring well under water table (m)

L_{of} = height of oil capillary fringe in porous media (m)

L_{ro} = height of residual oil in porous media (m)

L_{vo} = height of oil move vertically in porous media (m)

L_{mo} = height of mobile oil in porous media (m)

L_{io} = height of immobile oil in porous media (m)

L_{wf} = height of water capillary fringe in porous media (m)

D_w^{ow} = depth of interface of oil-water in monitoring well (m)

D_s^{ow} = depth of water capillary fringe in soil (m)

P_d^{ow} = oil-water displacement pressure (N/m^2)

S_{wr} = irreducible saturation of water

S_w = actual saturation of water

S_o = actual saturation of oil

P_d^{ao} = air-oil displacement pressure (N/m^2)

S_{or} = irreducible saturation of oil

Z = depth of immobile oil in soil (m)

P_c^{ow} = the pressure of interface of immobile oil in soil (N/m^2)

λ = BC model parameter

D_s^{aow} = depth of residual oil in soil (m)

P_c^{ao} = the immobile oil and mobile oil displacement pressure (N/m^2)

ϕ = porosity of soil

V_T = the total specific volume of oil in porous media (m^3/m^2)

K = the ratio of oil saturation to water saturation in oil mobile zone

S_{or} = residual oil saturation

S_{wr} = residual water saturation

V_m = the mobile specific volume of oil in porous media (m^3/m^2)

V_r = the residual specific volume of oil in porous media (m^3/m^2)

α_{ow} = VG model parameter (oil-water (m^{-1}))

α_{ao} = VG model parameter (air-oil (m^{-1}))

α = VG model parameter (m^{-1})

n = VG model parameter

h_{ow} = oil-water capillary head (m)

h_{ao} = air-oil capillary head (m)

ρ_{ro} = ratio of oil density with water density

h_d = air entry pressure in BC model (m)

β_{ow} = oil-water scaling factor

β_{ao} = air-oil scaling factor

Z_w^{ao} = elevation of interface of air-oil in monitoring well (m)

Z_s^{ao} = elevation of oil capillary fringe in soil (m)

Z_w^{ow} = elevation of interface of oil-water in monitoring well (m)

Z_s^{ow} = elevation of water capillary fringe in soil (m)

$S^*(h^*)$ = scaled saturation-pressure function

$\overline{S_w}$ = effective saturation of water

$\overline{S_t}$ = effective saturation of total fluid (oil +water)

S_m = water residual saturation

S_o = actual saturation of oil

V_{sfo} = specific oil volume in free phase oil area (m^3/m^2)

Z_u = elevation where oil saturation is zero (m)

V_{sfo}^T = total oil volume in free phase area (m^3)

A = free phase oil area (m^2)

V_{snf} = specific oil volume in non-free phase area (m^3/m^2)

F_r = a function of the volume of free phase oil, porosity, and oil thickness; it ranges from 0.2 to 0.5

L = the thickness of contaminated soil (m)

V_{snf}^T = total oil volume in non-free phase area (m^3)

V^T = total oil volume in free phase area and non-free phase area (m^3)

V_{sfo} = specific volume in porous media (m^3/m^2)

z_s^u = elevation where oil saturation is zero or level of leaked source (m)

N = number of soil layers between Z_s^{ow} and Z_s^u

ϕ_i = porosity of ith soil layer

S_{oi} = oil saturation of ith soil layer

z_{lb} = lower boundary of ith soil layer

z_{ub} = upper boundary of ith soil layer

Z_s^1 = elevation of interface between soil 1 and soil 2

ϕ_1 = porosity of soil 1

ϕ_2 = porosity of soil2

S_{o1} = oil saturation of soil 1

S_{o2} = oil saturation of soil 2

N = number of nodes

List of Abbreviation and Acronyms

CFR:	Code of federal regulations
LNAPL:	Light non-aqueous phase liquids
UST:	Underground storage tank
BTEX:	Benzene, toluene, ethyl-benzene, and xylene
SERM:	Saskatchewan Environment and Resource Management
TPH:	Total petroleum hydrocarbons

Chapter 1

Introduction

1.1 Introduction

Oil spill is a significant environmental pollution problem. Over 315,000 releases from leaking underground storage tanks (USTs) were reported by USA environmental agencies as of March 1996. The us Federal regulations state that at UST sites where investigations indicate the presence of free products, owners and operators must remove those free products to the maximum extent practicable as determined by the implementing agency (40 CFR 280.64, API Interactive LNAPL guide; http://www.api.org/ehs/groundwater/lnapl/).

Each release represents a potential threat to human health and the environment; appropriate remedial steps must be taken to assess the risk and minimize the impact. LNAPL can migrate significant distances if the release source (e.g., a leaking underground storage tank) is not eliminated. The migrating free-phase LNAPL may have the potential to impact surface water bodies, water supply wells, and underground utilities. Explosive vapours released from LNAPL may migrate into utilities or other confined spaces and accumulate at concentrations representing an explosion hazard. Also LNAPL present a vapour and toxicity risk: Volatilize from LNAPL and migration into indoor or ambient air, and direct contact with LNAPL in soil, groundwater or surface water may present risks to human health or the ecology.

Releases of petroleum products may occur above ground (*e.g.*, spills, leaks from exposed piping) or below ground (*e.g.*, leaks from tanks or piping). The recovery of a product above ground is relatively routine. Effective methods for cleaning up these releases from the ground surface, surface water bodies, or sewers and other underground conduits are well established. By contrast, the recovery of a product from below the ground is usually much more difficult, more costly, and less effective. The released product first soaks into the soil, and only if the volume of release is large enough will the free product accumulate at the water table. The soil will retain a significant portion of the product, but as this portion is immobile, it does not contribute to that portion termed "free product".

Petroleum products typically produced, stored, and distributed include gasoline, middle distillates (diesel, kerosene), and heavy fuel and lubricating oils. These products vary in chemical composition and physical properties. The characteristics of these

product types in conjunction with the hydrogeology conditions at the site and the manner in which the product is released are the primary factors that influence the movement and distribution of LNAPL in the subsurface. When oil is accidentally released at the surface or from an underground pipe or storage tank, oil migrates vertically downward under the force of gravity (Figure 1.1). When the volume of the release is sufficient, the LNAPL will migrate through the unsaturated zone to the capillary fringe and water table. The increasing water content in the capillary fringe and the effects of buoyancy will impede the vertical movement of the LNAPL near the water table. As a result, the less dense oil will begin to migrate laterally along the water table. In general, the lateral oil migration will preferentially flow with the water table gradient. However, if the rate of downward vertical LNAPL movement from the surface is greater than the lateral migration, the oil will begin to mount vertically and the oil flow may become radial. In addition, the downward migration into the aquifer will increase, thereby displacing water from the aquifer porous space.

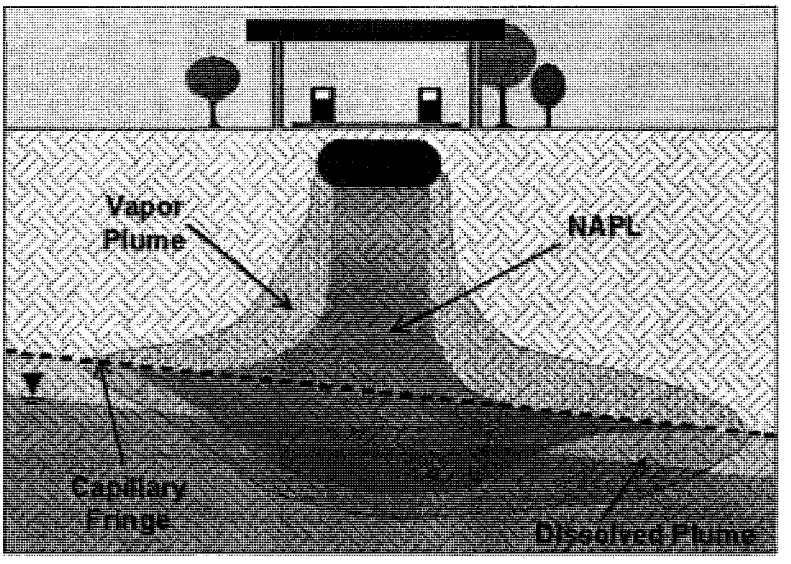

Figure 1.1 LNAPL release to the subsurface (API Interactive LNAPL guide, http://www.api.org/ehs/groundwater/lnapl/)

The important properties of hydrocarbons and geologic media must be considered when designing a free product recovery system. The first step is to estimate the volume of Hydrocarbons. Therefore, methods for evaluating recoverability of subsurface Hydrocarbons are very important. This method need to characterize the extent of the free product at a site as well as to estimate the volume of the free product.

Low density non-aqueous phase liquids (LNAPL) can accumulate as contaminants in the unsaturated zone and enter a saturated zone by being transported by the groundwater flow. In order to estimate the distribution and volume of the LNAPL, monitoring a well system is a commonplace practice. Many observations have been obtained that relate the thickness of the oil observed in monitoring wells to the actual thickness in the subsurface. And some empirical formulae have been obtained (De Pastrovich et al., 1979 and Lenhard and Parker, 1990a). However, the applications of these empirical relationships are very limited to specific soil types and fluids.

The quantitative understanding of petroleum distribution in subsurface media and its recovery was developed in the 1930s. In the past two decades, methods have been reported to analyze the actual LNAPL thickness and volume in petroleum-contaminated sites. For example, De Pastrovich et al. (1979) and Hall et al. (1984) based the estimations of oil volume on hydrocarbon density and release rate. Lenhard and Parker (1990a), Farr et al. (1990) have developed an integrated method to calculate the free LNAPL volume (specific volume) in porous media using the observed thickness of the oil in the monitoring well. Marinelli and Durnford (1996) have suggested to further

evaluate which model (van Genuchten or Brook-Corey model) is more consistent with field soils and soil layering effects on oil drainage. More recently, Sleep et al. (2000) have pointed out that the existence of layered soil would invalidate calculations based on assumptions of soil homogeneity.

Thus, it is seen that previous studies were limited to observations and theoretical analysis. Specifically, few methods of estimating oil volume in the subsurface have considered the effects of heterogeneous (i.e., layered soil), which could mislead or give the incorrect results. Very limited model validation through laboratory or field scale studies could be found. Moreover, there is no integrated user-friendly system. The present thesis study is intended to extend previous efforts on the accurate calculation of the oil volume in the subsurface after an accidental release.

1.2 Research objectives

The objectives of the present thesis study are the following:

1) To develop a new oil volume computation method, based on an integrated analysis of the oil properties, the characteristics of subsurface porous media, and the interactions between oil, soil, groundwater, and the site investigation;

2) To develop a pilot-scale experiment in the laboratory with actual oil spills and observations to validate the developed oil volume model;

3) To apply the developed and validated method to a field case study; and

4) To develop a user-friendly modeling code for technology transfer.

1.3 Organization of this thesis

The present thesis is organized as follows,

Chapter 1 is the background and research objectives of this thesis study.

Chapter 2 reviews previous modeling systems and significant parameters of modeling.

Chapter 3 describes the derivation of a computation module and examines the proposed modeling through two cases.

Chapter 4 validates the model through a pilot-scale system experiment. This experiment had as its goal to test these commonly applied techniques using data generated in a pilot-scale test.

Chapter 5 develops a user-friendly computation system. Also this system is applied to a real site.

Chapter 6 includes a model sensitivity analysis. A sensitivity analysis was conducted to evaluate the impact of changes in selected variable parameters. The variables and associated values were used for the pilot-scale experiment case.

Chapter 7 gives conclusions, research contributions, and recommendations for future study.

Chapter 2

Literature review

In this chapter, first the interaction of spilled oil and groundwater as well as related physical parameters of the system is briefly presented. Then previous studies on the estimation of oil volume in the porous media are reviewed. A short summary and discussion are presented at the end.

2.1 Spilled oil in groundwater system

Understanding of LNAPL behavior in groundwater is important for the choice and implementation of an effective clean up strategy.

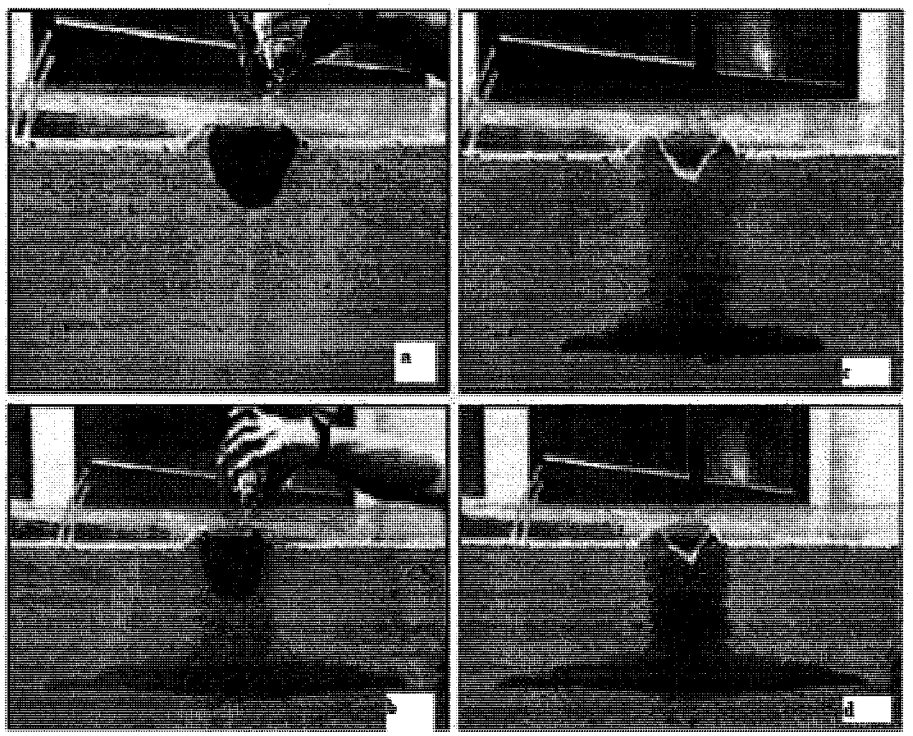

Figure 2.1 Accumulation of oil released to the subsurface
(http://www.api.org/ehs/groundwater/lnapl/)

Figure 2.1 shows a simple experiment that shows how oil is released to the soil and accumulates above groundwater. According to this experiment (API Interactive LNAPL Guide- http://www.api.org/ehs/groundwater/lnapl/), Figure 2.1-a shows an LNAPL that has just been released into the soil. The LNAPL does not reach the capillary fringe. There would probably not be any accumulation of the free product if the release of the LNAPL were to be stopped at this point. In Figure 2.1-b, the LNAPL is still being released and the volume of the release has grown large enough for the free product to begin accumulating on, and displacing, the capillary fringe. The free product is beginning to displace the capillary fringe and some of the LNAPL are dissolving into the groundwater. In Figure 2.1-c, d; Residual hydrocarbons remain in the soil beneath the UST. The free product plume has spread extensively.

Figure 2.2 shows the progression of a typical petroleum product released from an underground storage tank.

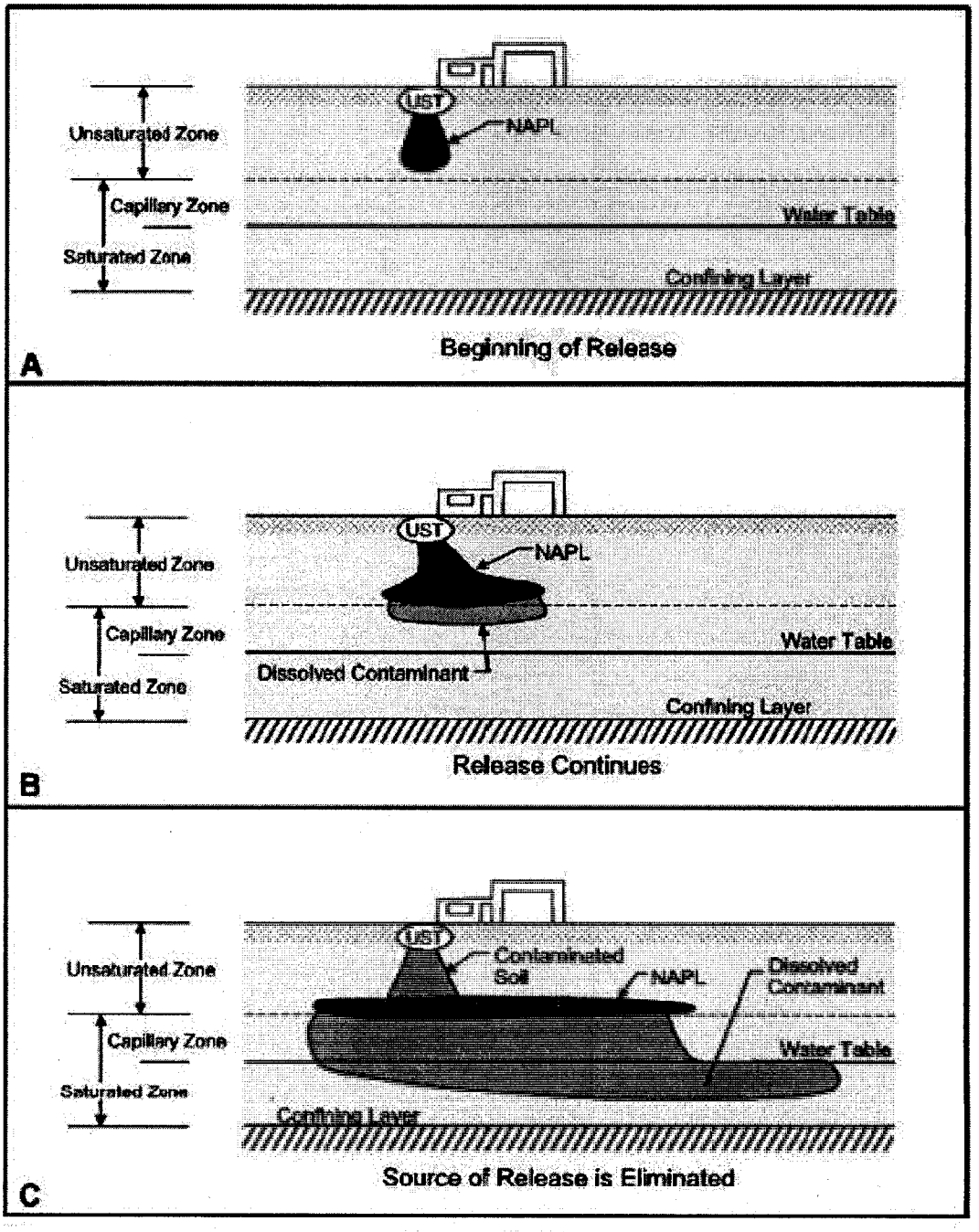

Figure 2.2 Progression of a typical petroleum product released from an underground storage tank (EPA510-R-96-001, September 1996)

The process shown above is very complex. It is based on fluid and geological properties and conditions. Some of the related characteristics are briefly reviewed.

The physical properties of fluids that are most significant to free product recovery and migration are density and viscosity. Common petroleum hydrocarbons tend to accumulate above the water table because of their low density. Viscosity is a factor controlling the mobility and recoverability of liquid hydrocarbons. A third fluid property is interfacial tension, which is important because it determines how easily a geologic medium will be wetted with a fluid. It is also important because it controls (with porous size) the height of the capillary rise in a porous media. All three properties are inversely related to temperature.

2.2 Previous observations and experimental studies on oil volume estimation

2.2.1 Field observation

Fluid physics indicate that, at equilibrium, the observed LNAPL thickness in an observation well is greater than the actual thickness in the aquifer, although there is an apparent volume exaggeration by wells. The depth down to the groundwater and the apparent thickness of an LNAPL in monitoring wells can be measured with an oil/water interface probe (ORS Model #1068013 or equivalent). The thickness of an LNAPL in a monitoring well typically exceeds the thickness of LNAPL in the subsurface by a factor estimated to range between 2 and 10. Due to this difference, the LNAPL thickness

measured in a monitoring well is commonly referred to as the "observed or apparent thickness" and is not an accurate measurement of the LNAPL thickness in the subsurface.

2.2.2 Correlation between observed and actual oil thickness

Many studies have been performed to correlate LNAPL thickness in a monitoring well to actual LNAPL thickness. These studies have produced correlations that can be used to estimate the actual LNAPL thickness from the observed LNAPL thickness measured in a monitoring well.

Because of the LNAPL thickness, observations made in monitoring wells are only an estimation of the actual volume of LNAPL in the aquifer. To determine the actual LNAPL thickness, it is necessary to collect and visually analyze the observed thickness in the monitoring well. This was done by de Pastrovich et al. (1979) using the CONCAWE method. They came to the conclusion that the actual thickness is approximately four times the observed thickness. Kramer (1982) and Yaniga and Demko (1983) have respectively proposed a difference between the actual oil thickness and the observed thickness in the monitoring well of 2–3 times, 2.5–3 times and 5–10 times approximately in each case. Shephard (1983) and Hall et al. (1984) included the grain size in the Equations. Schiegg (1985) included capillary heights and Corey (1986) proposed the Brooks-Corey model. Parker et al. (1987) and Parker and Lenhard (1989) went further, incorporating soil saturation into their Equations. This improved the accuracy of the estimation of the oil volume. Figure 2.3 illustrates this relationship.

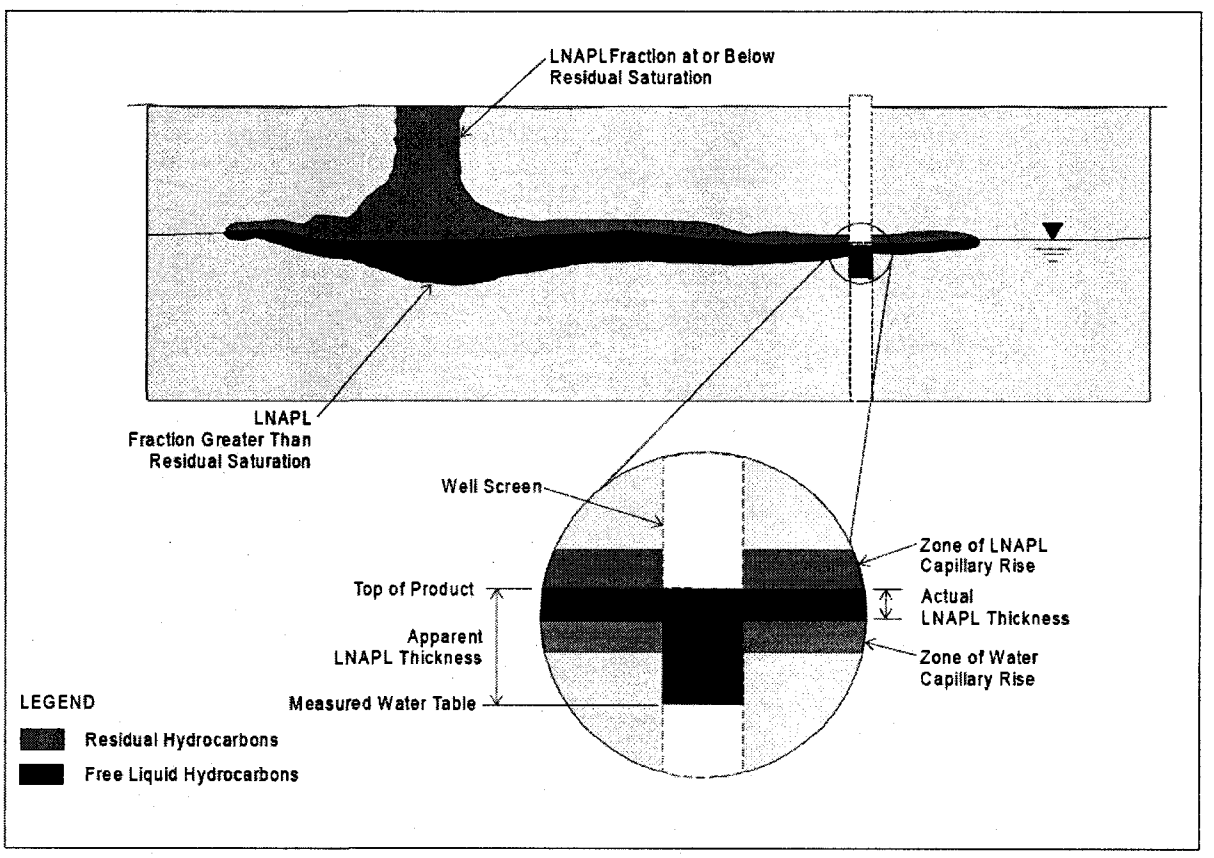

Figure 2.3 Observed versus actual LNAPL thickness (De Pastrovich et al (1979))

It has been demonstrated that the thickness of the LNAPL in a monitoring well is greater than the thickness of the LNAPL in the formation (De Pastrovich et al., 1979 and Lenhard and Parker, 1990a); and that the apparent thickness in a monitoring well can be from 2 to 10 times greater than the actual LNAPL thickness in the formation (Mercer and Cohen, 1990). Lenhard and Parker (1990a) have developed an Equation (2-1) to estimate the actual LNAPL thickness in the formation using the apparent LNAPL thickness in the monitoring well.

$$D_O = \frac{r_{ro}\, b_{ao}\, H_o}{b_{ao}\, r_{ro} - b_{ow}\,(1 - r_{ro})} \qquad (2\text{-}1)$$

where:

D_o = actual thickness of LNAPL in the formation

H_o = apparent LNAPL thickness in the well

r_{ro} = density of LNAPL

b_{ao} = air/oil scaling factor = s_{aw}/s_{ao}

b_{ow} = oil/water scaling factor = s_{aw}/s_{ow}

s_{aw} = surface tension of uncontaminated water (72.75 dynes/cm @ 20°C)

s_{ao} = surface tension of LNAPL (26.8 dynes/cm for JP-5)

$s_{ow} = s_{aw} - s_{ao}$ = interfacial tension between water and LNAPL

2.2.3 Experimental studies

Previously, laboratory experimental studies were rarely found. Also the experimental studies were almost in homogeneous condition. They did not consider heterogeneous conditions and layer effects (Wickramanayake et al., 1991 and Sleep et al., 2000).

2.3 Previous models of calculating oil volume in the porous media

The quantitative understanding of petroleum distribution in subsurface media and the recovery of petroleum was developed in the 1930s at Princeton and other universities. This understanding established the role of interfacial and capillary forces in determining the distribution of oil in subsurface media. Previous studies on the calculation of the volume of oil when it is spilled into porous media are reviewed below.

Studies presented by De Pastrovich et al. (1979):

In the past two decades, there have been reports about methods for the analysis of the actual LNAPL thickness and volume in petroleum contaminated sites. For example, De Pastrovich et al. (1979) and Hall et al. (1984) made estimations based on hydrocarbon density and release rate. These studies have tried to relate the measured thickness in the monitoring well to the "actual LNAPL thickness" with the ratio of 4:1 (De Pastrovich et al., 1979). Based on laboratory studies and a review of many of these methods, Hampton and Miller (1988) have pointed out that the relationships investigated in their study were not sufficient to reliably predict hydrocarbon thickness in the formation.

Studies presented by Lenhard and Parker (1990a) and Farr et al. (1990):

A few methods reflecting more complex relationships incorporating the properties of the porous medium have been developed. Simultaneously and separately, Farr et al. (1990) and Lenhard and Parker (1990a) investigated the theoretical basis for estimating LNAPL volume in porous media under vertical equilibrium conditions taking into consideration the fluid and media properties. These efforts corroborated one other and thereby enhancing the validity of each individual study. Wickramanayake et al. (1991) compared the methods proposed by De Pastrovich et al. (1979), Hall et al. (1984), and Lenhard and Parker (1990a) to estimate the LNAPL volume from an artificial release. The method proposed by Lenhard and Parker (1990a) was found with an accurate estimate of LNAPL release after the system had reached equilibrium.

During the same period of time, Lenhard and Parker (1990a) and Farr et al. (1990) developed an integrated method to calculate the free LNAPL volume (specific volume) in porous media using the apparent thickness of oil in the monitoring well. An analytical solution based on the Brook-Corey model was also obtained. Their research was based on two assumptions: the existence of hydrostatic equilibrium between the well and the adjacent porous media, and the homogeneity of porous media. The first assumption makes it possible to connect the thickness of the oil in the well with the distribution of the LNAPL in the porous media. The second assumption facilitates the analytical solution based on the Brooks-Corey capillary pressure-saturation model (BC model). Although the integrated method was applied more widely than empirical formulae, the method considered only homogeneous soils. The specific volume showed no relations to the groundwater table in the homogeneous soils. Basing our conclusions on the available soil type and fluid properties, the actual specific volume in the porous media is proportional to the apparent thickness in the monitoring well under the assumption of homogeneity. Wickramanayake et al. (1991) compared the total oil volume in a pilot-scale sand tank with the calculation employing the method of Lenhard and Parker (1990a) and concluded that there is a fairly accurate fit based on the van Ganuchten (1980) model.

Studies presented by Durnford et al. (1991):

Few previous studies have been adequately evaluated under a variety of field conditions especially in the majority of soils and aquifers with heterogeneous characteristics. These studies were limited to homogeneous sites. Furthermore, several

potential limitations in the application of many of these methods were identified by Durnford et al. (1991): (1) water table fluctuations can result in differences in "actual LNAPL thickness"; (2) uncertainties exist in the measurements of capillary pressure-saturation relationships when using methods incorporating soil and fluid properties; and (3) it is difficult to evaluate the spatial variability in subsurface properties (heterogeneity) and its effects on the distribution of LNAPL inside.

Studies presented by Marinelli and Durnford (1996) and Sleep et al. (2000):

More recently, Marinelli and Durnford (1996) have suggested the need to further evaluate which model (VG or BC model) is more consistent with field soils and soil layering effects on oil drainage. Moreover, Sleep et al. (2000) thought that the existence of soil layering would invalidate calculations based on assumptions of soil homogeneity. From the engineering point of view, specific oil volume estimations of free phase oil in the stratified soils are more significant due to almost no existence of homogeneous soils in the real world.

2.4 Discussion and summary

In summary, four methods of calculating the LNAPL volume associated with a LNAPL spill site have been available since the 1970s. Much of the understanding of the distribution and mobility of spilled LANPL is useful for establishing a modeling method. However, previous studies were limited to the following areas:

1) Heterogeneous soil: Few of these studies considered the effects of heterogeneous soil, i.e. the layering effects, which directly affect the oil volume estimation results or simply result in an incorrect estimation.

2) Validation: Very few of the model validations in these studies were through laboratory and field scale experiments.

3) Selectivity: These studies do not present an integrated consideration of both properties and characteristics associated with subsurface soil and groundwater and spilled LNAPL.

4) Interface: A few user-friendly systems and extensive unstable analyses could be found.

The present thesis is intended to address the issues given above by extending previous model development and by creating a model validation experiment.

Chapter 3

Development of an oil volume computation system

Low density non-aqueous phase liquids (LNAPL) as contaminants can accumulate in unsaturated zones and enter saturated zones are transported by the groundwater flow. In order to estimate the distribution and volume of LNAPL, monitoring a well system is a commonplace practice. In this chapter, an oil volume computation system is developed and examined through similar literature case studies.

3.1 Development of a conceptual model

The present study focuses on developing a method to estimate free phase LNAPL as indicated in Figure 3.1. The steps are (1) to construct a conceptual model based on; (2) to

define the level of different fluids; (3) to determine the physical interactions between oil and the groundwater system; and (4) to develop the mathematical model;

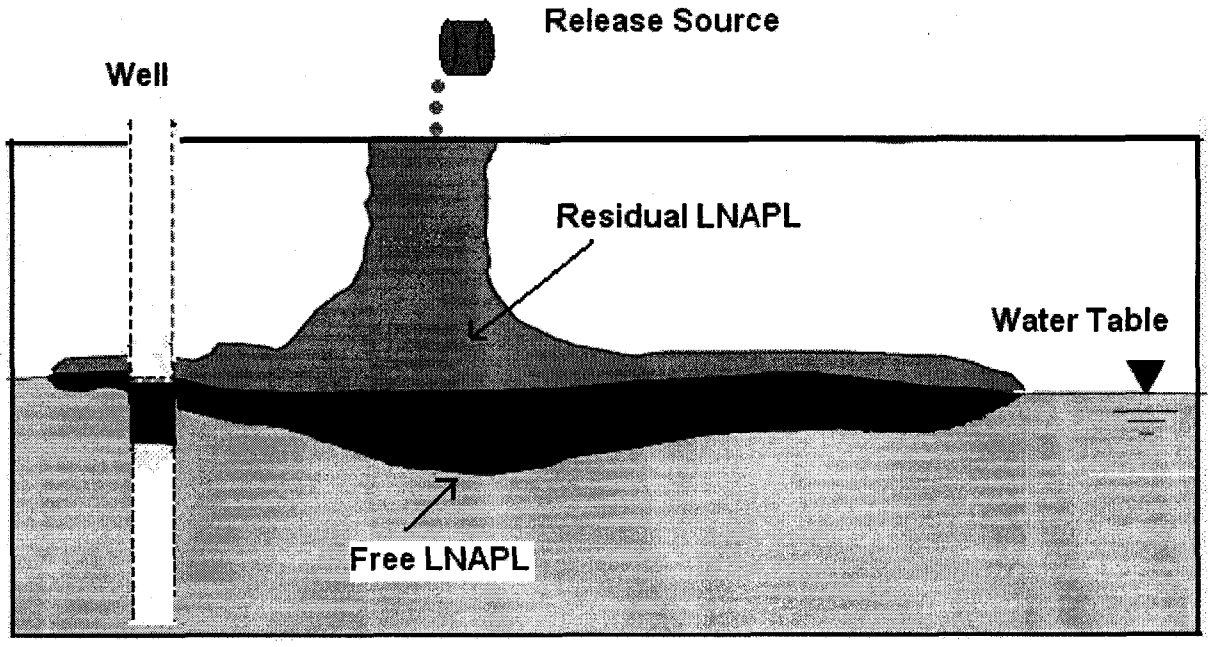

Figure 3.1 Condition of LNAPL and water in porous media

The subsurface can be divided into two zones based on water content: the unsaturated zone and the saturated zone. The movement of petroleum hydrocarbons in the subsurface is fundamentally different in the unsaturated and saturated zones. It is commonly accepted that the boundary between these two zones is the water table, which is the surface where water pressure equals atmospheric pressure. Below the water table, in the saturated zone, all porous and void spaces are filled with water and the water pressure is greater than the atmospheric pressure. Water pressures above the water table, in the unsaturated zone, are less than the atmospheric pressure, and the water may be considered to be under tension or suction. Directly above the water table is a relatively

thin zone—the capillary fringe—that is saturated with water but the water pressure is less than the atmospheric pressure. The capillary fringe is thicker in fine-grained media and thinner in coarse-grained media. Above the capillary fringe in the unsaturated zone, voids and porous spaces are filled primarily with air and varying amounts of water as either liquid or vapor (Figure 3.1).

3.2 Oil volume computation

3.2.1 Calculations of phase-to-phase elevation corresponding to the oil saturation in the porous media

The majority of petroleum hydrocarbons stored in USTs are lighter than water, which means that they float. A free product generally moves in the same direction as the flow of groundwater. This movement is strongly influenced by soil heterogeneity and anisotropy, and the design and operation of an effective free-product recovery system is dependent upon the accurate characterization of the hydrogeology conditions at the site. It is extremely important to realize that the elevations of liquid surfaces in a monitoring well containing both groundwater and free products are not representative of the hydraulic head at that location. The measurement must first be corrected to account for the thickness of the free product. Other critical factors to consider are the total volume of the release and the depth down to the groundwater.

The following formulae are mainly based on two assumptions:

- Hydrostatic equilibrium between the well and porous media.
- Homogeneous porous media.

The depth to the water table is an important factor that affects how the free product migrates and how its recovery should be approached. Except for very deep water tables, the depth to the water table can be determined through relatively inexpensive borings or monitoring wells (or well points). The depth to the water table will indicate the potential for petroleum hydrocarbons to reach the water table, where the free product can then be collected in wells or trenches. All other factors being equal, a greater depth to the water table requires that the volume of liquid petroleum hydrocarbons be greater if they are to reach the water table.

According to the equilibrium of pressure on the interface of oil-water in the well, we have Figure 3.2 (extended from Fetter, 1998):

$$\rho_w L_w = \rho_o \mathrm{T} \qquad [3\text{-}1]$$

$$L_w = \frac{\rho_o}{\rho_w} \mathrm{T} \qquad [3\text{-}2]$$

where,

T= apparent oil thickness in monitoring well (m);

ρ_o, ρ_w = oil and water densities, respectively (kg/m^3);

L_w= apparent thickness in monitoring well under water table (m).

The interface between oil, water and air phases in the well and aquifer can be expressed by Equation [3-3]:

$$D_w^{ao} = D_s^{ao} + \frac{P_d^{ao}}{\rho_o g} \quad [3\text{-}3]$$

where,

D_w^{ao} = depth of interface of air-oil in monitoring well (m);

D_s^{ao} = depth of oil capillary fringe in soil (m);

P_d^{ao} = air-oil displacement pressure (N/m^2).

It is evident that the difference is the oil capillary fringe (Figure 3.2),

$$D_w^{ao} = D_s^{ao} + L_{of} \quad [3\text{-}4]$$

where (Figure 3.2),

L_{of} = height of oil capillary fringe in porous media (m);

L_{ro} = height of residual oil in porous media (m);

L_{vo} = height of oil move vertically in porous media (m);

L_{mo} = height of mobile oil in porous media (m);

L_{io} = height of immobile oil in porous media (m);

L_{wf} = height of water capillary fringe in porous media (m).

$$L_{of} = \frac{P_d^{ao}}{\rho_o g} \quad [3\text{-}5]$$

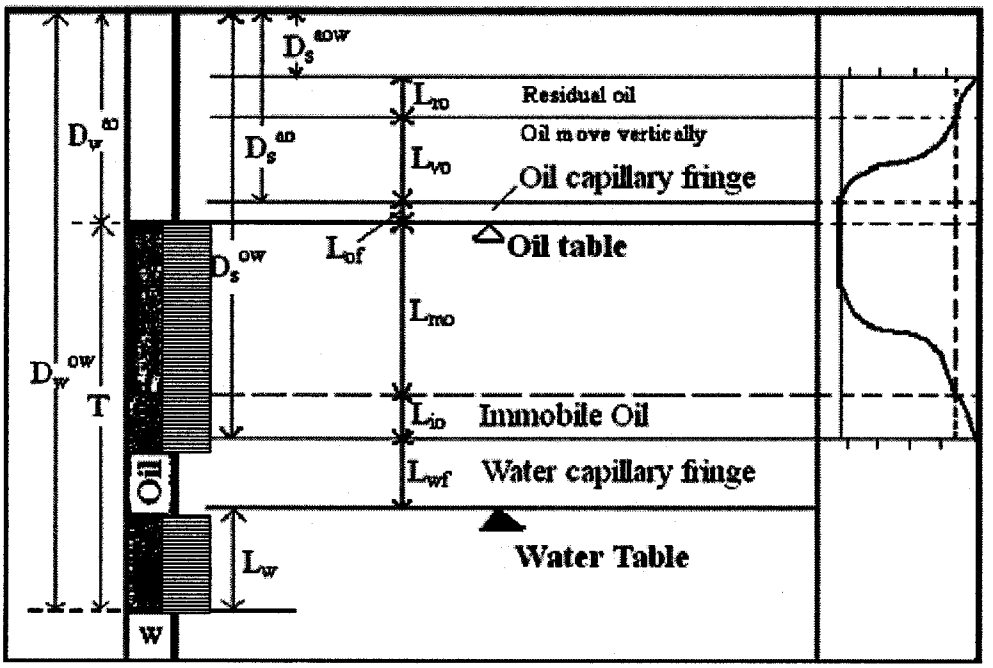

Figure 3.2 Conceptual diagrams for heights in porous media (Extended from Fetter (1998))

Similarly, the difference between the oil-water interface in the well and the aquifer is expressed as:

$$D_w^{ow} = D_s^{ow} + \frac{P_d^{ow}}{\Delta \rho g} \qquad [3\text{-}6]$$

where,

$\Delta \rho = \rho_w - \rho_o$ (g/cm^3);

D_w^{ow} = depth of interface of oil-water in monitoring well (m);

D_s^{ow} = depth of water capillary fringe in soil (m);

P_d^{ow} = oil-water displacement pressure (N/m^2).

In Figure 3.2, this difference consists of the water capillary fringe and the water table difference.

$$D_w^{ow} = D_s^{ow} + L_{wf} + L_w \qquad [3\text{-}7]$$

So, the height of the water capillary fringe is expressed as:

$$L_{wf} = \frac{P_d^{ow}}{\Delta \rho g} - \frac{\rho_o}{\rho_w} T \qquad [3\text{-}8]$$

Three-phase saturation relations are based on the work of Lenhard and Parker (1987):

$$S_o + S_w = 1, \quad P_c^{ao} \le P_d^{ao} \qquad [3\text{-}9]$$

$$S_w = (1 - S_{wr}) \left(\frac{P_c^{ow}}{P_d^{ow}} \right)^{-\lambda} + S_{wr}, \quad P_c^{ow} \ge P_d^{ow} \qquad [3\text{-}10]$$

where,

S_{wr} = irreducible saturation of water; S_w = actual saturation of water; S_o = actual saturation of oil; P_d^{ao} = air-oil displacement pressure (N/m^2).

Oil saturation equals the oil residual saturation in the porous media at the upper boundary of immobile oil, i.e. $S_o = S_{or}$. Combining with Equations [3-9] and [3-10], we get the following:

$$S_{or} = (1 - S_{wr}) \left[1 - \left(\frac{P_c^{ow}}{P_d^{ow}} \right)^{-\lambda} \right] \qquad [3\text{-}11]$$

where,

S_{or} = irreducible saturation of oil.

And the corresponding depth can be expressed in Equation [3-12] (Figure 3.2):

$$Z = D_w^{ow} - (L_w + L_{wf} + L_{io}) \qquad [3\text{-}12]$$

where,

Z= depth of immobile oil in soil (m).

Therefore, Equation [3-13] exists:

$$P_c^{ow} = \Delta\rho g\left(D_w^{ow} - P_d^{ow}/\Delta\rho g - Z\right) + P_d^{ow} \qquad [3\text{-}13]$$

where,

P_c^{ow} = the pressure of interface of immobile oil in soil (N/m^2).

The height of the immobile oil zone above the water capillary fringe based on Equations [3-9]-[3-13] is as follows (Brooks, R.H. and Corey, A.T., 1964):

$$L_{io} = \frac{P_d^{ow}}{\Delta\rho g}\left[\left(\frac{1 - S_{wr} - S_{or}}{1 - S_{wr}}\right)^{-\frac{1}{\lambda}} - 1\right] \qquad [3\text{-}14]$$

where,

λ = BC parameter (Brooks-Corey model).

The mobile oil zone can be calculated by Equation [3-15] (Figure 3.2):

$$L_{mo} = T - \frac{P_d^{ow}}{\Delta\rho g} - L_{io} \qquad [3\text{-}15]$$

Equation [3-14] is substituted for [3-15]; we obtain Equation [3-16],

$$L_{mo} = T - \frac{P_d^{ow}}{\Delta\rho g}\left(\frac{1 - S_{wr} - S_{or}}{1 - S_{wr}}\right)^{-\frac{1}{\lambda}} \qquad [3\text{-}16]$$

At the depth of D_s^{aow} (depth of residual oil in soil), oil saturation is zero. We can calculate this depth based on the relationship of water saturation and total (oil and water) saturation. Total liquid saturation is expressed as:

$$S_o + S_w = (1 - S_{wr})\left(\frac{P_c^{ao}}{P_d^{ao}}\right)^{-\lambda} + S_{wr}, \quad P_c^{ao} \geq P_d^{ao} \qquad [3\text{-}17]$$

From Equations [3-17] and [3-10] and the conditions of Equations [3-18] and [3-19], the depth of the point at which oil saturation is zero can be acquired by Equation [3-20].

$$(S_o + S_w) - S_w = 0 \qquad [3\text{-}18]$$

$$P_c^{ao} = \rho_o g\left(D_w^{ao} - P_d^{ao} / \rho_o g - Z\right) + P_d^{ao} \qquad [3\text{-}19]$$

where,

P_c^{ao} = the immobile oil and mobile oil displacement pressure.

$$D_s^{aow} = D_w^{ow} - \left(\frac{P_d^{aw}\rho_o g}{P_d^{aw}\rho_o g - P_d^{ao}\Delta\rho g}\right)T \qquad [3\text{-}20]$$

In Figure 3.2, the height of the oil staying in the air-oil-water phase (three dimensions) is as follows:

$$L_{vo} + L_{ro} = D_s^{ao} - D_s^{aow} \qquad [3\text{-}21]$$

Substituting Equation [3-20] in [3-21], we get Equation [3-22].

$$L_{vo} + L_{ro} = \left(\frac{P_d^{ao}\Delta\rho g}{P_d^{aw}\rho_o g - P_d^{ao}\Delta\rho g}\right)T - \frac{P_d^{ao}}{\rho_o g} \qquad [3\text{-}22]$$

Equation [3-22] is the height of the residual oil and oil moves vertically in soil. Equations [3-5], [3-14], [3-15] and [3-22] are important for oil volume calculations. They clearly show the different height of oil in soil. Through these Equations, we deduct the volume of oil in porous media.

3.2.2 BC model

The Brooks-Corey (BC) model evaluates the volume of an LNAPL using the thicknesses in wells compared to the capillary displacement porous-entry pressure (Farr et al., 1990). The use of this concept involves consideration of some of the same theoretical constructs (e.g., scaling parameters to obtain capillary parameters) as the background to analyze LNAPL volume and mobility.

Specific volume is defined as the volume of a substance per unit area, expressed in cubic meter per square meter (m^3/m^2).. Using a specific volume, it is possible to represent the distribution of oil in porous media. The total specific volume of oil in porous media can approximately be expressed as Equation [3-23]:

$$V_T = \phi\left[(L_{vo} + L_{ro}) \times \frac{1 - S_{wr}}{2} + L_{of} \times (1 - S_{wr}) + L_{mo} \times K \times (1 - S_{wr}) + L_{io} \times \frac{S_{or}}{2}\right] \quad [3\text{-}23]$$

where,

ϕ= porosity of soil;

T= apparent oil thickness in monitoring well (m);

V_T= the total specific volume of oil in porous media (m^3/m^2).

K is the ratio of oil saturation to water saturation in oil mobile zones. S_{or} and S_{wr} are residual oil and water saturation, respectively. K is proportional to T (apparent oil thickness in monitoring well). Thus Equation [3-24] is obtained:

$$V_T = \phi(1 - S_{wr})T\left(\frac{1}{2} \times \frac{P_d^{ao}\Delta\rho g}{P_d^{aw}\rho_o g - P_d^{ao}\Delta\rho g} + K\right) + A \times \phi \quad [3\text{-}24]$$

where,

$$A=\frac{1-S_{wr}}{2}\times\frac{P_d^{ao}}{\rho_o g}+\frac{P_d^{ow}}{\Delta\rho g}\left(\frac{1-S_{wr}-S_{or}}{1-S_{wr}}\right)^{-\frac{1}{\lambda}}\times\left[\frac{S_{or}}{2}-K\left(1-S_{wr}\right)\right]-\frac{S_{or}}{2}\times\frac{P_d^{ow}}{\Delta\rho g}$$

The free phase oil volume (specific volume under ideal discharge conditions) is as follows:

$$V_m=V_T-V_r \qquad [3\text{-}25]$$

where,

V_m = the free phase specific volume of oil in porous media (m^3/m^2);

V_r = the residual phase specific volume of oil in porous media (m^3/m^2).

The residual oil volume in porous media is as follows:

$$V_r=\phi\left(D_s^{ow}-D_s^{aow}\right)S_{or} \qquad [3\text{-}26]$$

Based on Equations [3-24], [3-25], [3-26], the free phase oil specific volume is the following:

$$V_m=\phi\times\frac{P_d^{ao}\Delta\rho g}{P_d^{ow}\rho_o g-P_d^{ao}\Delta\rho g}T\left(\frac{1-S_{wr}-2S_{or}}{2}\right)+\phi\left(1-S_{wr}\right)KT+B\times\phi \qquad [3\text{-}27]$$

where, B is constant, i.e.

$$B=\frac{1-S_{wr}}{2}\times\frac{P_d^{ao}}{\rho_o g}+\frac{P_d^{ow}}{\Delta\rho g}\left(\frac{1-S_{wr}-S_{or}}{1-S_{wr}}\right)^{-\frac{1}{\lambda}}\times\left[\frac{S_{or}}{2}-K\left(1-S_{wr}\right)\right]+\frac{S_{or}}{2}\times\frac{P_d^{ow}}{\Delta\rho g}$$

If oil in porous media is extended over a soil surface, $D_s^{aow} \leq 0$, the total specific volume and the mobile oil specific volume are calculated by Equations [3-28] and [3-29], respectively.

$$V_T = \phi K(1 - S_{wr})T + C\phi \qquad [3\text{-}28]$$

$$V_m = \phi K(1 - S_{wr})T - \phi S_{or} T + D\phi \qquad [3\text{-}29]$$

where, c and d are constants expressed in the following:

$$C = D_w^{ao} \times \frac{1 - S_{wr}}{2} + \frac{1 - S_{wr}}{2} \times \frac{P_d^{ao}}{\rho_o g} + \frac{P_d^{ow}}{\Delta\rho g}\left(\frac{1 - S_{wr} - S_{or}}{1 - S_{wr}}\right)^{-\frac{1}{\lambda}} \times \left[\frac{S_{or}}{2} - K(1 - S_{wr})\right] - \frac{S_{or}}{2} \times \frac{P_d^{ow}}{\Delta\rho g}$$

$$D = D_w^{ao} \times \frac{1 - S_{wr} - 2S_{or}}{2} + \frac{1 - S_{wr}}{2} \times \frac{P_d^{ao}}{\rho_o g} + \frac{P_d^{ow}}{\Delta\rho g}\left(\frac{1 - S_{wr} - S_{or}}{1 - S_{wr}}\right)^{-\frac{1}{\lambda}} \times \left[\frac{S_{or}}{2} - K(1 - S_{wr})\right] + \frac{S_{or}}{2} \times \frac{P_d^{ow}}{\Delta\rho g}$$

Using the Equation above to calculate the case in the article by Farr et al. (1990), it was found that K is important, which determines the accuracy compared with the analytical results. K is within a range of 0.3-0.7 and increases along with T. So it would not fit well with the analytical curve except by adjusting the K value. The reason is that both water and oil saturations in the soil are complex. Simply using ($1\text{-}s_{WT}$) or $1/2(1\text{-}s_{WT})$ for oil saturation causes erroneous results.

3.2.3 VG model

Another concept is to employ actual saturation at the half depth as representative saturation. From this point, a computational method -VG can be obtained. The analyses are as follows:

For BC model parameters, V_m is obtained:

$$V_m = \phi\left(L_{mo} + L_{io} + L_{of}\right) \times S_o \Big|_{\frac{1}{2}\left(D_s^{ao} + D_s^{ow}\right)} \qquad [3\text{-}30]$$

Given $Z = D_s^{ao} + \frac{1}{2}\left(D_s^{ow} - D_s^{ao}\right)$, Equation [3-31] is obtained based on Equations [3-5], [3-9], [3-10], and [3-15]:

$$V_m = \phi\left(1 - S_{wr}\right)\left(T - \frac{P_d^{ow}}{\Delta\rho g} + \frac{P_d^{ao}}{\rho_o g}\right)\left[1 - \left(\frac{1}{2}\frac{\Delta\rho g}{P_d^{ow}}T + \frac{1}{2}\frac{\Delta\rho g}{P_d^{ow}}\frac{P_d^{ao}}{\rho_o g} + \frac{1}{2}\right)^{-\lambda}\right] \qquad [3\text{-}31]$$

Similar deductions can be obtained for VG model V_m calculation (van Ganuchten, M.T., 1980):

$$V_m = \phi\left(L_{mo} + L_{io}\right) \times S_o \Big|_{\frac{1}{2}\left(D_s^{ao} + D_s^{ow}\right)} \qquad [3\text{-}32]$$

When P_d^{ao} and P_d^{ow} are assumed to be zero, and $L_{mo} + L_{io} = T$, utilizing Equations [3-33] and [3-34] gives the specific volume of oil (Equation [3-35]) based on VG parameters:

$$S_o + S_w = 1 \qquad [3\text{-}33]$$

$$S_w = \left(1 - S_{wr}\right)\left(\frac{1}{1 + \left(\alpha_{ow} P_c^{ow}\right)}\right)^{1-1/n} + S_{wr} \qquad [3\text{-}34]$$

$$V_m = \phi(1 - S_{wr})T\left[1 - \left(\frac{1}{1 + \left(\frac{1}{2}\alpha_{ow} T\Delta\rho g\right)^n}\right)^{1-1/n}\right] \qquad [3\text{-}35]$$

where,

α_{ow}= VG model parameter (oil-water); and n= VG model parameter.

From Equation [3-31], if V_m>0.0, $T \geq \frac{P_d^{ow}}{\Delta\rho g} - \frac{P_d^{ao}}{\rho_o g}$. That is in concordance with the result (Lenhard and Parker, 1990a).

3.2.4 Total oil volume calculation

3.2.4.1 Calculation of the total volume of spilled oil in a groundwater system

When an underground storage tank (UST) leaks oil, the leaked oil will spread in two directions: vertically and laterally. If there is enough leaked oil, it will reach the groundwater capillary fringe and the groundwater table, thus producing free oil in porous media. Free oil will flow in a lateral direction because of the pressure difference in the media. The spread of leaked oil shows the apparent complexity in the real world due to the heterogeneity of the porous media. Site investigation using monitoring wells and core samples in the leaked oil area usually produces three kinds of free phase oil results: free oil accumulated in the wells; no free oil in the wells but with a certain thickness in core samples; no oil is found in the wells and samples. According to the above-mentioned

analysis, a site can be divided into three areas, i.e., the free phase oil area, the non-free phase oil area, and the non-contaminated area (Figure 3.3).

The free phase oil area is the area where free oil accumulates in the monitoring. The non-free phase oil area is the area in which free oil cannot be found in the monitoring well, but it is evident that the soil is contaminated. Non-contaminated area is defined as an area where the soil is not contaminated by a concerned source of leaked oil.

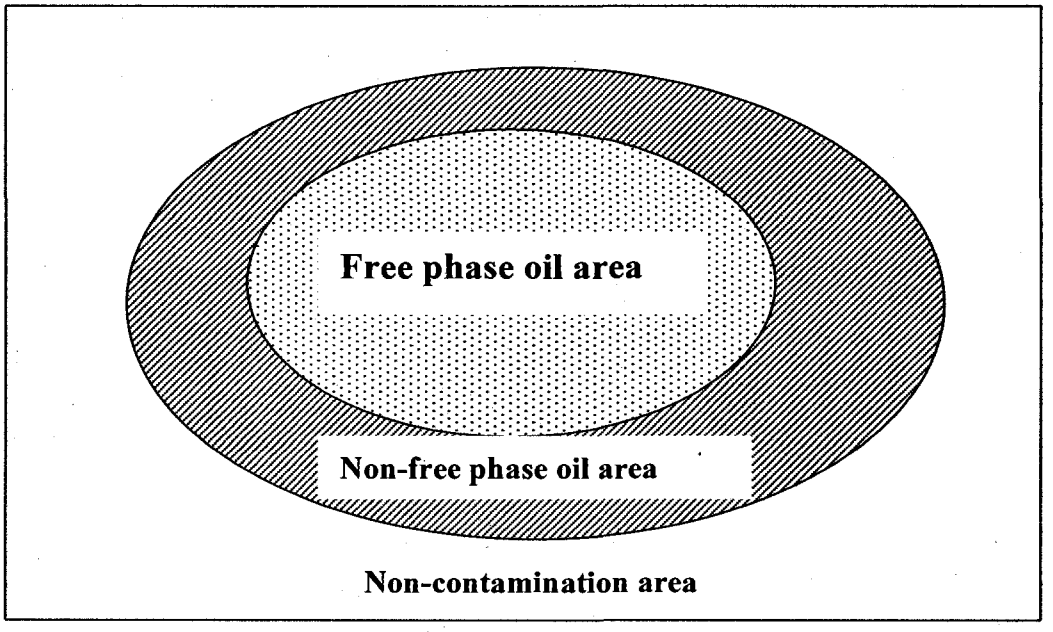

Figure 3.3 Delimitation of contamination areas

3.2.4.2 Oil volume estimation in free phase oil area

Lenhard and Parker (1990a), Farr et al. (1990) proposed formulas to calculate specific volumes in the free-phase oil area. Their Equations are identical after a conversion between models of parameters (Lenhard and Parker, 1990b). These related studies are

referred to in the development of methods of estimating oil volume in the free-phase oil area in below.

First, vertical equilibrium pressure distribution and the relationships between fluid levels (air-oil and oil-water) in the monitoring well and porous media are built under the condition of hydrostatic equilibrium (Equations [3-36]-[3-39]).

$$h_{ow} = (1 - \rho_{ro})(z - z_s^{ow}) \quad [3\text{-}36]$$

$$h_{ao} = \rho_{ro}(z - z_s^{ao}) \quad [3\text{-}37]$$

$$z_s^{ow} = z_w^{ow} + \frac{h_d}{(1-\rho_{ro})\beta_{ow}} \quad [3\text{-}38]$$

$$z_s^{ao} = z_w^{ao} + \frac{h_d}{\rho_{ro}\beta_{ao}} \quad [3\text{-}39]$$

where,

h_{ow}, h_{ao}=oil-water, air-oil capillary head, respectively (m); ρ_{ro}=ratio of oil density with water density; h_d=air entry pressure in BC model (m); β_{ow}=oil-water scaling factor; β_{ao}=air-oil scaling factor; Z_w^{ao}=elevation of interface of air-oil in monitoring well (m); Z_s^{ao}=elevation of oil capillary fringe in soil (m); Z_w^{ow}=elevation of interface of oil-water in monitoring well (m); Z_s^{ow}=elevation of water capillary fringe in soil (m).

Secondly, the decision concerning the distribution of oil saturation is based on three-phase relationships between fluid content and capillary pressures (Lenhard and Parker, 1987,1988), which are the extensions of the two-phase relationships of the Brooks-Corey (BC) concept or the van Ganuchten (VG) concept (Equations [3-40]-[3-47]).

$$\overline{S_w}(\beta_{ow} h_{ow}) = S^*(h^*) \quad [3\text{-}40]$$

$$\overline{S_t}(\beta_{ao} h_{ao}) = S^*(h^*) \quad [3\text{-}41]$$

$$\overline{S_w} = \frac{S_w - S_m}{1 - S_m} \quad [3\text{-}42]$$

$$\overline{S_t} = \frac{S_w + S_o - S_m}{1 - S_m} \quad [3\text{-}43]$$

$$S^*(h^*) = (h_d / h^*)^{\lambda} \qquad h^* > h_d \quad [3\text{-}44]$$

$$S^*(h^*) = 1 \qquad h^* \le h_d \quad [3\text{-}45]$$

$$S^*(h^*) = \left[1 + (\alpha h^*)^n\right]^{-m} \qquad h^* > 0 \quad [3\text{-}46]$$

$$S^*(h^*) = 1 \qquad h^* \le 0 \quad [3\text{-}47]$$

where,

$S^*(h^*)$= scaled saturation-pressure function; $\overline{S_w}$= effective saturation of water; $\overline{S_t}$= effective saturation of total fluid (oil +water); S_m= water residual saturation; and S_o= actual saturation of oil.

Last, the specific volume of free-phase oil is obtained by the integration of the oil saturation in the soil (Equation [3-48]).

$$V_{sfo} = \int_{Z_s}^{Z_u} \phi S_o dz \quad [3\text{-}48]$$

where,

V_{sfo}= specific oil volume in free phase oil area; Z_u = elevation where oil saturation is zero.

An analytical solution is acquired based on BC model (Equations [3-49a] and [3-49b]).

$$V_{sfo}=\frac{\phi(1-S_m)}{1-\rho_{ro}}(A-B)-\frac{\phi(1-S_m)}{(1-\rho_{ro})(1-\lambda)}\cdot B^{\lambda}(A^{1-\lambda}-B^{1-\lambda}) \quad Z_s^{ao}>z_u \qquad [3\text{-}49a]$$

$$V_{sfo}=\frac{\phi(1-S_m)}{1-\rho_{ro}}(C-B)-\frac{\phi(1-S_m)}{(1-\rho_{ro})(1-\lambda)}\cdot B^{\lambda}(C^{1-\lambda}-B^{1-\lambda})+\frac{\phi S_m}{\rho_{ro}}(D-E)+\frac{\phi(1-S_m)}{(1-\rho_{ro})(1-\lambda)}\cdot$$

$$E^{\lambda}(D^{1-\lambda}-E^{1-\lambda})-\frac{\phi S_m}{1-\rho_{ro}}(A-C)-\frac{\phi(1-S_m)}{(1-\rho_{ro})(1-\lambda)}\cdot B^{\lambda}(A^{1-\lambda}-C^{1-\lambda}) \quad Z_s^{ao}\le z_u \qquad [3\text{-}49b]$$

where,

ϕ= porosity of soil; λ = BC model parameter.

The development of Equation [3-48] is based on the configuration shown in Figure 3.4 and is for the area of oil saturation distribution along with the vertical contamination zone (Figure 3.4).

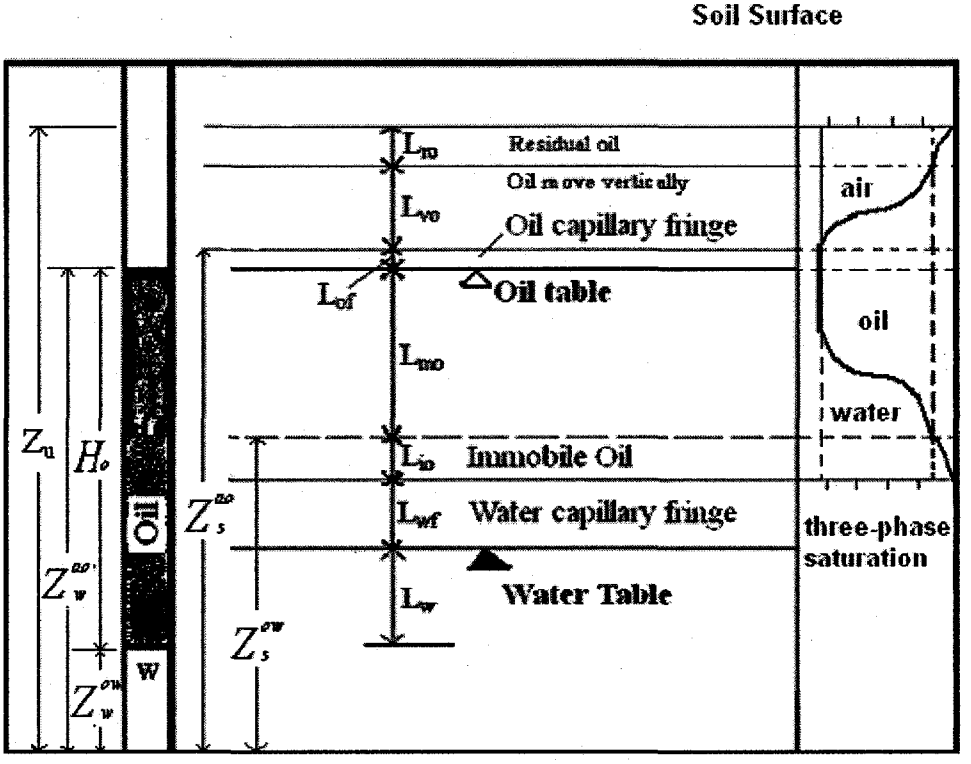

Figure 3.4 Conceptual diagram of oil in the monitoring well

The total oil volume in the free-phase oil area is the integration of specific oil volume over the whole free-phase oil area (Equation [3-50]):

$$V_{sfo}^{T} = \iint_{A1} V_{sfo} dA \qquad [3\text{-}50]$$

where,

V_{sfo}^{T} = total oil volume in free phase area; A=free phase oil area.

3.2.4.3 Oil volume estimation in non-free phase oil area

Equation [3-48] expresses the general method for calculating the specific oil volume in the soil; it is also applicable to non-free phase oil area,

$$V_{snf} = \int_{z_l}^{z_u} \phi S_o dz \qquad [3\text{-}51]$$

where,

V_{snf} = specific oil volume in non-free phase area.

Determinations of oil saturation and the upper and lower limitation of the integration range influence the accuracy of the specific volume of the non-free phase oil. The non-free phase oil area is produced when oil spreads in the vertical or lateral direction and the amount of oil is less compared to the amount in the free phase oil area. In this area, oil is in the form of oil residual saturation; and air, oil, water co-exist in the soil, i.e., the three-phase condition. S_o equals S_{or} when the oil is in the three-phase condition.

Residual oil saturation (S_{or}) can be expressed as Equation [3-52].

$$S_{or} = F_r S_m(1 - S_m) \quad [3\text{-}52]$$

where,

F_r is a function of the volume of free phase oil, porosity, and oil thickness; it ranges from 0.2 to 0.5.

The upper limitation z_u and lower limitation z_L are determined by the thickness of the contaminated soil. The specific volume of oil in the non-free phase area is calculated as follows:

$$V_{snf} = \phi S_{or} L \quad [3\text{-}53]$$

where,

L = the thickness of contaminated soil (m).

Similarly, the total oil volume in the non-free phase oil area is the integration of the specific oil volume over the whole non-free phase oil area (Equation [3-20]).

$$V_{snf}^{T} = \iint_{A2} V_{snf} dA \quad [3\text{-}54]$$

where,

V_{snf}^{T} = total oil volume in non-free phase area.

3.2.4.4 Total oil volume calculation

The total oil volume in the site is the sum of the oil volume in the free phase oil area and in the non-free phase oil area.

$$V^{T} = \iint_{A1} V_{sfo} dA + \iint_{A2} V_{snf} dA \quad [3\text{-}55]$$

where,

V^{T} = total oil volume in free phase area and non-free phase area.

3.2.5 Volume estimation of free phase oil in stratified soils

3.2.5.1 Specific volume estimation of free phase oil in homogeneous soil

Figure 3.5 shows that the subsurface porous media is assumed to be homogeneous.

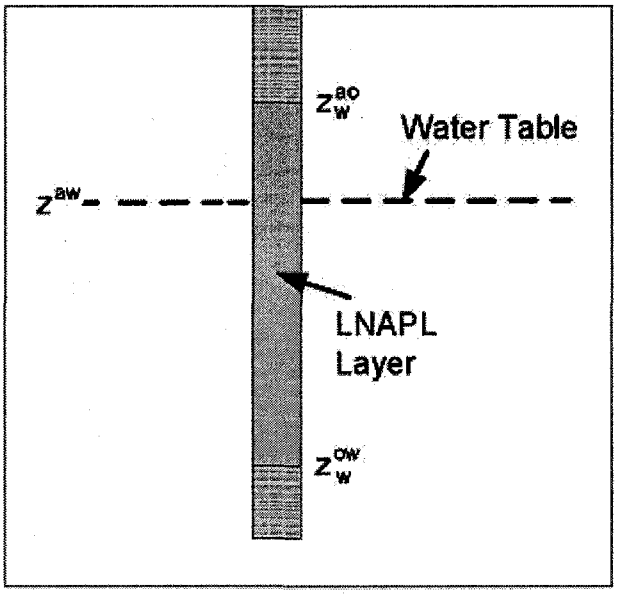

Figure 3.5 The subsurface porous media is assumed to be homogeneous

Vertical equilibrium pressure distribution and the relationships between fluid levels (air-oil and oil-water) in the monitoring well and porous media are built under the condition of hydrostatic equilibrium based on the van Ganuchten (VG) concept (Equations [3-1]-[3-4]).

$$h_{ow} = (1 - \rho_{ro})(z - z_w^{ow}) \quad [3\text{-}56]$$

$$h_{ao} = \rho_{ro}(z - z_w^{ao}) \quad [3\text{-}57]$$

$$z_s^{ow} = z_w^{ow} \quad [3\text{-}58]$$

$$z_s^{ao} = z_w^{ao} \qquad [3\text{-}59]$$

The decision about the distribution of oil saturation is based on three-phase relationships between fluid content and capillary pressures (Lenhard and Parker, 1987), which are the extensions of two-phase relationships of VG concept (Equations [3-40]-[3-43], [3-60]-[3-61]).

$$S^*(h^*) = \left[1 + (\alpha h^*)^n\right]^m \qquad h^* > 0 \qquad [3\text{-}60]$$

$$S^*(h^*) = 1 \qquad h^* \le 0 \qquad [3\text{-}61]$$

The specific volume of free phase oil is obtained by the integration of oil saturation in the soil (Equation [3-62]).

$$V_{sfo} = \int_{z_s}^{z_s^u} \phi S_o dz \qquad [3\text{-}62]$$

where,

V_{sfo} = specific volume in porous media;

z_s^u =elevation where the oil saturation is zero or at the level of the leaked source; it can be expressed as Equation [3-63] (Lenhard and Parker, 1990b).

$$z_s^u = \frac{\beta_{ao}\rho_{ro} z_w^{ao} - \beta_{ow}\left(1-\rho_{ro}\right) z_w^{ow}}{\beta_{ao}\rho_{ro} - \beta_{ow}\left(1-\rho_{ro}\right)} \qquad [3\text{-}63]$$

In this section, the specific volume of free phase oil in homogeneous soil has been obtained. The following gives the specific volume of free phase oil in stratification soils.

3.2.5.2 Estimation of free phase oil in stratified soils

The method developed in Section 3.2.5.1 is based on the assumption that the site is homogeneous. The present section is to extend the method to consider soil layering effects. Figure 3.6 gives one example of soil heterogeneity.

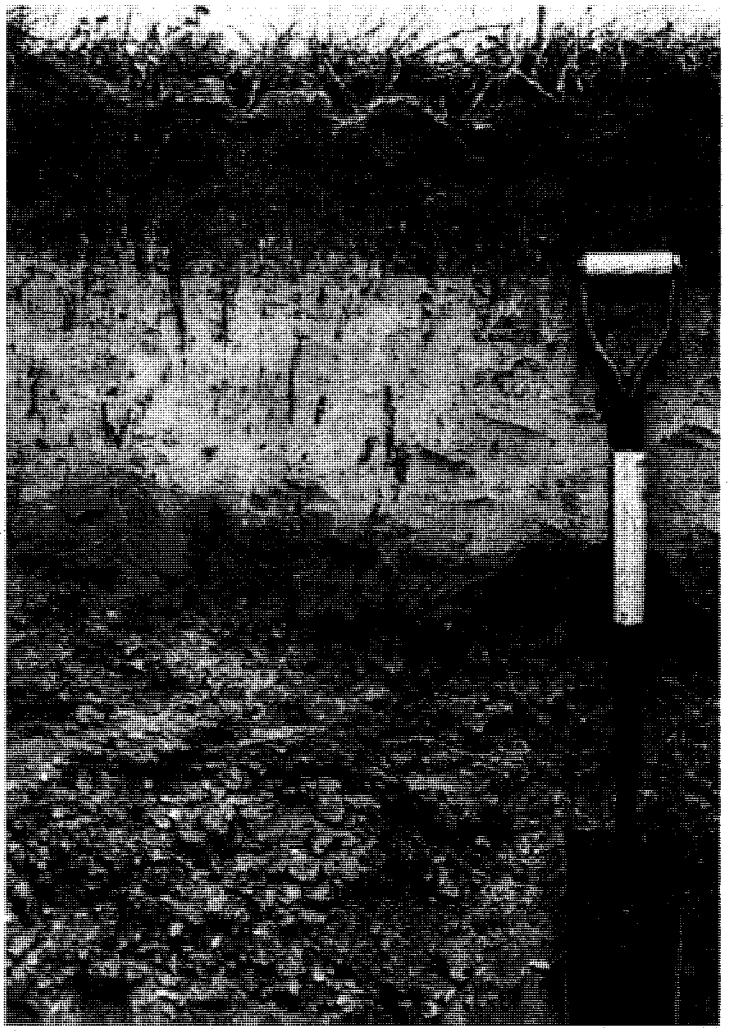

Figure 3.6 Soil heterogeneity (API Interactive LNAPL guide, 2004)

Figure 3.7 shows a monitoring well with an LNAPL layer located between the air-NAPL interface z_{ao} and the NAPL-water interface z_{ow}. The elevation of the water table,

z_{aw}, provides the data for fluid levels. While the water table is not present because of the LNAPL layer, its elevation is easily determined from the elevations z_{ao} and z_{ow}, and the LNAPL density ρ_o. For the example shown in Figure 3.7, the interface between the upper Layer 1 and the lower Layer 2 is at elevation z_{12} located beneath the water table. This interface could be located above, below, or at the water table. The texture characteristics of each layer and the contrast across the interface will strongly influence the resulting LNAPL saturation distribution. Figure 3.7 should be compared with Figure 3.5.

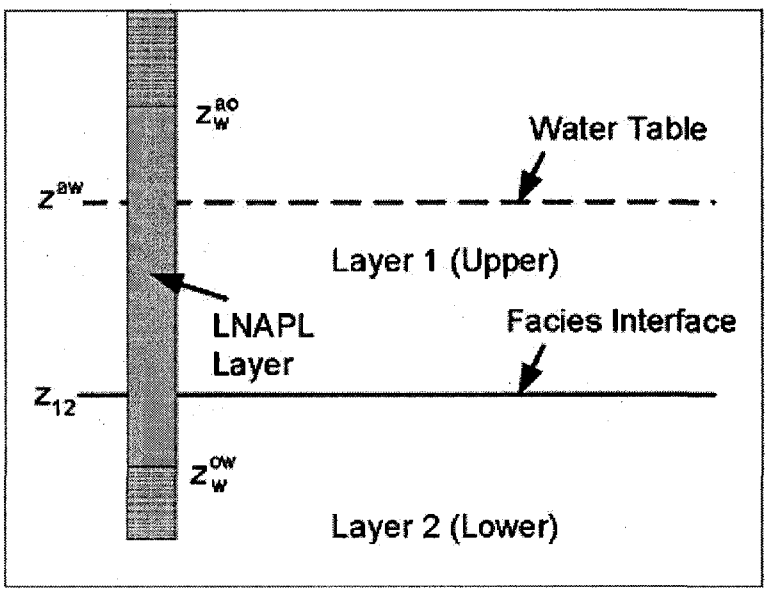

Figure 3.7 The simple heterogeneity in subsurface porous media

For the heterogeneous soil system, the texture characteristics that must be defined for each layer include the porosity *n*, the van Genuchten parameters N and α, the irreducible water saturation s_{wr}, and the residual LNAPL saturation values for the vadose zone and the saturated zone, s_{orv} and s_{ors}. The fluid properties include the LNAPL density ρ_o (it is assumed that the water density is $1 g/cm^3$), and the water and LNAPL surface and interfacial tensions, σ_{aw}, σ_{ao}, and σ_{ow}.

The integration pattern of Equation [3-62] can be analogized to calculate the specific volume of free phase oil in stratified soils (Equation [3-64]).

$$V_{sfo}=\sum_{i=1}^{N}\int_{z_{Lb}}^{z_{ub}}\phi_i S_{oi}\,dz \qquad [3\text{-}64]$$

where,

N= number of soil layers between Z_s^{ow} and Z_s^{u};

ϕ_i = porosity of ith soil layer;

S_{oi} = oil saturation of ith soil layer;

z_{lb} = lower boundary of ith soil layer; z_{lb} should greater than Z_s^{ow}.

z_{ub} = upper boundary of ith soil layer; z_{ub} should less than Z_s^{u}.

For a two-layer soils profile, when soil 1 is underlying soil 2, the Equation [3-13] is simplified to Equation [3-65].

$$V_{sfo}=\int_{Z_s^{ow}}^{Z_s^{l}}\phi_1 S_{o1}dz+\int_{Z_s^{l}}^{Z_s^{u}}\phi_2 S_{o2}dz \qquad [3\text{-}65]$$

where,

Z_s^{l} = elevation of interface between soil 1 and soil 2, it should be situated between z_s^{ow} and z_s^{u}.

ϕ_1, ϕ_2 = porosity of soil 1 and soil2, respectively;

S_{o1}, S_{o2} = oil saturation of soil 1and soil 2, respectively.

3.2.5.3 Total free phase oil volume estimation

The total free phase oil volume in the site is the sum of the specific volume in every node multiplied by the area designated to that node (Equation [3-66]).

$$V_{sfo}^{T} = \sum_{i=1}^{n} \left(V_{sfo} \times A \right)_{i} \qquad [3\text{-}66]$$

where,

A= area designated to node i;

V_{sfo} = specific volume in node i;

n= number of nodes.

3.3 Testing of the proposed modeling approach

This section discusses the proposed modeling through two examples. The first example is based on a single layer soil. The other one is based on stratified soils. The effects of soil layering on the specific volume in porous media are discussed.

3.3.1 Case 1

This case deals with single-layer soil. The input data are adapted from Lenhard and Parker (1990a). The LNAPL specific volumes are predicted as a function of well hydrocarbon thickness. Hydrocarbon specific volumes are estimated by the developed model and compared with the literature data.

For a single-layer condition, outcomes based on the van Genuthten (VG) model are expected to be the same as reported in the literature (i.e. Lenhard and Parker, (1990a)). Particularly, the VG model parameter α_{ao} is given as in Equation [3-67] (Farr et al., 1990).

$$\alpha_{ao} = \alpha \times \beta_{ao} \qquad [3\text{-}67]$$

where, α_{ao}=VG model parameter (air-oil); α is VG model parameter (m^{-1}); β_{ao} is the scaling factor. Both of them are used in the method of Lenhard and Parker (1990a). α_{ao} is an input parameter in the method of Farr et al (1990), which depends on the properties of soil and fluid. Farr et al. (1990) had a misconception about α_{ao}. They thought α_{ao} depends only on the property of the soil.

Two types of soil are chosen to compare the results reported in Farr et al. (1990) with those reported by Lenhard and Parker (1990a), respectively. The input and output data are shown in Tables 3.1 and 3.2.

Table 3.1 Input data from Lenhard and Parker (1990a)

			van Genuchten parameter	
Soil types	Porosity	Irreducible water saturation S_m	n	α (m^{-1})
Soil 1	0.43	0.13	2.434	0.027
Soil 2	0.43	0.58	1.645	0.185
Fluid Properties	Density ratio, ρ_{ro}		0.73	
	Air-oil scaling factor		3.20	
	Oil-water scaling factor		1.45	

Table 3.2 Comparison of specific volume with VG model

Predicted LNAPL specific volumes from well hydrocarbon thickness			
Well hydrocarbon thickness (cm)		Specific volumes(cm^3/cm^2)	
		(literature)	VG(predicts)
Soil 1	30	0.2	0.08
	60	1.6	0.32
	100	6.7	5.7
	150	17.2	16.7
	200	30.3	30.0
	250	45	44.5
	300	60.7	59.7
Soil 2	30	1.5	1.3
	60	4.7	4.8
	100	9.9	10.0
	150	17	16.9
	200	24.5	24.3
	250	32.2	32.0
	300	40	39.7

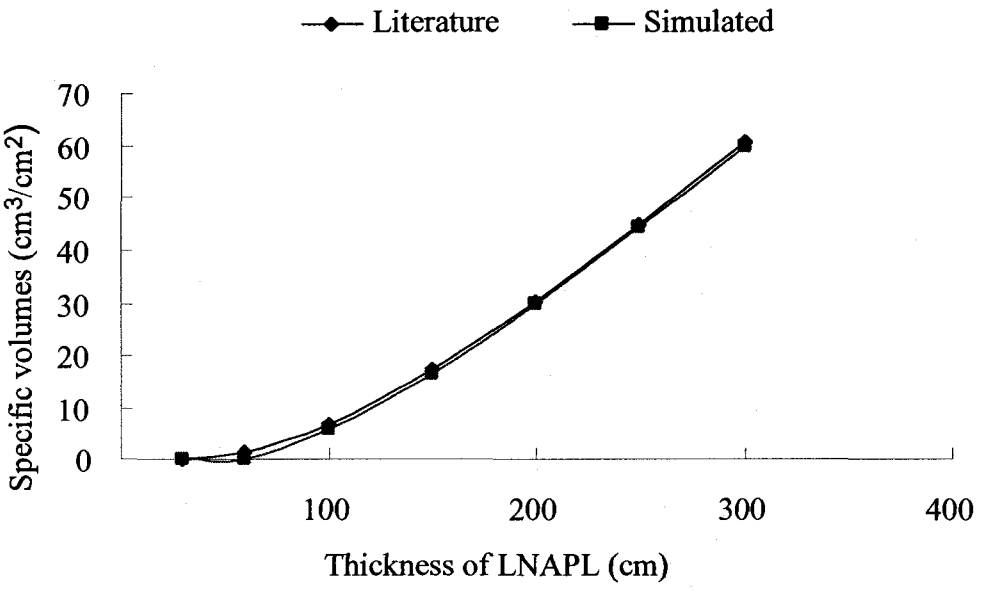

Figure 3.8 Comparison of LNAPL specific volumes with VG model results for soil 1 (Literature-Lenhard and Parker (1990a))

In Figure 3.8, series 1 is literature data in soil 1. Series 2 is the simulation outputs data with VG parameters for soil 1. Figure 3.8 shows that the simulation results are the same between this case study and Lenhard and Parker (1990a) with the soil 1 condition.

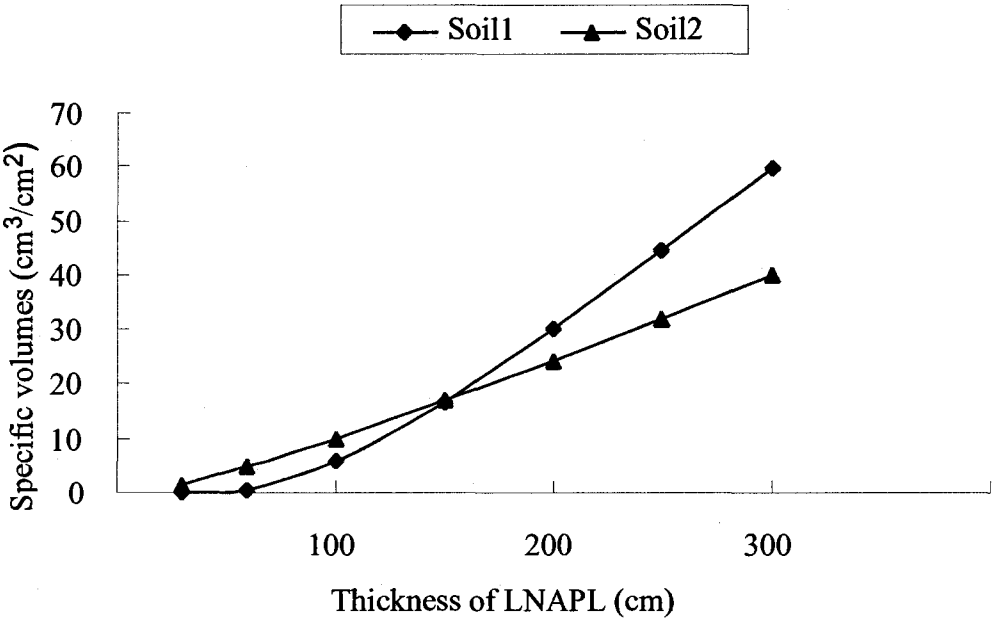

Figure 3.9 Comparison of LNAPL specific volumes with VG model results for soils 1 and 2

Figure 3.9 shows the different results of specific volumes obtained for soil 1 and soil 2. It clearly indicates that the soil layering effects will influence the results. Therefore, it is important to consider soil layering effects in the estimation of the volume of an LNAPL.

3.3.2 Case 2

(A) Description of the example case with a testing run

The same example with information given in Table 3.1 is used here. However, soil 1 is below soil 2 as shown in Figure 3.10. The thickness of soil 1 is 0.838 m and that of soil 2 is 0.864 m.

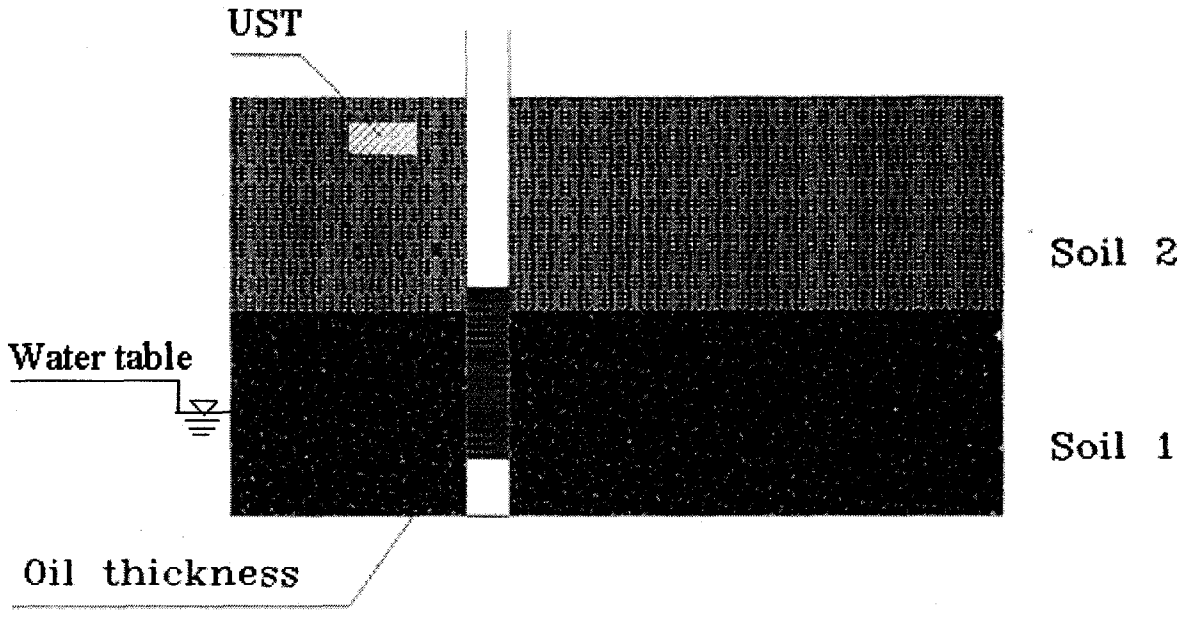

Figure 3.10 Site conditions and monitoring wells in the study domain

The site parameters include geological properties and porous medium properties. They include water dynamic viscosity, water density, water surface tension, average recharge rate, water saturation, air entry head, residential water saturation, van Genuchten's α, van Genuchten's n, etc. The porous medium properties include hydraulic conductivity in three dimensions, the ratio of horizontal to vertical hydraulic conductivity, porosity, bulk density, surface ground elevation, groundwater elevation, groundwater gradient and direction. The data used in this hydrological study are given in Table 3.3.

Table 3.3 Input data for hypothetical case

Soil parameters			Fluid parameters	
	Soil 1	Soil 2		
Porosity	0.33	0.3	Density ratio	0.867
S_m	0.25	0.25	β_{ao}	1.655
n	4.3	5.0	β_{ow}	2.526
α	2.5 m^{-1}	4.0 m^{-1}		

Note: the parameters of soil 1, soil 2 and fluid are adapted from Sleep et al. (2000).

where,

n, α is the van Genuchten parameters n and α; β_{ao} is air–oil scaling factor; and β_{ow} is oil-water scaling factor.

The model is run using the input data given in Table 3.3. Table 3.4 gives the modeling results for a two-layer soil system compared to literature results. Specifically, for the same site condition, Sleep et al. (2000) and Lenhard and Parker (1990a) reported with a specific oil volume of 9.7×10^{-3} and 1.11×10^{-2} m^3/m^2, respectively, considering soil layering effect, the proposal method gives 1.38×10^{-2} m^3/m^2 just for soil 1 and 2.87×10^{-2} m^3/m^2 for the two-layer system.

Table 3.4 Comparison of specific volume

	Specific volume (m^3/m^2)		
Conditions	Sleep et al. (2000)	Lenhard and Parker (1990a)	Stratified method
Water level is 0.04m; apparent thickness of oil is 0.8 m	9.7×10^{-3}	1.11×10^{-2}	#1.38×10^{-2} 2.87×10^{-2}

No stratification is considered, entire soil is soil 1.

Sleep et al. (2000) obtained the results based on the parameters of soil 1 in Table 3.3. When the effect of soil layering is considered, the specific volume in porous media is larger than the results based on homogeneous soil.

(B) Further comparison analyses

The following scenarios are designed to apply the developed method to estimate the oil in the stratified soils.

- Scenario 1: only soil 1 is considered (Figure 3.11);
- Scenario 2: only soil 2 is considered (Figure 3.12);
- Scenario 3: both soil 1 and soil 2 are considered; soil 1 is located above soil 2 (Figure 3.13);
- Scenario 4: both soil 1 and soil 2 are considered; soil 1 is located below soil 2 (Figure 3.14).

The basic parameters for soil 1, soil 2, fluid and fluid levels in the monitoring well are enumerated in Table 3.5.

Table 3.5 Input data for hypothetical case study

Soil parameters			Fluid parameters	
	Soil 1	Soil 2		
Porosity	0.43	0.43	Density ratio	0.73
Sm	0.13	0.58	βao	3.2
n	2.434	1.645	βow	1.45
alpha	2.7 m-1	18.5 m-1		
Z_w^{ow} in the monitoring well is 87.0 m (assuming surface level is 100.0 m)				
Z_w^{ao} in the monitoring well is 90.0 m				

Source: the parameters of soil 1, soil 2 and fluid are modified from Lenhard and Parker (1990a).

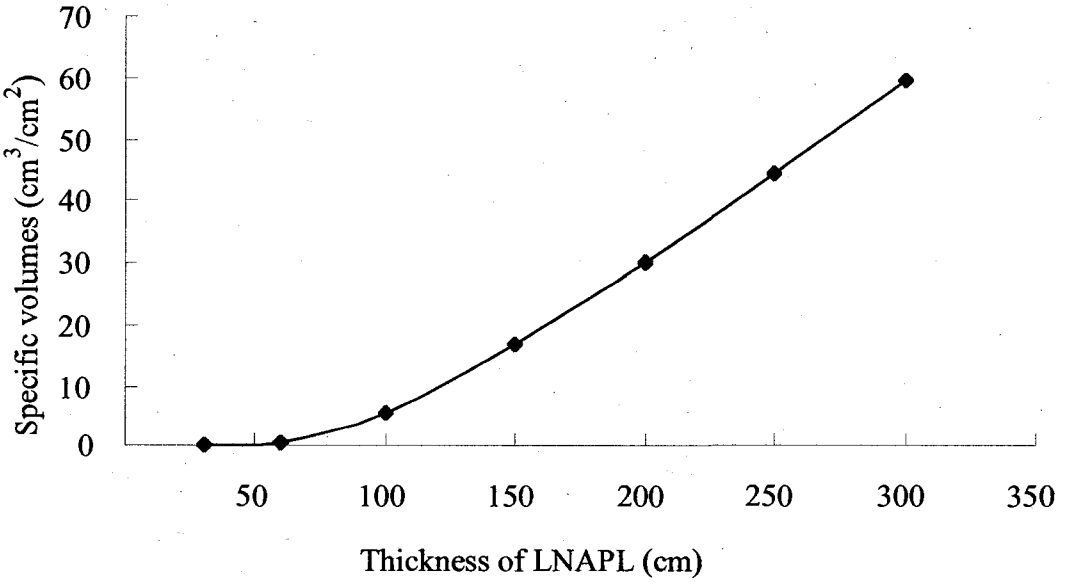

Figure 3.11 LNAPL specific volumes in soil 1

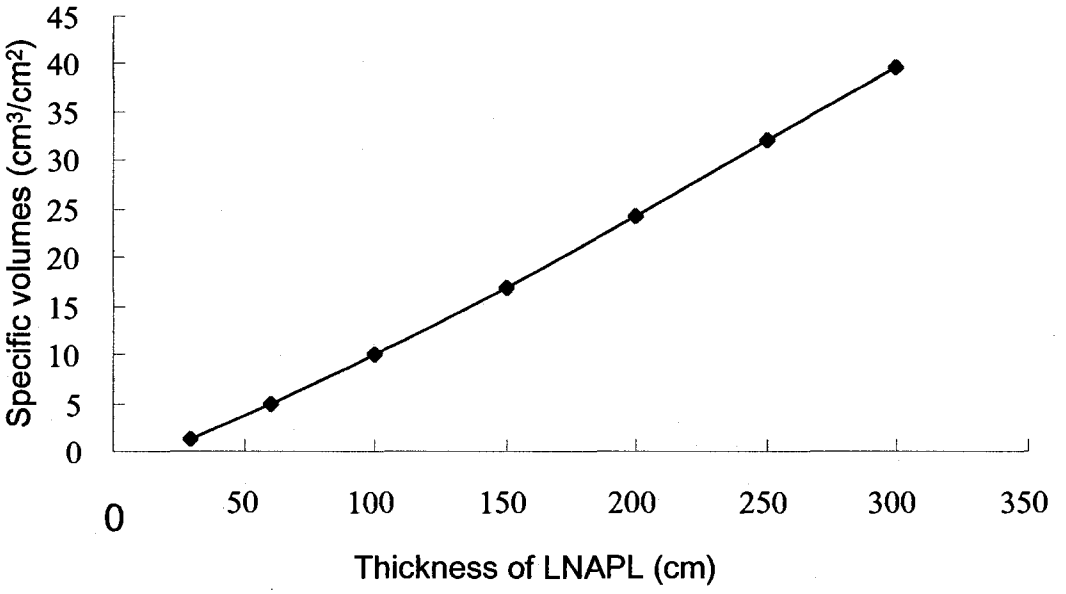

Figure 3.12 LNAPL specific volumes in soil 2

For scenarios 1 and 2, the soil compositions are actually homogeneous. Figures 3.11 and 3.12 show the specific volume in soils 1 and 2 according to different thickness of LNAPL in a well. The thickness of the LNAPL in the well is 3m. The results are V_{sfo} = 0.6069 m^3/m^2 for soil 1 and V_{sfo} = 0.4005 m^3/m^2 for soil 2, values which agree with the calculations made by Lenhard and Parker (1990a).

Under the conditions of scenarios 3 and 4, the specific oil volumes in porous media will vary with the elevations of the interface between soil 1 and soil 2 under the same apparent oil thickness in the monitoring well (Figures 3.13 and 3.14).

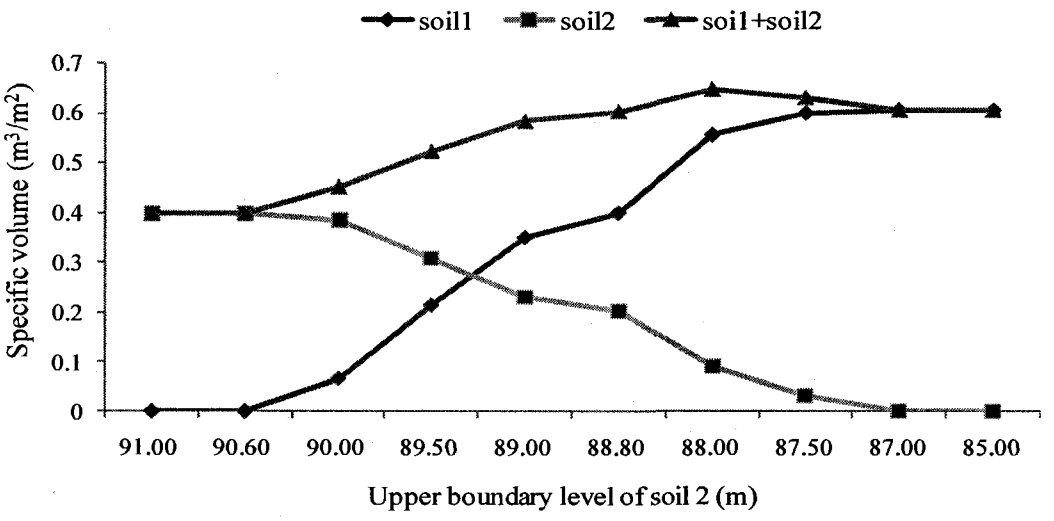

Figure 3.13 Specific volumes with soil 1 above soil 2

Figure 3.13 shows the specific volume with the variable elevation of the interface between soil 1 and soil 2. In this case, soil 1 is located above soil 2. The x-axis is the elevation of the interface of soil 1 and soil 2. Series 1 is the specific volume of soil 1 with the different level between soil 1 and soil 2. Series 2 is the specific volume of soil 2 with the different level between soil 1 and soil 2. Series 3 is the total specific volume of soil 1 and soil 2 with the different level between soil 1 and soil 2. It illustrates the fact that soil layering influences specific volume significantly. In this case, the maximum specific volume occurs at 87.8m; and it exceeds the range of only the soil 1 or soil 2.

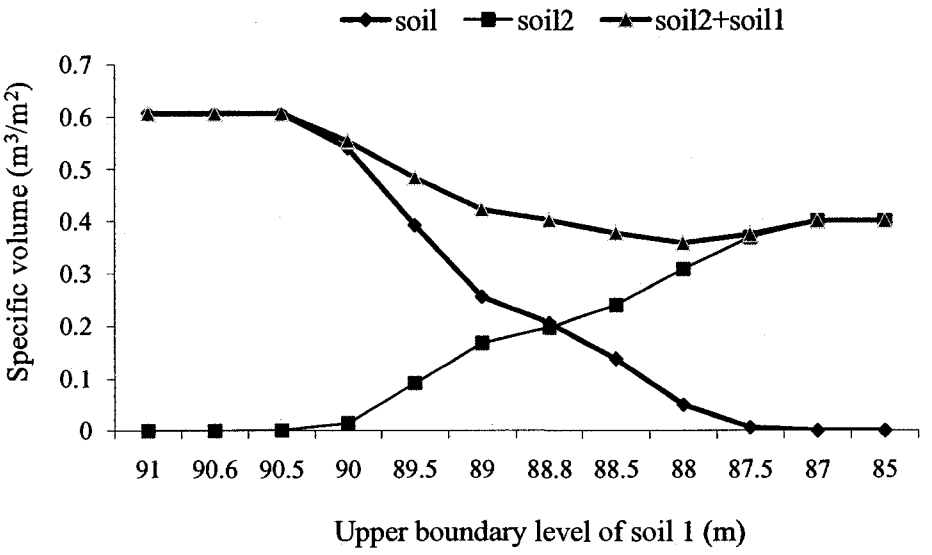

Figure 3.14 Specific volumes with soil 1 below soil 2

In this case, soil 2 is located above soil 1. Figure 3.14 shows the specific volume with the variable elevation of the interface between soil 1 and soil 2. The three series 1, 2, 3 are individual illustrations of specific volume with the different boundary level under the condition of soil 1, soil 2 and soil 1 + soil 2. The maximum specific volume occurs at 91m; and it exceeds the range of only the soil 1 or soil 2.

Given the identical apparent oil thickness in the monitoring well and depth of the interface of soils, the ordering of soils will affect the varied specific oil volume in porous media. For example, when the elevation of the interface of soils is 89.5 m, the specific oil volume is 0.524 m for soil 1 above soil 2 and 0.484 for soil 1 below soil 2.

3.3.3 Summary

The developed modeling method has been examined through a set of case studies. By applying the developed modeling method to two complete cases, the systematic operation and all the functions of the modeling are demonstrated and tested. A pilot-scale experiment is designed in Chapter 4 to finally validate the developed model.

Using the results from the case studies, a system to calculate total volume for sites of multi-type soils is developed. The effects of soil layering on specific oil volume in the porous media are discussed. Whereas it is only a system of two-layer soils, the results indicate the significance of the influence of the effects of stratified soils on the specific volume of free phase oil in the porous media. The specific oil volume in a two-layer porous media would extend the scope of specific oil volume, which is obtained assuming only one kind of soil is present under certain conditions.

After the thorough analysis of two cases, the values of the free phase LNAPL volume have been obtained. The result could serve as an important basis for considering the design of efficient remediation programs. The following conclusions are drawn:

1) The volume of free phase LNAPL in the subsurface of petroleum contaminated sites is highly sensitive to in-situ soil properties. Under different soil characteristics, the volumes could vary substantially even with the same observed oil thickness in monitoring wells.

2) The distribution of free phase LNAPL in the subsurface is related to site

conditions. Due to the heterogeneous characteristics of porous media in most sites, the distribution could be very different. Sequentially, the estimated volume of the free product will also be highly variable.

3) In addition to soil properties, the contaminant release history and fluid properties are other important factors affecting the estimation of the oil volume. The fluid properties such as density and viscosity partially decide the retention ability of a free phase LNAPL in the subsurface.

4) The estimation of free phase contaminants in petroleum contaminants is an important step before any remediation programs are designed. The results from this case study could help in the design of a cost-effective enhanced oil recovery (EOR) scheme for this site. In addition, the result can be incorporated into further sophisticated multi-phase, multi-component modeling of the subsurface contamination for the purpose of risk assessment.

In order to test the performance of the modeling method, the model has been applied to a pilot-scale experiment to validate this system. This application is achieved by comparing the observed data and the calculated results.

Chapter 4

Model validation through a pilot-scale experiment

4.1 A pilot-scale experiment

In this chapter, a pilot-scale oil-spill experiment is established and set up to validate the model developed.

4.1.1 Materials and method

The experiments were conducted is a customized 0.50m x 0.50m and 0.30m deep, open-top plastic tank with a drainage hole (Figure 4.3).

The tank was filled to a depth of 0.29m with fairly uniform washed silica sand. The particle size ranged from 0.1mm to 2mm in diameter.

The wells were developed using plastic pipe (ABS). The diameter of the pipe is 20mm. Altogether, using the stainless-steel made well screens. The hole of the well screen is 1x1 mm. The well is shown in Figure 4.1.

The LNAPL used in this experiment was lubricating oil (engine oil), which was chosen because it represents typical spilled oil and is relatively safety.

4.1.2 System set up and experiment

Many gaps were made by sawing the pipes to produce the wells. The distance between the gaps was 0.5cm. The wells were wrapped with stainless-steel well screens, each well extending to the bottom of the tank, were installed (Figure 4.1). The screens were used to prevent the sands from entering the wells.

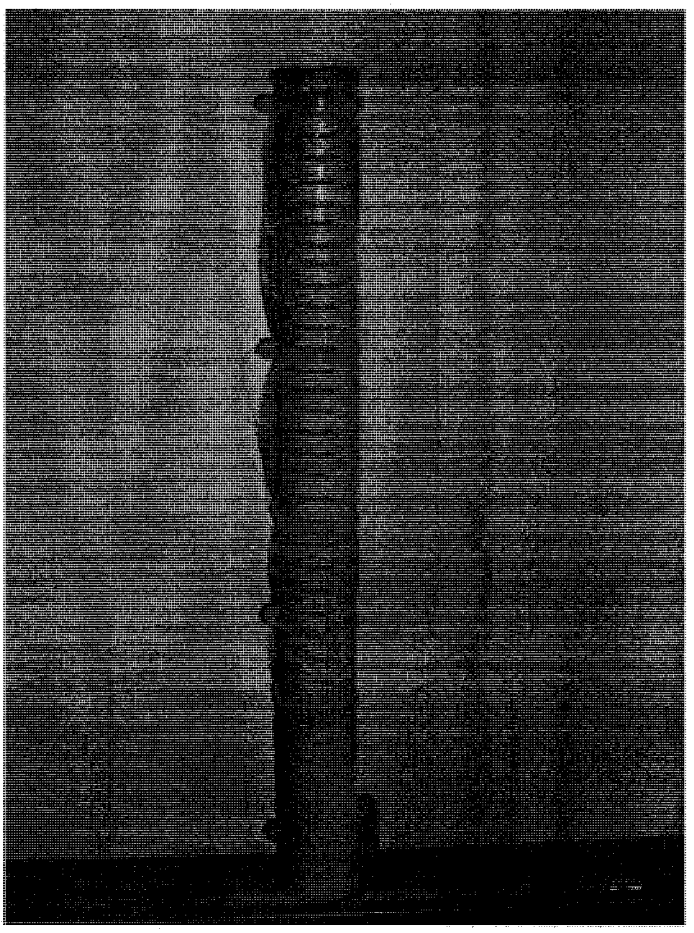

Figure 4.1 Picture of well that was wrapped with well screen

This system includes 12 wells. Four wells (wells 1-4) were located 10cm from the center of the tank (Figure 4.2). Another four wells (wells 5-8) were located 20cm from the center of the tank (Figure 4.2). The third four wells (wells 9-12) were located 25cm from the centre of the tank (Figure 4.2).

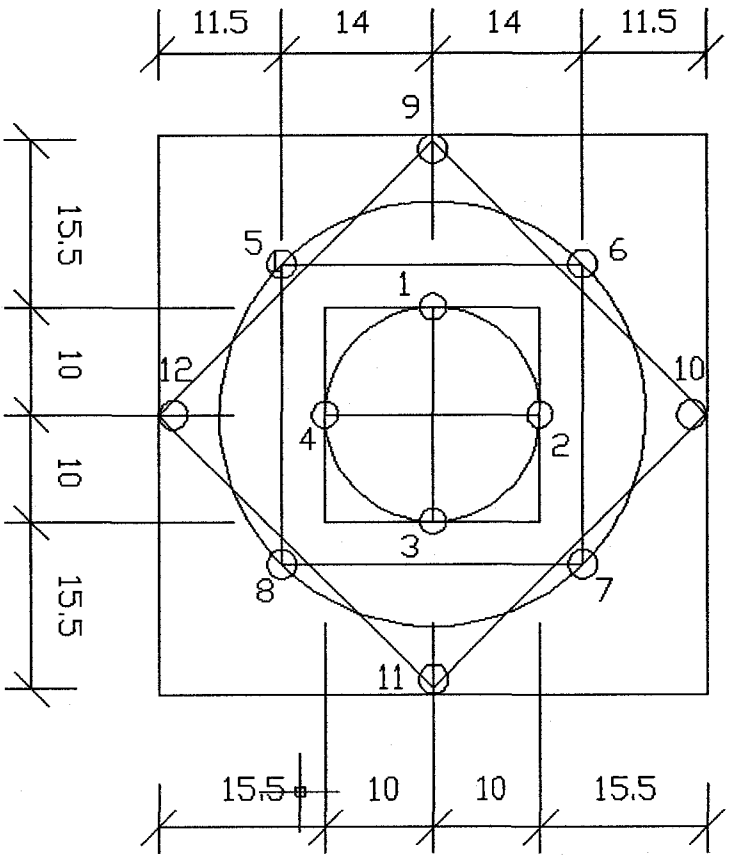

Figure 4.2 Layout of wells in tank

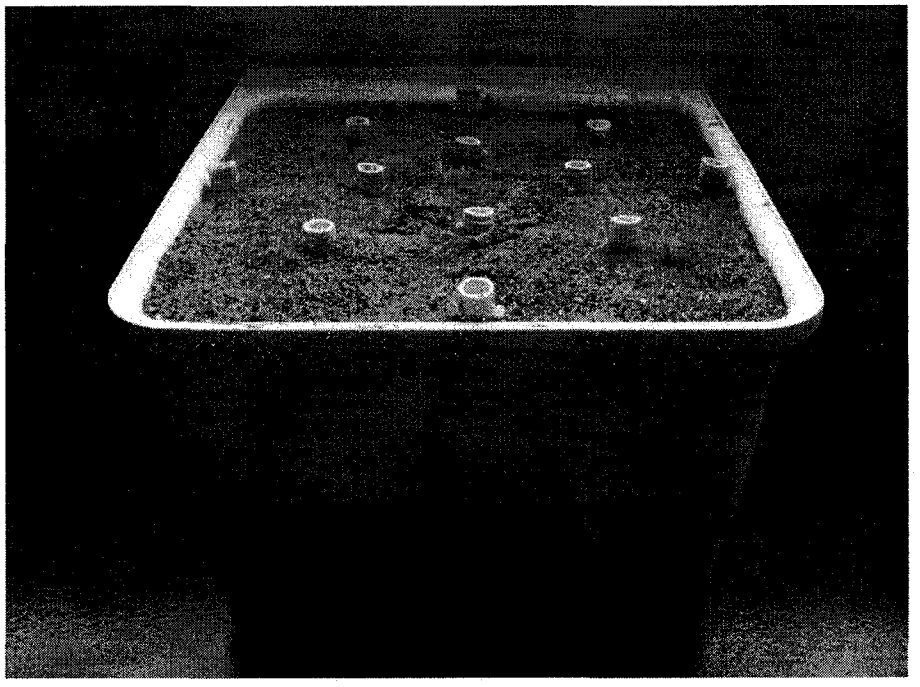

Figure 4.3 Picture of tank with wells and sand

The experimental validation process is shown in Figure 4.4.

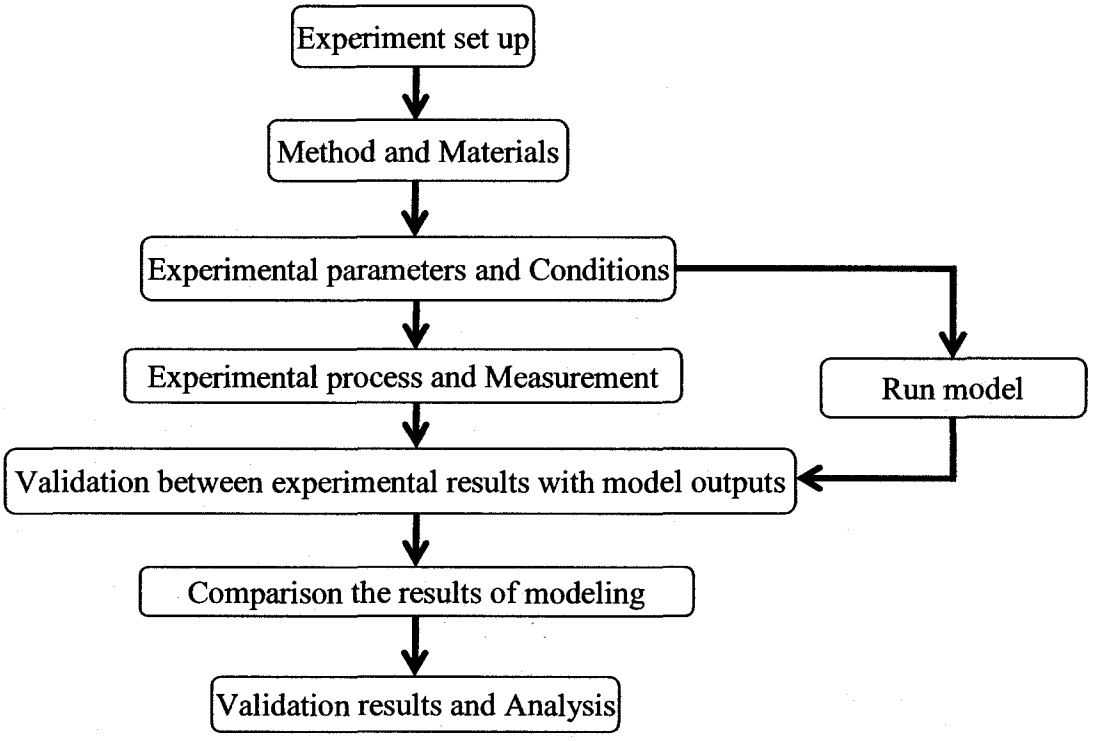

Figure 4.4 The experimental validation process flow chart

4.1.3 Preparation and analysis of data

Interfacial tension is the force of attraction between molecules at the interface of a liquid. These tensions are essential for calculating the spreading rates and the likely extent to which the oil will form oil-in-water and water-in-oil emulsions. The interfacial tensions of crude oils and oil products are dependent on the temperature and degree of weathering. The following tension values are at "0% Weathering Volume" - in other words, fresh oil.

Table 4.1 Surface tension and interfacial tension

Air-Oil (mN/M or dynes/cm)		
Temperature	Surface Tension (mN/m or dynes/cm)	
0	33.1	ESD 96
15	32.0	ESD 96
Oil-Seawater (mN/M or dynes/cm):		
Temperature	Oil-Seawater (mN/M or dynes/cm):	
0	6.4	ESD 96
15	NA	ESD 96
Oil-Water (mN/M or dynes/cm):		
Temperature	Oil-Water (mN/M or dynes/cm):	
0	10.5	ESD 96
15	7.1	ESD 96

Source: ESD 96, Lubricating Oil (Industrial, Teresso 150)

Table 4.2 Representative van Genuchten model parameters

Soil type	Saturated Water Content, q_m		Residual Water Content, q_{wr}		van Genuchten n		van Genuchten α (ft^{-1})	
	mean	std. dev.	mean	std. dev.	mean	std. dev.	mean	std. dev.
Sand	0.43	0.06	0.045	0.010	2.68	0.29	4.4	0.88

Source: After Carsell and Parish (1988)

Density, which refers to the mass per unit volume of a substance, is often presented as specific gravity (the ratio of a substance's density to that of some standard substance, usually water). The densities of petroleum hydrocarbons typically found in USTs are less than 1.0 and typically range from 0.75 g/ml to as high as 0.99 g/ml. Density varies as a function of several parameters, most notably temperature; however, in most subsurface

environments the temperature (and hence the density) remains relatively constant. The densities of some common petroleum hydrocarbons are presented in Table 4.1.

Table 4.3 Representative LNAPL density values (g/cm^3)

Fluid Type	Temp. 0 °C	Temp. 15 °C	Temp. 20 °C	Temp. 25 °C
Electrical Lubricating Oil	0.882	0.974	NA	NA
Electrical Lubricating Oil – used	0.883	0.874	NA	NA

Source: Charbeneau et al. (1999)

Residual saturation refers to the saturation level at which a continuous mass of petroleum hydrocarbons (NAPL) becomes discontinuous and immobilized by capillary forces (Newell et al., 1995). Residual saturation is important to free product recovery because it represents the amount of petroleum that cannot be recovered by pumping or gravity drainage.

Table 4.4 Representative residual saturation values

Soil Type	Residual Saturation, S_{wr}	Bubbling Pressure Head, Ψ_b (m)*	Porous Size Distribution Index, λ
Sand	0.10 (0.023)	0.069 (0.014)	1.68 (0.29)

Source: Charbeneau et al. (1999)

Table 4.5 Total porosity

Soil/ Rock Type	Minimum	Maximum	Midpoint
Sand	0.242	0.49	0.366

Source: Charbeneau et al. (1999)

4.2 Experiment results and comparison with modeling outputs

4.2.1 Experiment results

The lubricating oil was spilled in the centre of the tank as shown in Figure 4.5. The tank was filled with water to 14cm from the bottom (water table). The quantity of oil added was 150ml each time until the oil thickness did not change. A condition of equilibrium is reached if the oil thickness result is the same the last three times.

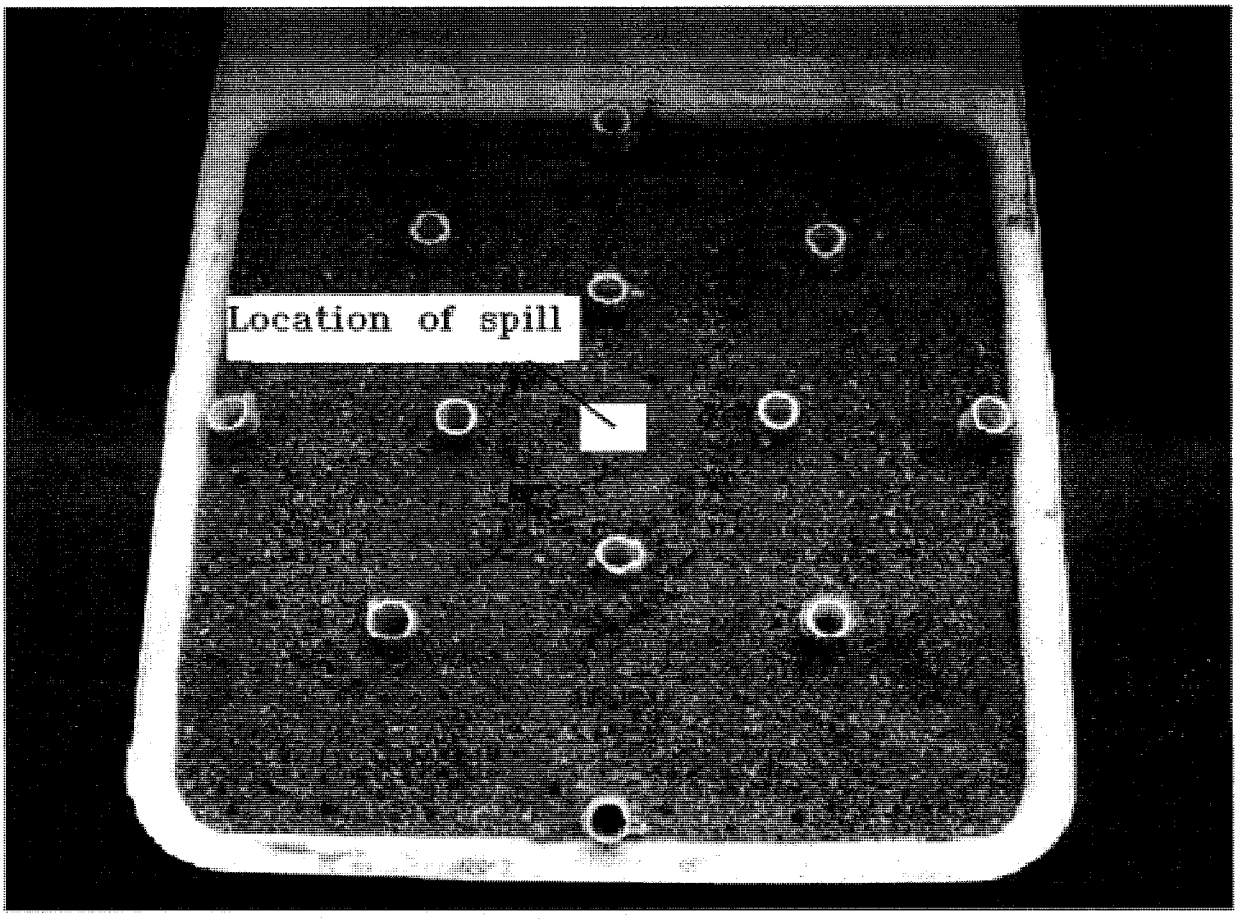

Figure 4.5 Location of oil spill

Data sheet of experiment

No.	Depth type	Added Volume (ml)	Total Volume (ml)	Date	Measuring time	Depth (mm) Well No. 1	2	3	4	5	6	7	8	9	10	11	12
1	Oil level																
	Water level																
2	Oil level																
	Water level																
3	Oil level																
	Water level																
4	Oil level																
	Water level																
5	Oil level																
	Water level																
6	Oil level																
	Water level																
7	Oil level																
	Water level																
8	Oil level																
	Water level																
9	Oil level																
	Water level																
Note: Each measurement was recorded when three readings were the same at equilibrium.																	

Figure 4.6 shows the distribution of the LNAPL thickness in the tank.

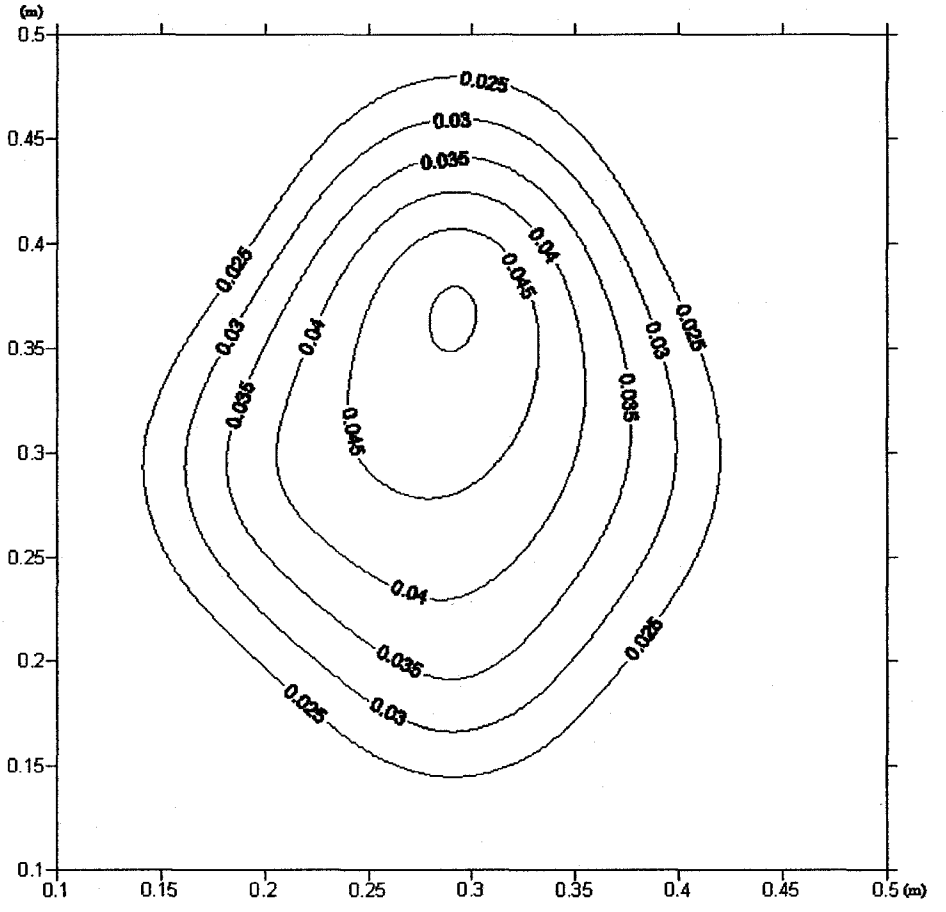

Figure 4.6 LNAPL thickness contour with a 600ml spill in the tank (0.5 x 0.5m)

4.2.2 Modeling and experimental results

In this section, both VG- and BC-based modeling methods were used to predict the total oil volume for the 600ml and 750ml spill scenarios.

4.2.2.1 Computational mesh

First, the computational mesh of modeling is built based on the experimental pilot setup.

Because the size of the tank was 50 x 50cm, we divided it into 10 x 10cm space. Each mesh was 5 x 5cm. All the wells were located as shown in Figure 4.7.

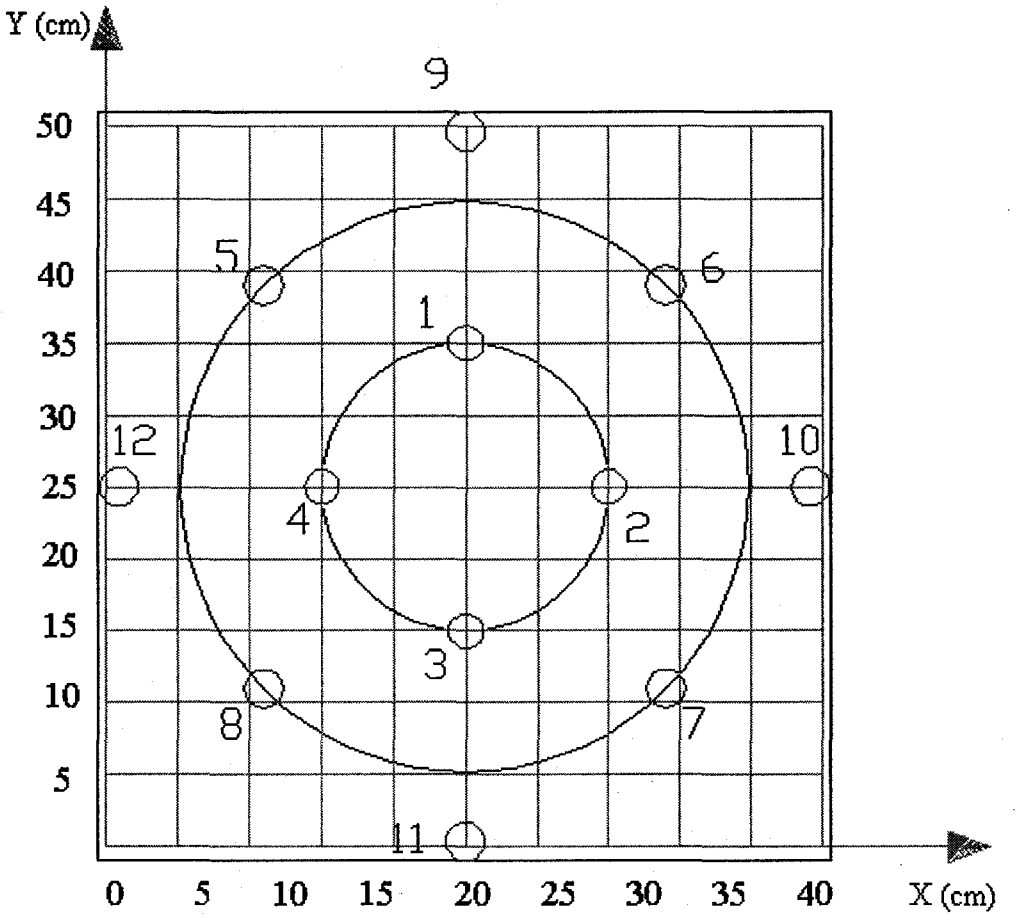

Figure 4.7 Setup of computational meshes

The axis of x, y of the wells is shown in Table 4.7. These coordinate data will be input into the modeling system.

Table 4.6 Location of wells in computational mesh

Well	MW1	MW2	MW3	MW4	MW5	MW6
Location (x,y) cm	25, 35	35, 25	25, 15	15, 25	10, 40	40, 40
Well	MW7	MW8	MW9	MW10	MW11	MW12
Location (x,y) cm	40, 10	10, 10	25, 50	50, 25	25, 0	0, 25

4.2.2.2 Results of VG-based model for a 600ml spill

Based on Section 4.1.3, experimental data were prepared for a VG model. The specific volume and total volume were obtained through the modeling system.

The model, as described in Chapter 3, was run for an experimental oil spill of 600ml. The results of VG modeling give 571.7 ml. The difference may come from:

1) The measurement of the level of oil and water

2) The measurement of porosity

3) Change of the oil surface tension under different room temperature

4) Numerical calculation such as the interpolation

Table 4.7 gives the parameters used in the VG model. The parameters include porosity, residual saturation, VG parameter, density ratio, air-oil scaling factor and oil-water scaling factor.

Table 4.7 Parameters for VG model

			van Genuchten parameter	
Soil types	Porosity	Irreducible water residual saturation S_m	n	α (m^{-1})
Sand	0.334	0.01	2.97	17.33
Fluid	Density ratio, ρ_{ro}		0.86	
Properties	Air-oil scaling factor		10.394	
	Oil-water scaling factor		2.275	

Table 4.8 gives the experimental data including the oil level and water level of the wells. It shows the locations of the observed well and the experimental data for a 600ml spill.

Table 4.8 Wells data input for 600ml spill

	X (m)	Y (m)	Oil level (m)	Water level (m)
MW1	0.25	0.35	0.155	0.213
MW2	0.35	0.25	0.163	0.195
MW3	0.25	0.15	0.158	0.196
MW4	0.15	0.25	0.156	0.197
MW5	0.1	0.4	0.190	0.190
MW6	0.4	0.4	0.190	0.190
MW7	0.4	0.1	0.190	0.190
MW8	0.1	0.1	0.190	0.190

Table 4.9 shows the modeling outputs for the specific volume for a 600ml spill. MW 1~8 wells are the observation wells. Table 4.9 shows that different specific volumes are obtained for different wells and oil thicknesses in wells.

Table 4.9 Specific volume of observed well for 600ml spill based on VG modeling (m^3/m^2)

	X (m)	Y (m)	Oil level (m)	Water level (m)	Oil thickness (m)	Specific volume(m^3/m^2)
MW1	0.25	0.35	0.155	0.213	0.058	0. 0125827
MW2	0.35	0.25	0.163	0.195	0.032	0.00537560
MW3	0.25	0.15	0.158	0.196	0.038	0.00672632
MW4	0.15	0.25	0.156	0.197	0.041	0.00765514
MW5	0.1	0.4	0.190	0.190	0	0
MW6	0.4	0.4	0.190	0.190	0	0
MW7	0.4	0.1	0.190	0.190	0	0
MW8	0.1	0.1	0.190	0.190	0	0

The generation of the contour in Figure 4.8 is based on the results of modeling for a 600ml spill. The results of the modeling system have the specific volume at every location of the computation mesh in the tank. Then, the software Surfer is used to produce the contour of the oil specific volume. Figure 4.8 shows the distribution of oil specific volume for a 600ml spill in the tank.

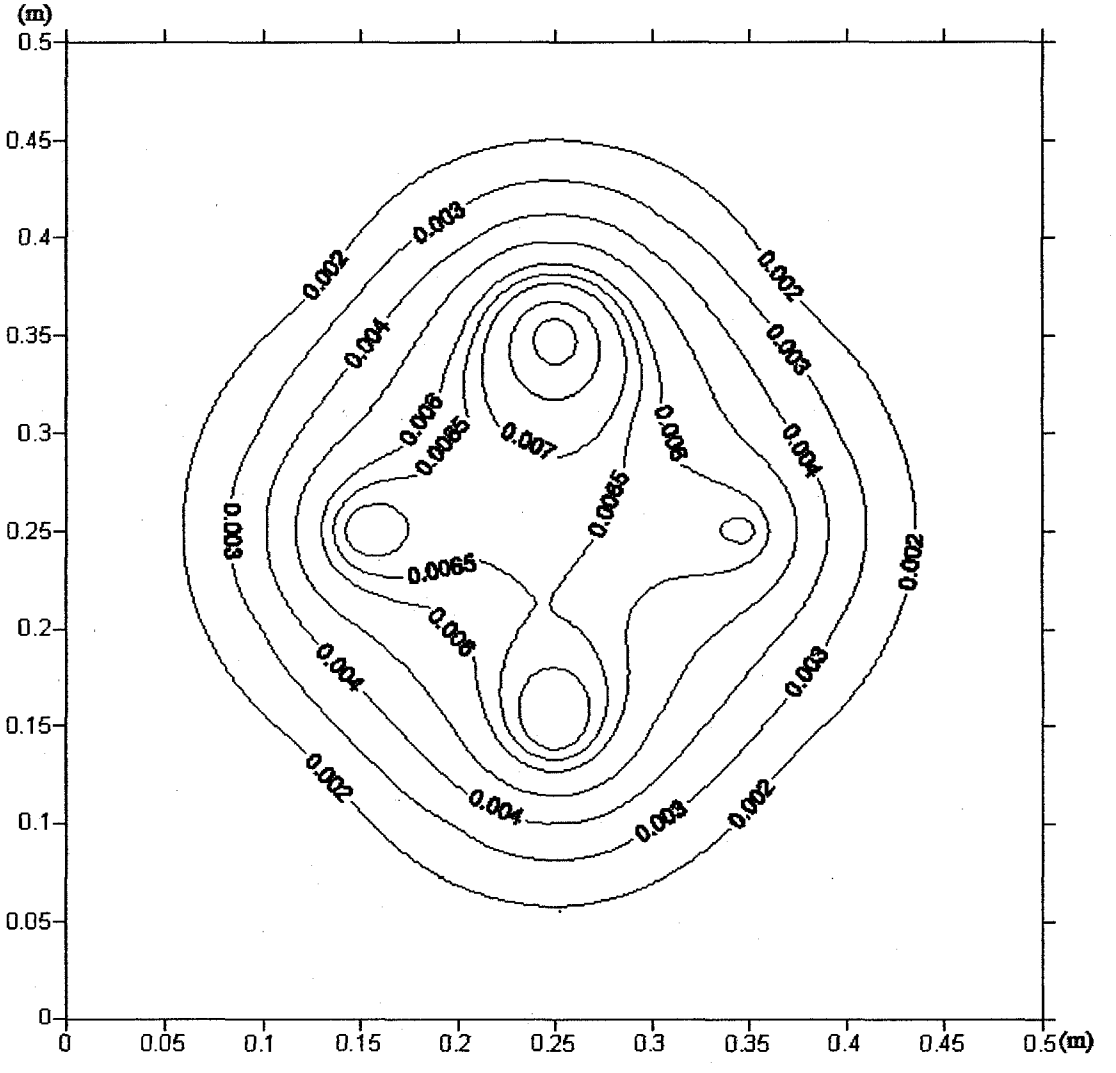

Figure 4.8 LNAPL specific volume contour of VG model for a 600ml spill

4.2.2.3 Results of VG-based model for a 750ml spill

Based on Section 4.1.3, experimental data were prepared for a VG model. The specific volume and total volume for 750ml spill were obtained through the modeling system.

The model was run for an experimental oil spill of 750ml. The results of VG modeling give 704.2ml. The input data are shown in Tables 4.7, 4.10.

Table 4.10 gives the experimental data including the oil level and the water level of the wells. It shows the locations of the observed well and the experimental data for a 750ml spill.

Table 4.10 Wells data input for a 750ml spill

	X (m)	Y (m)	Oil level (m)	Water level (m)
MW1	0.25	0.35	0.209	0.268
MW2	0.35	0.25	0.195	0.236
MW3	0.25	0.15	0.200	0.248
MW4	0.15	0.25	0.205	0.252
MW5	0.1	0.4	0.223	0.234
MW6	0.4	0.4	0.224	0.231
MW7	0.4	0.1	0.25	0.25
MW8	0.1	0.1	0.25	0.25
MW9	0.25	0.5	0.196	0.204
MW10	0.5	0.25	0.25	0.25
MW11	0.25	0	0.25	0.25
MW12	0	0.25	0.25	0.25

Table 4.11 shows the modeling outputs for a 750ml spill. MW 1~12 wells are the observation wells. Table 4.11 shows that different specific volumes were obtained for different wells and oil thickness in wells.

Table 4.11 Specific volume of an observed well for a 750ml spill based on VG model (m^3/m^2)

	X (m)	Y (m)	Oil level (m)	Water level (m)	Oil thickness (m)	Specific volume (m^3/m^2)
MW1	0.25	0.35	0.209	0.268	0.059	0.0128416
MW2	0.35	0.25	0.195	0.236	0.041	0.0076504
MW3	0.25	0.15	0.200	0.248	0.048	0.0094997
MW4	0.15	0.25	0.205	0.252	0.047	0.0095341
MW5	0.1	0.4	0.223	0.234	0.011	0.0004826
MW6	0.4	0.4	0.224	0.231	0.007	0.0000927
MW7	0.4	0.1	0.25	0.25	0	0
MW8	0.1	0.1	0.25	0.25	0	0
MW9	0.25	0.5	0.196	0.204	0.008	0.0016688
MW10	0.5	0.25	0.25	0.25	0	0
MW11	0.25	0	0.25	0.25	0	0
MW12	0	0.25	0.25	0.25	0	0

The generation of the contour in Figure 4.9 is based on the results of the modeling for a 750ml spill. The results of the modeling system have the specific volume at every location of the computation mesh in the tank. Then, the software-Surfer was used to produce the contour of oil specific volume. Figure 4.9 shows the distribution of oil specific volume for a 750ml spill in the tank.

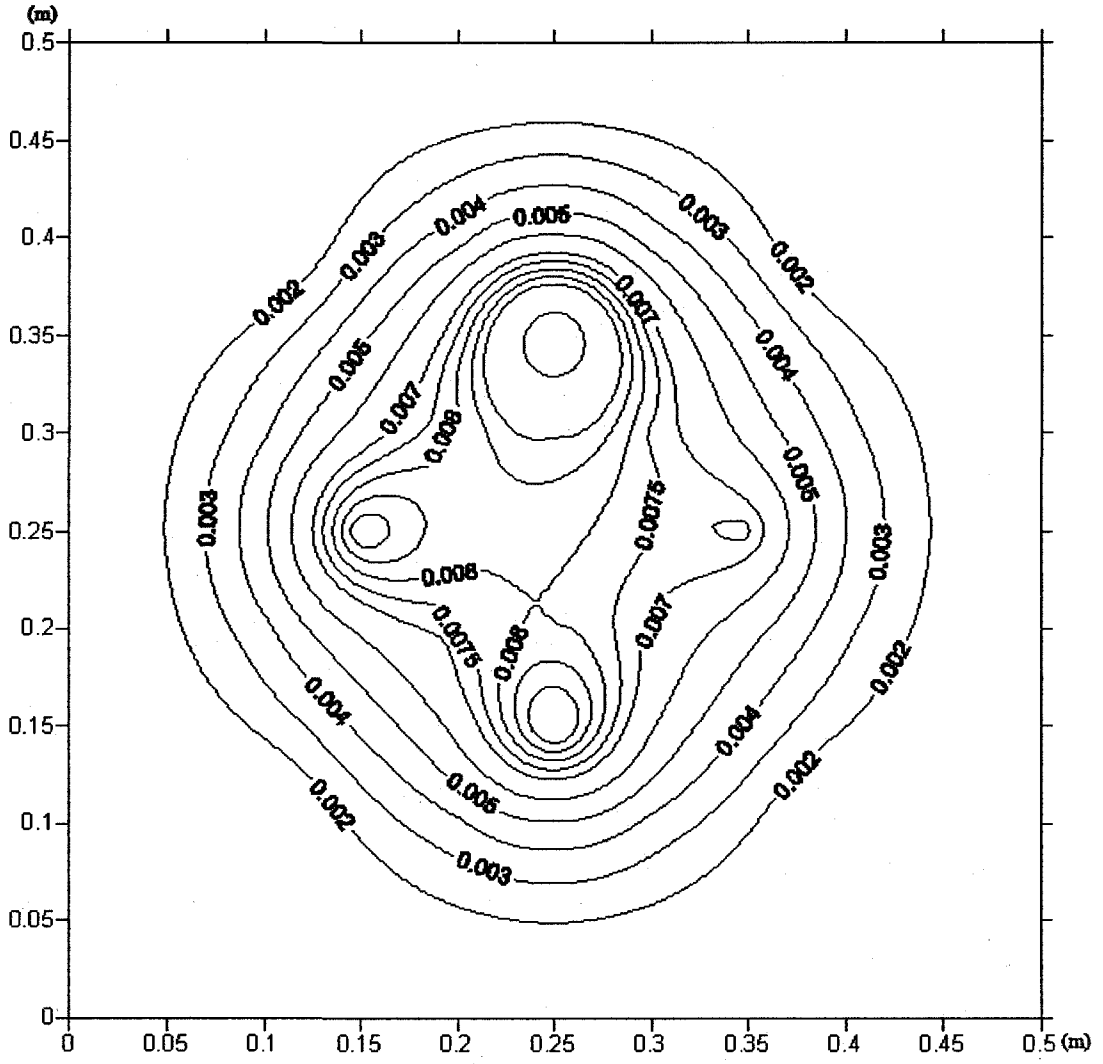

Figure 4.9 LNAPL specific volume contour of VG model for a 750ml spill

4.2.2.4 Results of BC-based model for a 600ml spill

The specific volume and total volume were obtained through the BC modeling system. The BC model was run for an experimental oil spill of 600ml. The results of the VG modeling give 480.1 ml.

The experimental data of the oil level and water level of the wells are same as in the previous section (Table 4.8). Table 4.8 shows the locations of the observed well and the experimental data for a 600ml spill.

Table 4.12 shows the parameters used in a BC model. The parameters include Porosity, Residual saturation, BC parameter, density ratio, air-oil scaling factor and oil-water scaling factor.

Table 4.12 Parameters for BC model

			BC parameter	
Soil types	Porosity	Irreducible water residual saturation S_m	H_d (m)	namda
Sand	0.334	0.01	0.045	1.13
Fluid	Density ratio, ρ_{ro}	0.86		
Properties	Air-oil scaling factor	10.394		
	Oil-water scaling factor	2.275		

Table 4.13 gives the parameters of the BC model. The parameters include Displacement Pressure Head (m) and Porous Size Distribution Index.

Table 4.13 Brooks and Corey Soil Parameters from Carsel and Parrish (1988)

Soil Texture	Porosity n	Irreducible water saturation, S_{wr}	ψ_{baw}	Porous size distribution index λ
Sand	0.43	0.105	0.045	1.13

Source: Carsel and Parrish (1988)

Table 4.14 shows the modeling outputs for the specific volume for a 600ml spill. MW 1~8 wells are the observation wells. Table 4.14 shows that different specific volumes are obtained for different wells and oil thicknesses in wells.

Table 4.14 Specific volume of the observed well for a 600ml spill based on BC model (m^3/m^2)

	X (m)	Y (m)	Oil level (m)	Water level (m)	Oil thickness (m)	Specific volume (m^3/m^2)
MW1	0.25	0.35	0.155	0.213	0.058	0.01084143
MW2	0.35	0.25	0.163	0.195	0.032	0.00425573
MW3	0.25	0.15	0.158	0.196	0.038	0.00562321
MW4	0.15	0.25	0.156	0.197	0.041	0.00656987
MW5	0.1	0.4	0.190	0.190	0	0
MW6	0.4	0.4	0.190	0.190	0	0
MW7	0.4	0.1	0.190	0.190	0	0
MW8	0.1	0.1	0.190	0.190	0	0

The generation of the contour in Figure 4.10 is based on the results of the BC modeling for a 600ml spill. The results of the modeling system have the specific volume at every location of the computation mesh in the tank. Then, the software-Surfer was used to produce the contour of oil specific volume. Figure 4.10 shows the distribution of oil specific volume for a 600ml spill in the tank.

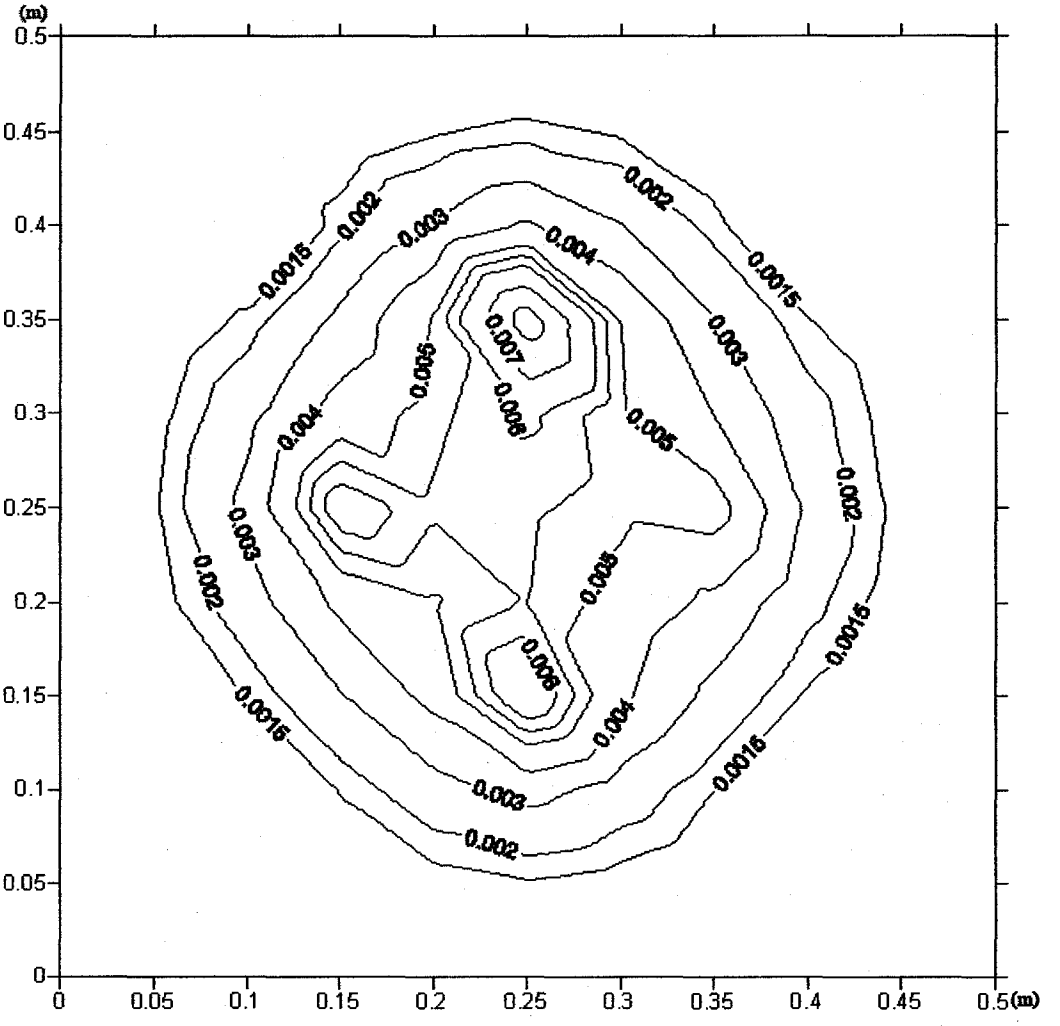

Figure 4.10 LNAPL specific volume contour of BC model for 600ml spill

4.2.2.5 Results of BC-based model for a 750ml spill

The specific volume and total volume for a 750ml spill had been calculated by using the BC modeling system. The model is run for an experimental oil spill of 750ml. The results of BC modeling give 603.3ml.

The input data are shown in Table 4.10 (Wells data input for a 750ml spill) and Table 4.12 (Parameters for BC model).

Table 4.10 gives the experiment data including the oil level and the water level of the wells. It shows the locations of the observed well and the experimental data for a 750ml spill (oil and water levels of wells).

Table 4.15 gives the specific volume of wells is calculated by the BC modeling system for a 750ml spill. MW 1~12 wells are the observed wells. Table 4.15 shows the different specific volume according to the different wells and the oil thicknesses in the wells.

Table 4.15 Specific volume for a 750ml spill based on BC model (m^3/m^2)

	X (m)	Y (m)	Oil level (m)	Water level (m)	Oil thickness (m)	Specific volume (m^3/m^2)
MW1	0.25	0.35	0.209	0.268	0.059	0.0112635
MW2	0.35	0.25	0.195	0.236	0.041	0.0065698
MW3	0.25	0.15	0.200	0.248	0.048	0.0082001
MW4	0.15	0.25	0.205	0.252	0.047	0.0080234
MW5	0.1	0.4	0.223	0.234	0.011	0.00029951
MW6	0.4	0.4	0.224	0.231	0.007	0
MW7	0.4	0.1	0.25	0.25	0	0
MW8	0.1	0.1	0.25	0.25	0	0
MW9	0.25	0.5	0.196	0.204	0.008	0.00003381
MW10	0.5	0.25	0.25	0.25	0	0
MW11	0.25	0	0.25	0.25	0	0
MW12	0	0.25	0.25	0.25	0	0

The generation of the contour on Figure 4.11 is based on the results of BC modeling for a 750ml spill. The results of the modeling system have the specific volume at every location of computation mesh in tank. Then, the contour of oil specific volume is drawn by using the software-Surfer. It shows the distribution of oil specific volume for a 750ml spill in the tank.

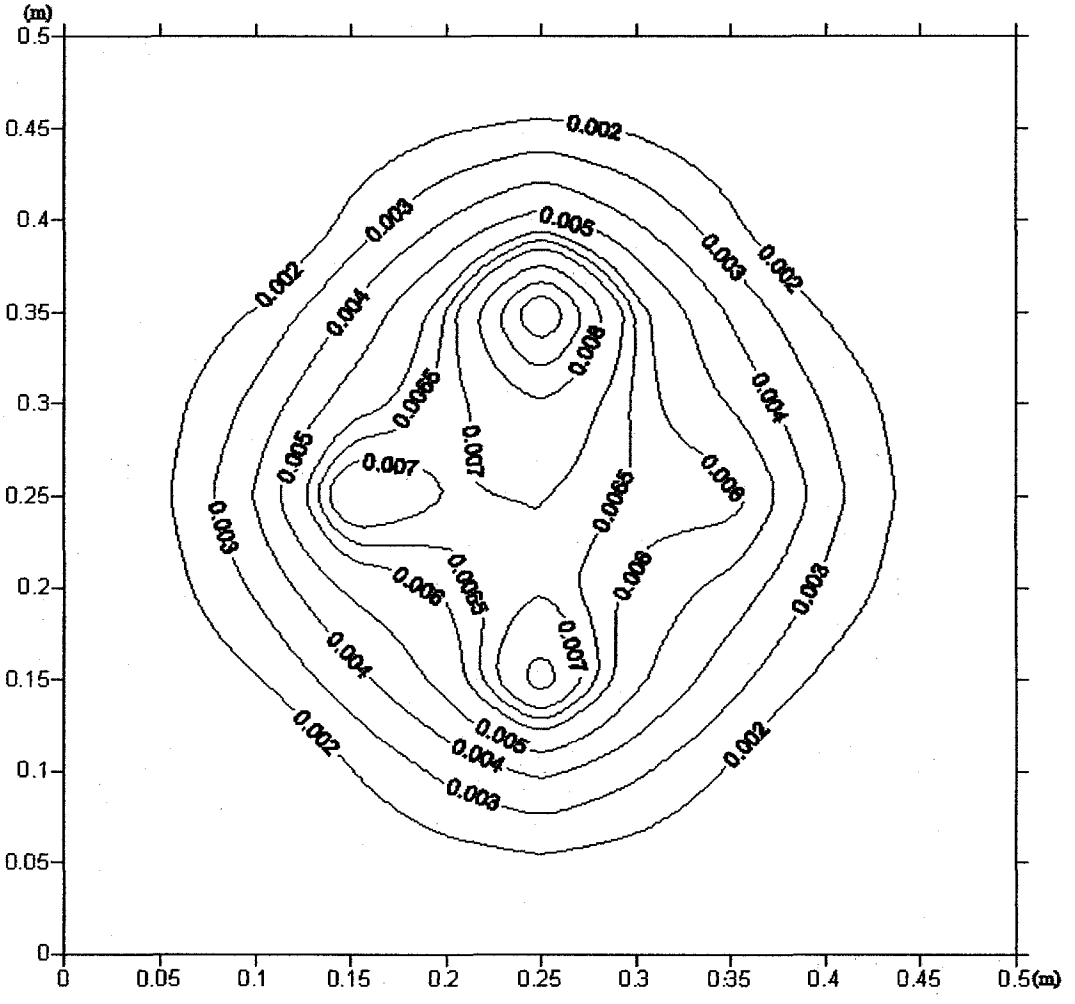

Figure 4.11 LNAPL specific volume contour of BC model for a 750ml spill

4.3 Validation results and discussion

The developed model was validated by using a pilot-scale experiment. The volume estimation using a VG model gave a fairly accurate estimate of the free liquid present in the porous space under equilibrium conditions.

4.3.1 A summary of experimental and modeling results

Specific Volumes were determined for each well using both van Genuchten and Brooks-Corey. The total volume was calculated by adding up the volume in approximately equal-sized grids around each well.

Table 4.16 Comparison of experimental and modeling results

Experimental oil spill / Modeling results	600ml		750ml	
VG-based model result (ml)	571.7	4.72% err	704.2	6.11% err
BC-based model result (ml)	480.1	20.1% err	603.3	19.6% err

Results obtained from VG and BC models are compared to the known oil volume in Table 4.16. When the oil in the sand appeared to stabilize and equilibrate with that in the wells, a good agreement between known and predicted oil volumes was obtained using the VG model.

The results of VG modeling are 571.7ml and 704.2ml towards to experimental spills of 600ml and 750ml; the percent error of results is 4.72% and 6.11%, respectively. The results of BC modeling are 480.1ml and 603.3ml towards to experimental spills of 600ml and 750ml; and the error in the results is 20.1% and 19.6%, respectively. The comparison shows that both VG- and BC-based models could generate reasonable results. The output

from VG-based model is better. The differences can be due to the uncertainties associated with the selected oil properties, interactions between oil and porous media, and output interpolations. More discussions are included in the next section.

In order to obtain reliable result from experimental results, the model parameters were calibrated based on an extensive literature survey. (Carsell and Parish, 1988 and Charbeneau et al., 1999).

4.3.2 Comparison of the VG- and BC-based modeling results

Based on Section 4.2, the specific volume has gotten through the modeling system's calculation. Also we obtain the contour of specific volume with VG and BC model using the software Surfer.

The Specific Volumes were determined for each well using both van Genuchten and Brooks-Corey. The total volume was calculated by adding up the volume in approximately equal-sized grids around each well. Figure 4.12 is the comparison of the specific volume of VG and BC model for a 600ml spill.

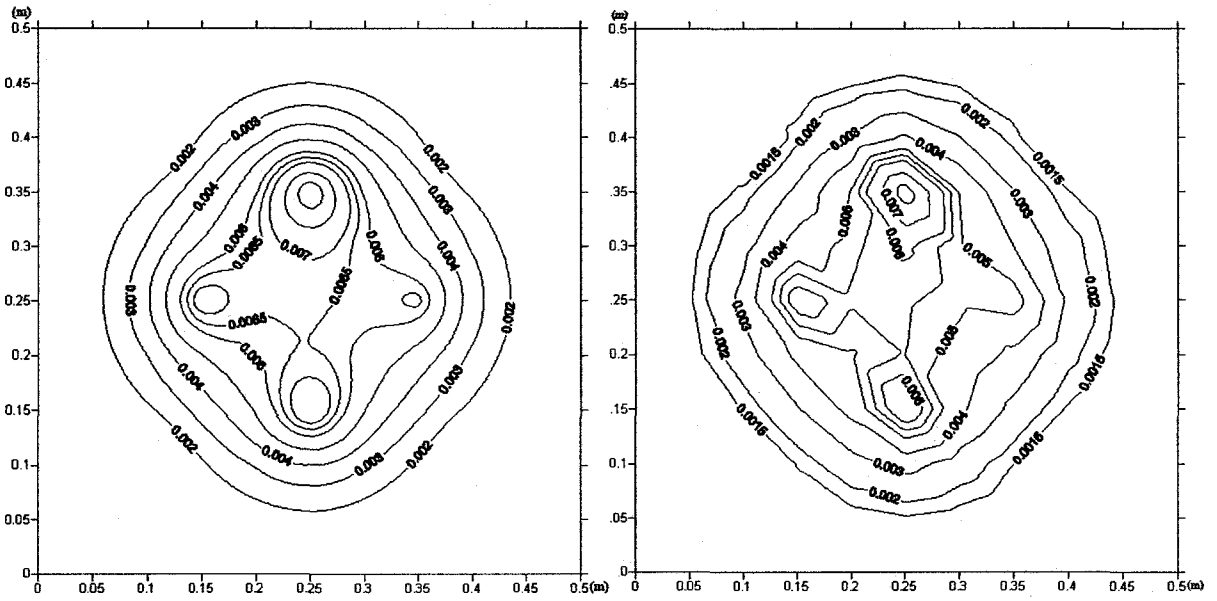

LNAPL specific volume contour of VG model under 600ml spill

LNAPL specific volume contour of BC model under 600ml spill

Figure 4.12 Comparison of the specific volume of the VG and BC models for a 600ml spill

Figure 4.13 is the comparison of the specific volume of the VG and BC models for a 750ml spill.

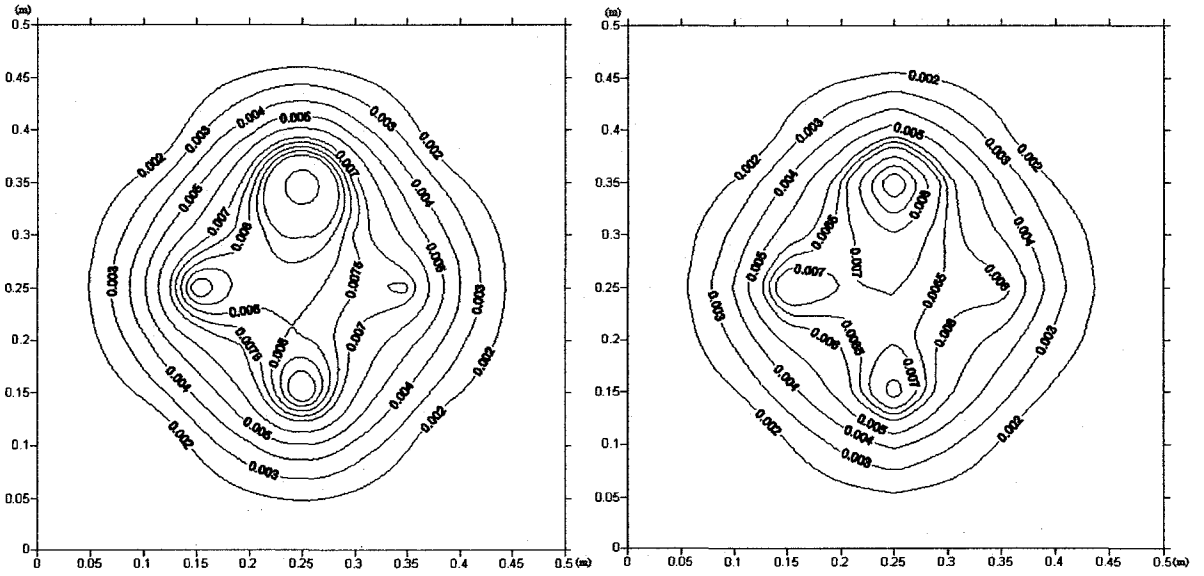

LNAPL specific volume contour of VG model under 750ml spill

LNAPL specific volume contour of BC model under 750ml spill

Figure 4.13 Comparison of the specific volume of the VG and BC models for a 750ml spill

Table 4.17 gives the comparison of specific volume between VG and BC modeling with different thicknesses of oil. The results of the VG model are larger than the BC model's and are closer to the real quantity of the spill.

Table 4.17 Result comparison for a 600ml spill

Thickness of NAPL in well (cm)	Specific volume of LNAPL (m^3/m^2)	
	VG model	BC model
0.058	0. 0125827	0.01084143
0.032	0.00537560	0.00425573
0.038	0.00672632	0.00562321
0.041	0.00765514	0.00656987

Figure 4.14 shows the comparison of the specific volume of the VG and BC model for a 600ml spill using the curve. The curve of the VG model is higher than that of the BC model. In addition, the specific volume of the LNAPL increases with the thickness of the LNAPL in the wells.

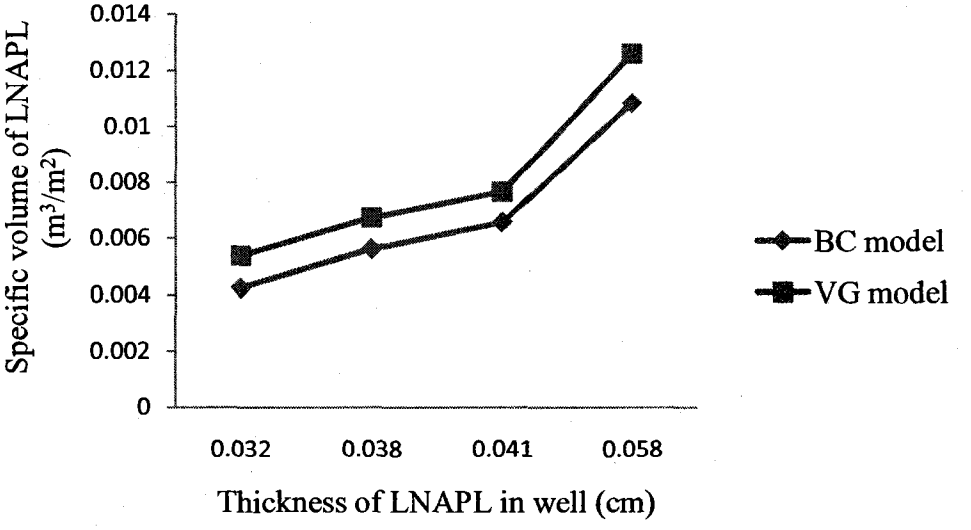

Figure 4.14 Comparison the LNAPL specific volume of the BC model for a 600ml spill with VG model

Table 4.18 presents the comparison of the specific volume between VG and BC modeling with different thicknesses of oil for a 750ml spill. The results of the VG model are larger than those of the BC model and are closer to the real quantity of the spill.

Table 4.18 Comparison of the results in the case of a 750ml spill

Thickness of NAPL in well (cm)	Specific volume of LNAPL (m^3/m^2)	
	VG model	BC model
0.059	0.0128416	0.0112635
0.041	0.0076504	0.0065698
0.048	0.0094997	0.0085925
0.047	0.0095341	0.0080234
0.011	0.0004826	0.0010503
0.007	0.0000927	0
0.008	0.0016688	0.00003381

Figure 4.15 presents the comparison of the specific volume of the VG and BC models for a 750ml spill using the curve. The curve of the VG model is higher than that of the BC model. In addition, the specific volume of the LNAPL increases with the thickness of the LNAPL in the wells.

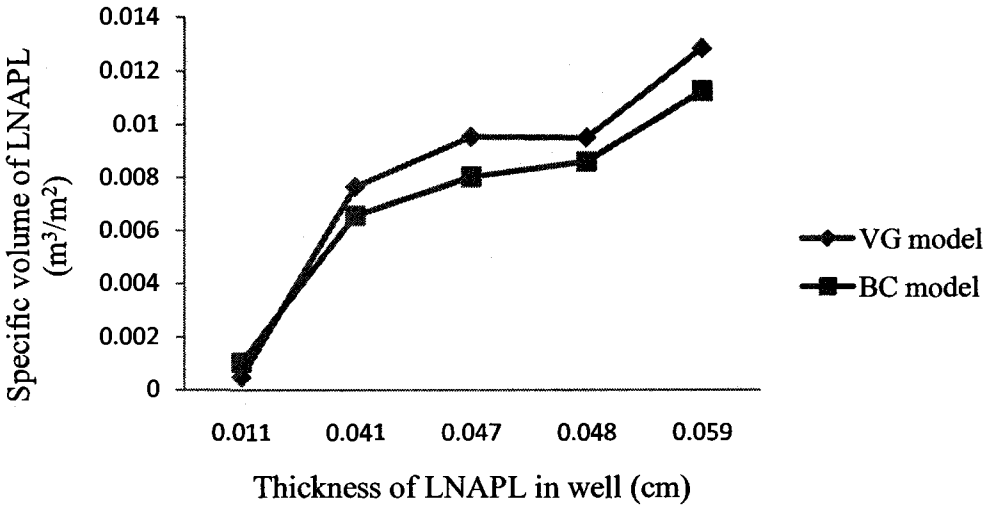

Figure 4.15 Comparison of the LNAPL specific volume of the BC model for a 750ml spill with VG model

In summary, the VG-based model outputs have a good match with the experiment. This agreement is to be expected only when equilibrium is reached because the model has been developed for the case where fluids in porous media adjacent to a monitoring well are in equilibrium with the fluid-level elevations in the well. Modeling, experiment and field observations confirm that the above assumption is reasonable. The reasons for the difference between the predicted and the actual oil volume using the BC model are various. One reason is that the Brook-Corey model assumes that a distinct water-saturated capillary fringe exists above the water table, which is different from the VG model and any contributed to the errors.

The fluidity of the LNAPL also makes it difficult to accurately measure their thickness in site monitoring wells. Additionally, the varying properties cause the LNAPL to behave differently in the subsurface. The presence of the LNAPL in several different geologic units further complicates the situation, as LNAPL will behave differently in different lithologies. As a result of all these factors, the LNAPL saturation profiles of spilled LNAPL in each of the geologic units at the site will differ.

Chapter 5

Application of the developed model to a petroleum contaminated site and development of a user-friendly computation system

5.1 Application to petroleum contaminated sites

In the present section, one real example is presented. For instance, the useful information in relation to site conditions and contamination situations has been obtained in the preparation of the data and provision of important bases for further simulating separation and recovery of condensate from the contaminated subsurface at the study site.

5.1.1 The study site

Figure 5.1 provides an overview of the study site, which is located at Hoosier, Saskatchewan, Canada. The site and facilities served and operated as a natural gas processing plant from the middle of 1960s until 1990. The plant utilized a series of scrubbers to remove condensate, recognized as an LNAPL, from the natural gas stream prior to transport in a regional transmission line. Throughout the operating history of the site, the waste condensate has been disposed of in two perforated underground storage tanks (USTs) (Figure 5.2). From 1992 to 1998, a number of site investigations and monitoring works were conducted.

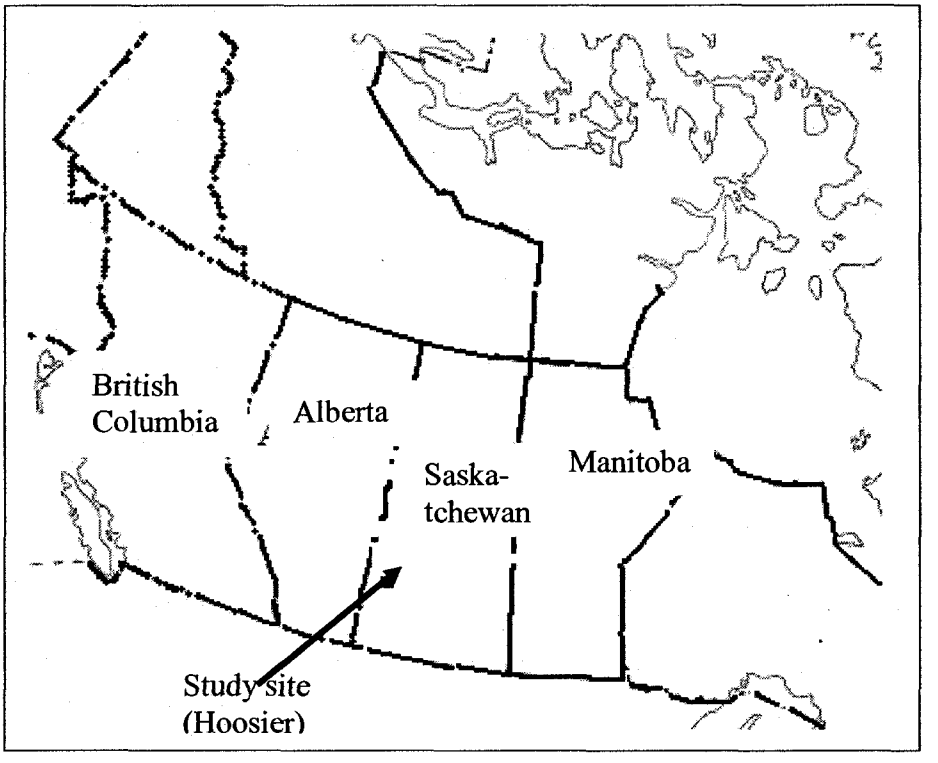

Figure 5.1 The study site

The soil stratigraphy at the depth of 0.05 m to 0.15 m consists of a thin sand and gravel fill. Clay till underlies the fill and extends to depths varying from 1.1 m to 1`2.2

m. Sand underlies the clay till in most areas of the site except the immediate south. Clay till underlies the sand over most of the site. The sand was discontinuous and ranged in thickness between 0.02 m and 5.5 m. The sand was generally encountered at the depths of 5.0 m to 12.0 m.

Groundwater was encountered between 4.5 m and 10 m below the surface. Around UST2 area, the groundwater table was encountered at depths of 5.7 m to 9.1 m below the surface, while it was 4.7 m to 9.2 m deep north of the UST2. Figure 11 describes a graphical display of groundwater flow direction and a vertical view of the water table at the study site. It is indicated that the general groundwater flow direction is towards the south, with the gradient of the water table being approximately from northeast to southwest. The only exception is to the immediate south of the site, where higher gradients can be found at some spots. The groundwater table is predominately located within the clay-till soils.

The investigation results of the site contamination conditions show that (1) elevated concentrations of total petroleum hydrocarbons (TPH), benzene and toluene, as well as elevated combustible vapor, were detected at levels above the local soil quality guidelines for commercial/industrial areas (SERM, 1995); (2) residual hydrocarbon concentrations in soils were at levels above the local soil quality guidelines for industrial/commercial areas (SERM, 1995); (3) free phase products were encountered in several monitoring wells with a thickness ranging from 20 mm to 450 mm. The residual phase hydrocarbons and free phase hydrocarbons were present in fractured clay till near the water table and in the vadose zone above the discontinuous sand stratum under the three USTs; and (4) the peak dissolved concentrations of BTEX (benzene, toluene, ethyl-benzene, and xylene) in

groundwater were close to or higher than the regulated standards in the local non-potable groundwater quality guidelines (SERM, 1995). For example, a highly contaminated area was beside the UST1 with a peak benzene concentration of 7.22 mg/L and a peak toluene concentration of 5.9 mg/L.

Site investigation results indicate that the leaked condensate and its constituents have been contaminating the soil and groundwater inside and around the site. The separation and recovery of the condensate are required to prevent the spreading of contaminants to the surrounding communities.

5.1.2 Site simulation

Site investigation results in 5.1.1 are used to develop a conceptual model and to prepare model simulations. The simulation area is considered a two-dimensional domain. The area is 100×80 m^2 with a depth of 14.0 m (Figures 5.3 and 5.4). In the 2D computational mesh system, the total number of nodes is 99 with a computational mesh of 11×9. The distribution of monitoring wells is described in Figure 5.2. Figures 5.3 and 5.4 show the main profiles of the study site. According to the site investigation, two types of soils are related to the estimation of the specific oil volume in porous media. The interface between two kinds of soils ranges from 5.8 m to 13.7 m. The soils and fluid parameters are enumerated in Table 5.1. The distributions of apparent oil thickness in monitoring wells and the interface depths of soils are shown in Table 5.2.

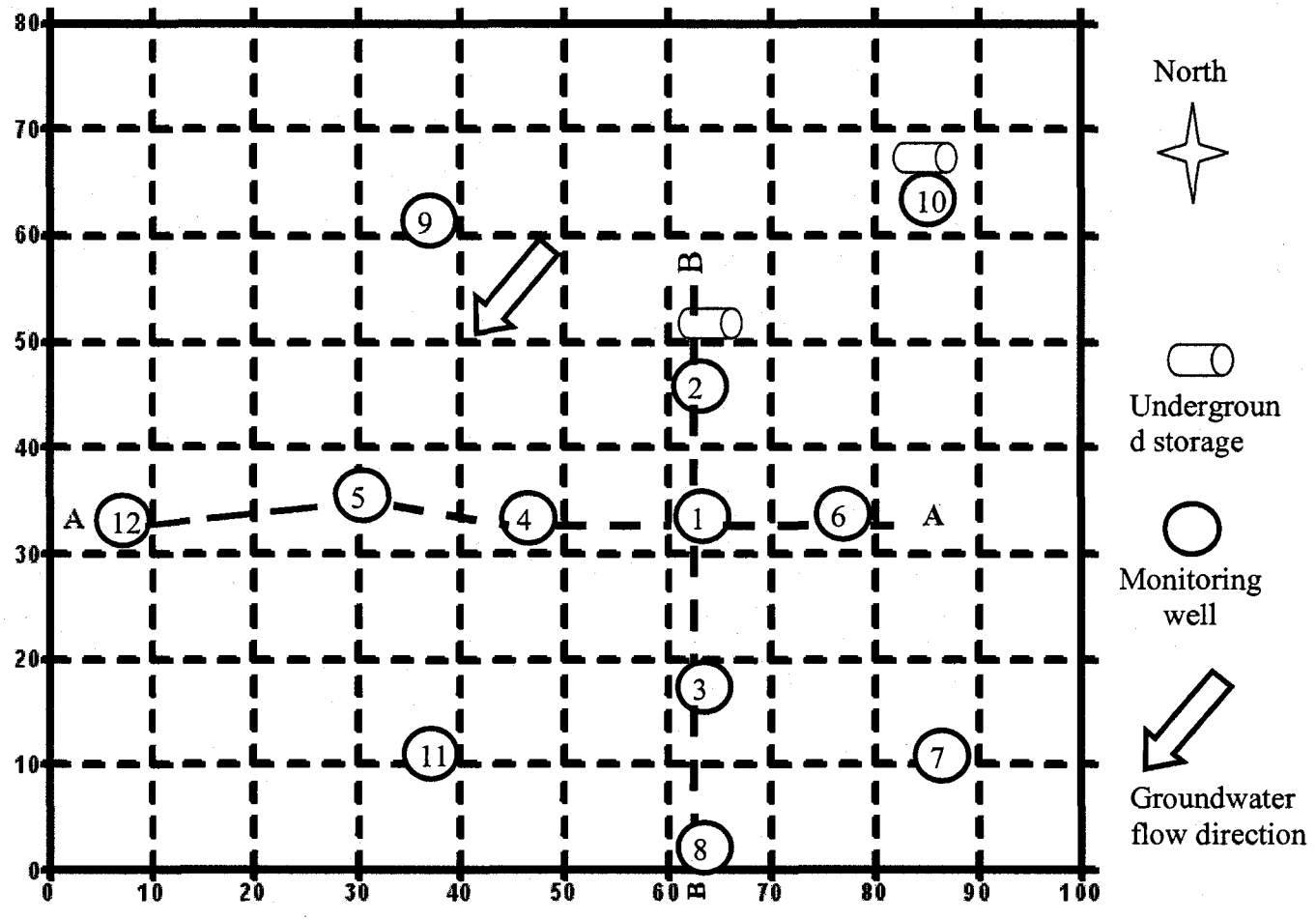

Figure 5.2 Distribution of monitoring wells and mesh delimitation in the study domain

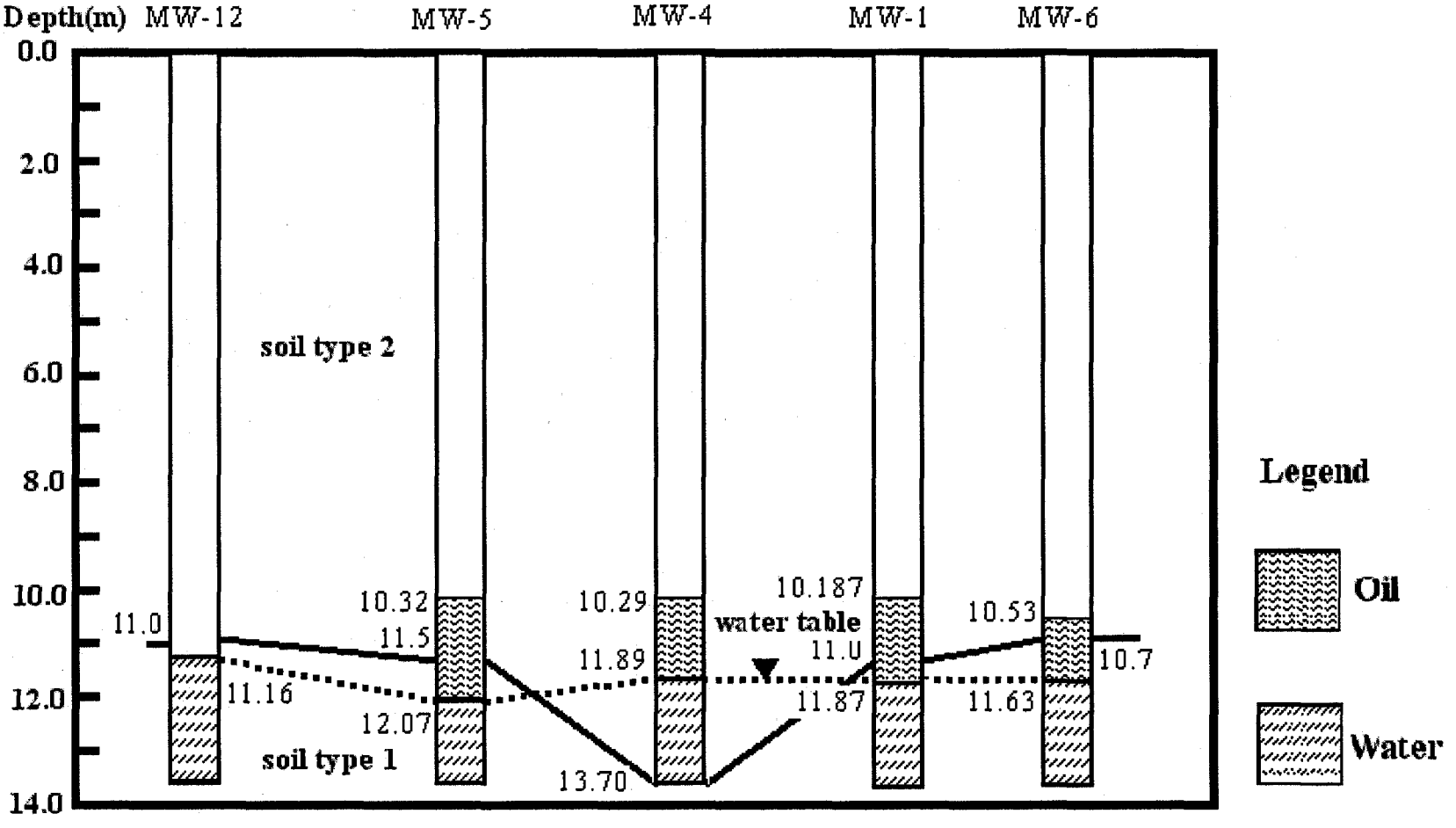

Figure 5.3 Schematic of soil stratigraphy and distributions of oil in monitoring wells

(A-A profile)

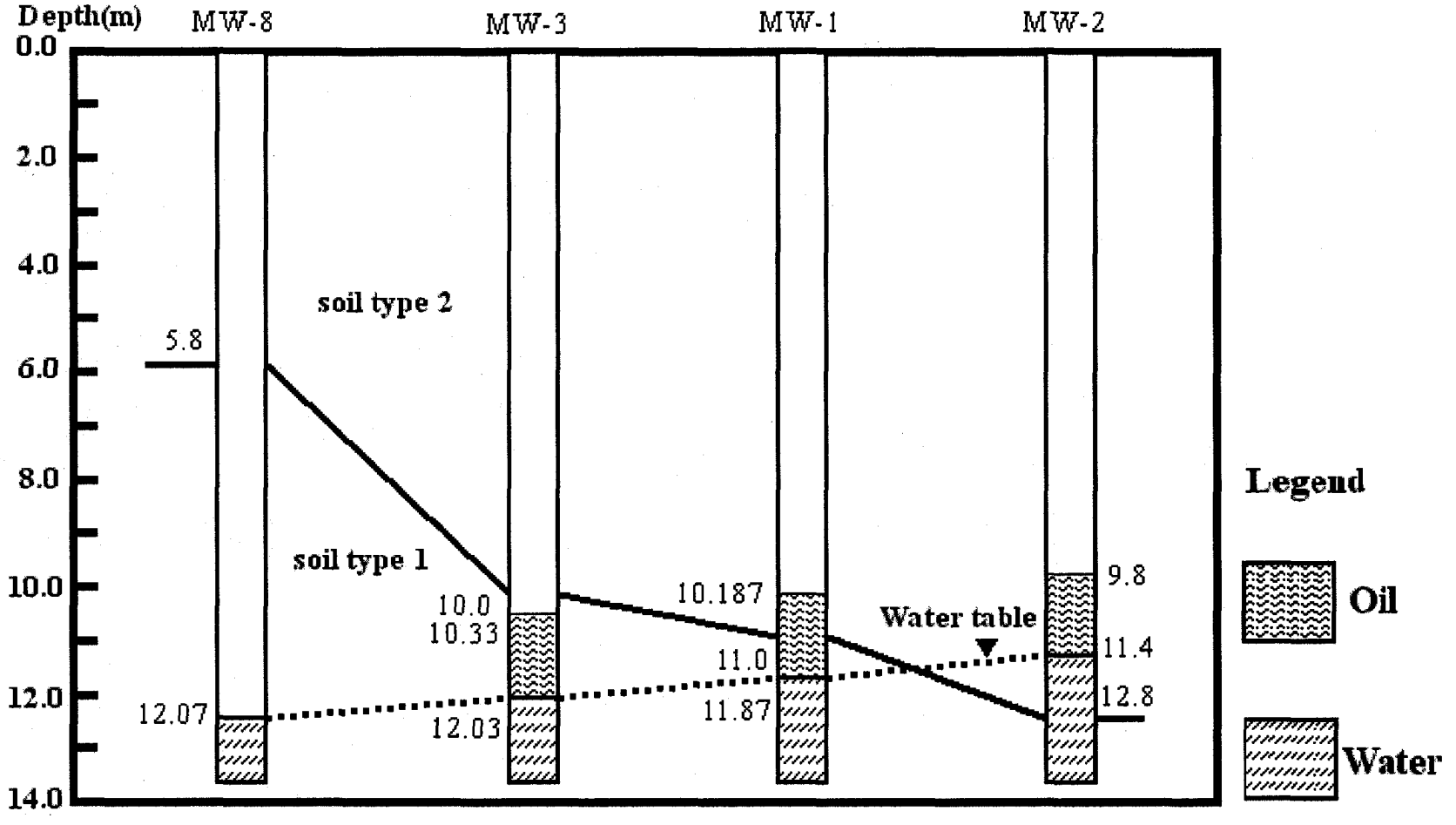

Figure 5.4 Schematic of soil stratigraphy and distributions of oil in monitoring wells (B-B profile)

5.1 Soil and fluid properties

Soil types	Porosity	Irreducible water saturation S_m	van Genuchten parameter		BC parameters	
			n	α (m^{-1})	λ	h_d (m)
Soil 1	0.36	0.100	3.50	1.80	1.55	0.39
Soil 2	0.34	0.069	1.98	1.03	0.74	0.60
Fluid Properties	Density ratio, ρ_{ro}		0.78			
	Air-oil scaling factor		3.02			
	Oil-water scaling factor		1.50			

Table 5.2 Depths of oil and soil interfaces in monitoring wells

Well number	X (m)	Y (m)	Dao (m)	Dow (m)	Z_s^1 (m)
MW-1	61.84	34.96	10.187	11.87	11.0
MW-2	61.46	46.24	9.8	11.45	12.8
MW-3	61.47	18.8	10.33	12.03	10.0
MW-4	45.68	34.96	10.29	11.89	13.7
MW-5	29.89	35.34	10.32	12.07	11.5
MW-6	76.88	34.96	10.53	11.63	10.7
MW-7	85.96	10.9	11.99	11.99	5.6
MW-8	61.47	2.63	12.07	12.07	5.8
MW-9	37.41	62.03	8.25	8.25	12.3
MW-10	84.02	63.91	7.51	7.51	10.4
MW-11	37.41	10.9	11.94	11.94	9.4
MW-12	5.16	34.34	11.16	11.16	11.0

5.1.3 Results

All parameters are input through a user-friendly interface (module 1 in interface). Then, Module 2 in the system of interface is employed to calculate the specific oil volume at the locations of the monitoring wells. Finally, the specific oil volume at all computational nodes and the total free-phase oil volume are computed in Module 3 and displayed by the user-friendly interface. In this case, iteration converge criterion, 0.00001, is designated for the finite difference method.

Both BC and VG models are used to simulate the distribution of the leaked LNAPL in the contaminated soil and groundwater. Parameters for BC model (Table 5.1) are derived from the conversion of the VG model (Lenhard et al., 1989). Figures 5.5 and 5.6 illustrate the specific volume (m^3/m^2) distribution contours for the VG model and BC model, respectively.

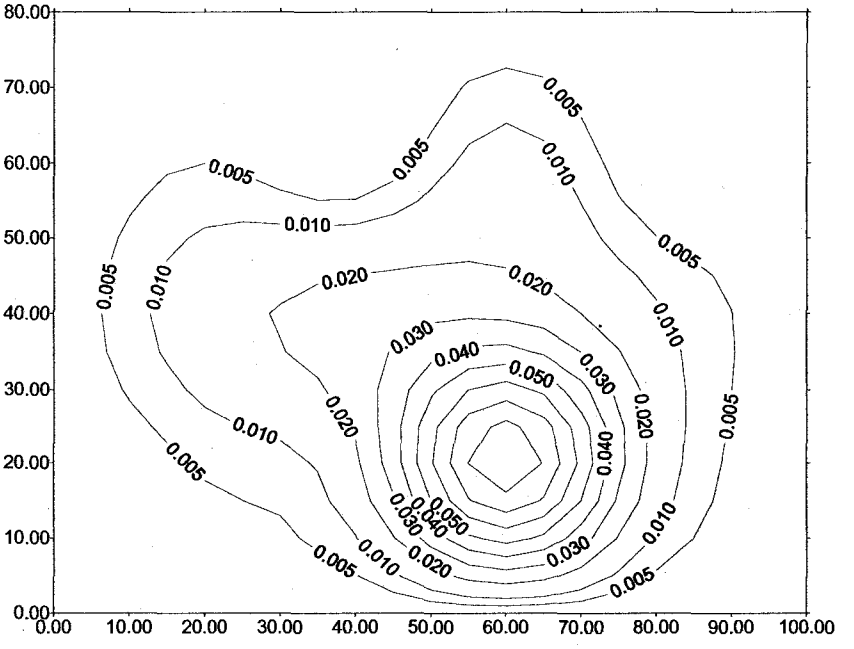

Figure 5.5 Specific volume distribution in stratified soils based on VG model

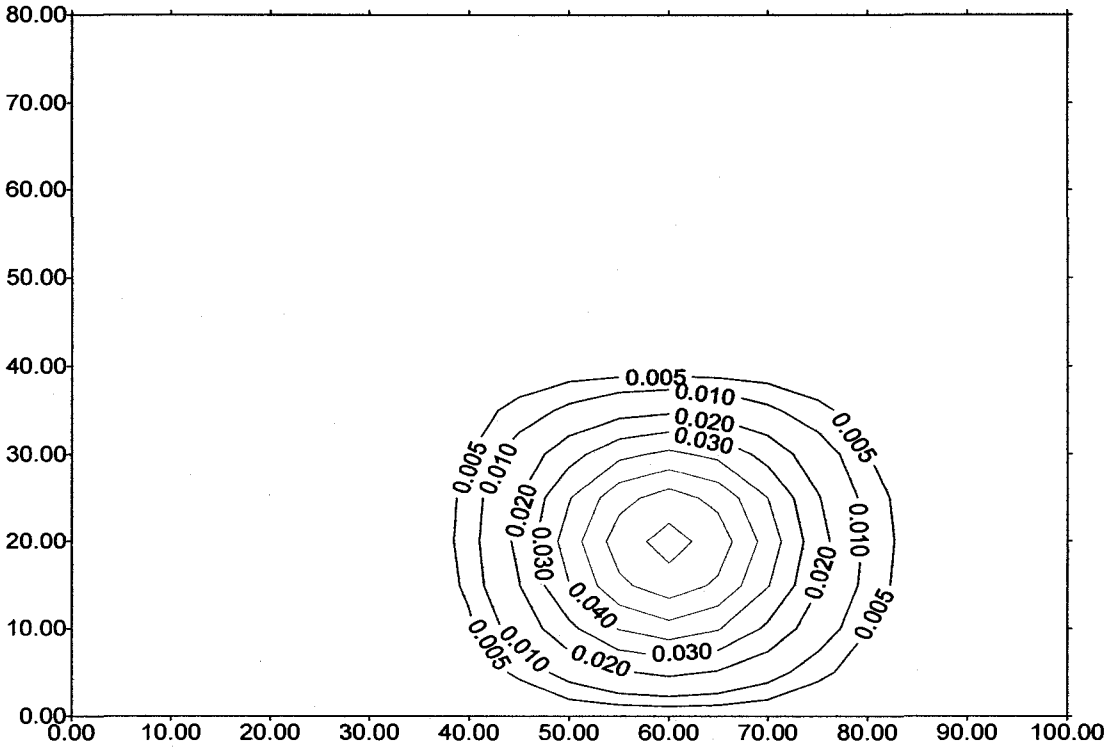

Figure 5.6 Specific volume distribution in stratified soils based on BC model

By comparison, Figures 5.7 to 5.8 show the specific oil volume assuming the site is homogeneous. Specifically, Figures 5.7 and 5.8 display the distribution of the specific oil volume in soil type 1 (lower soil) based on VG and BC models, respectively; the specific oil volume in soil type 2 (upper soil) based on VG and BC models is shown in Figures 5.9 and 5.10.

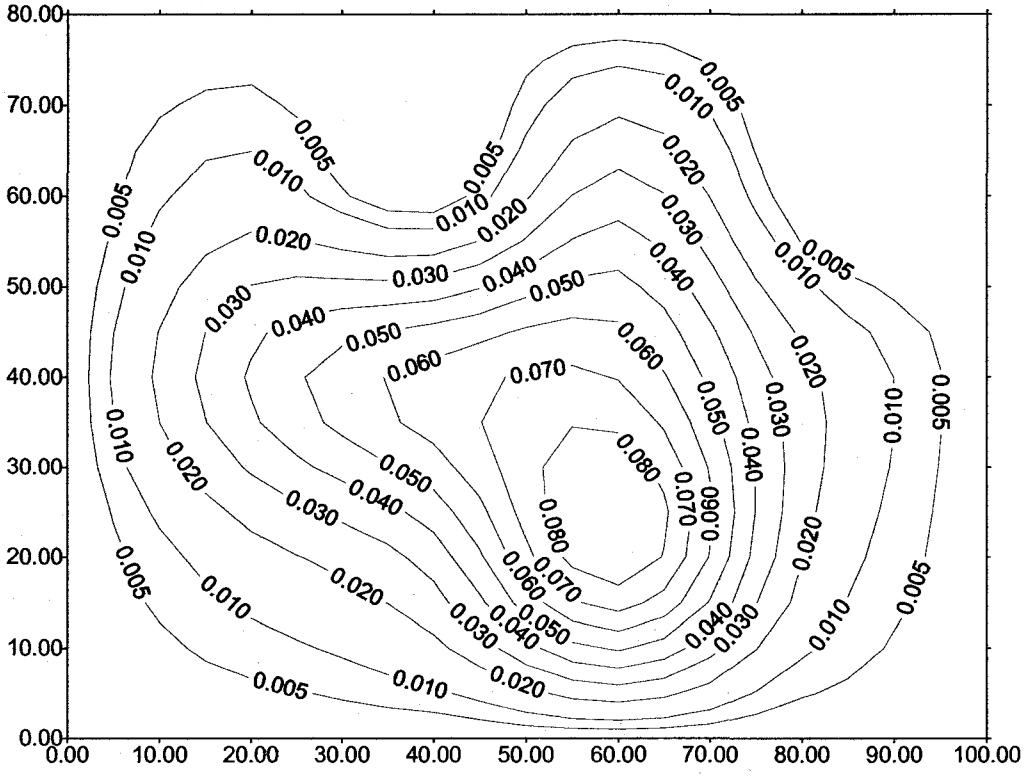

Figure 5.7 Specific oil volume distribution in soil 1 based on VG model

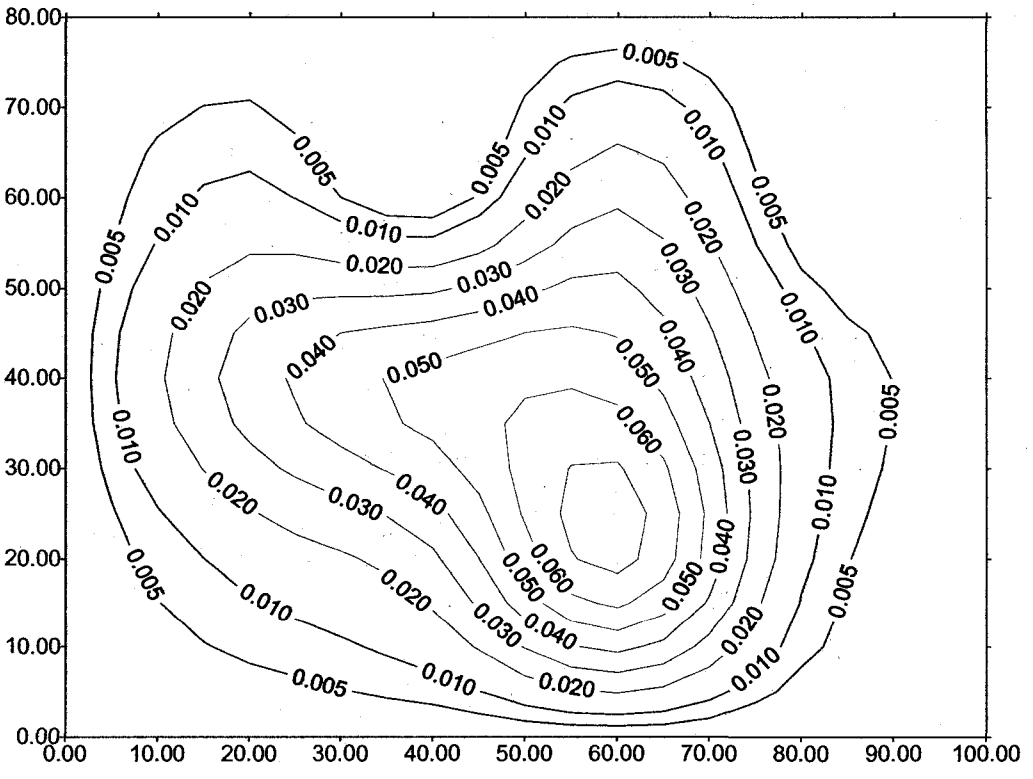

Figure 5.8 Specific oil volume distribution in soil 1 based on BC model

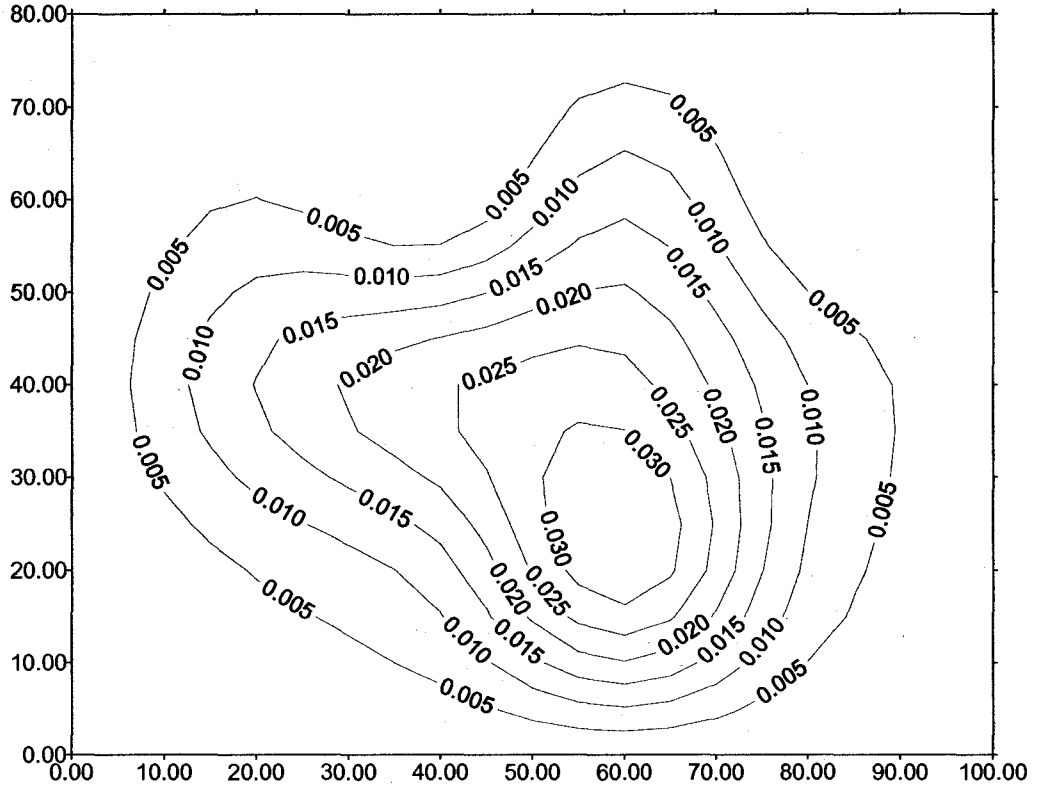

Figure 5.9 Specific oil volume distribution in soil 2 based on VG model

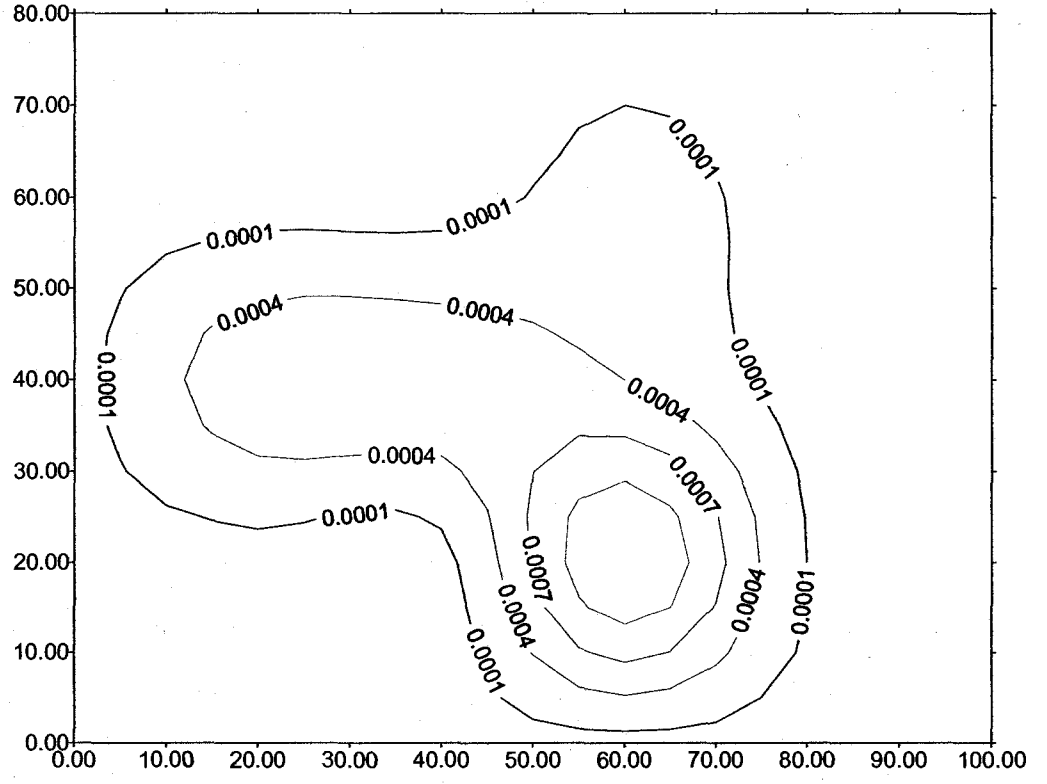

Figure 5.10 Specific oil volume distribution in soil 2 based on BC model

The total free-phase oil volumes are shown in Figure 5.11 for both VG model and BC model. Since non-zero apparent oil thickness occurs only in six monitoring wells, i.e. MW-1 to MW-6, the specific oil volume in porous media corresponding to these monitoring wells is shown in Figure 5.12 for VG model and Table 5.3 for BC model.

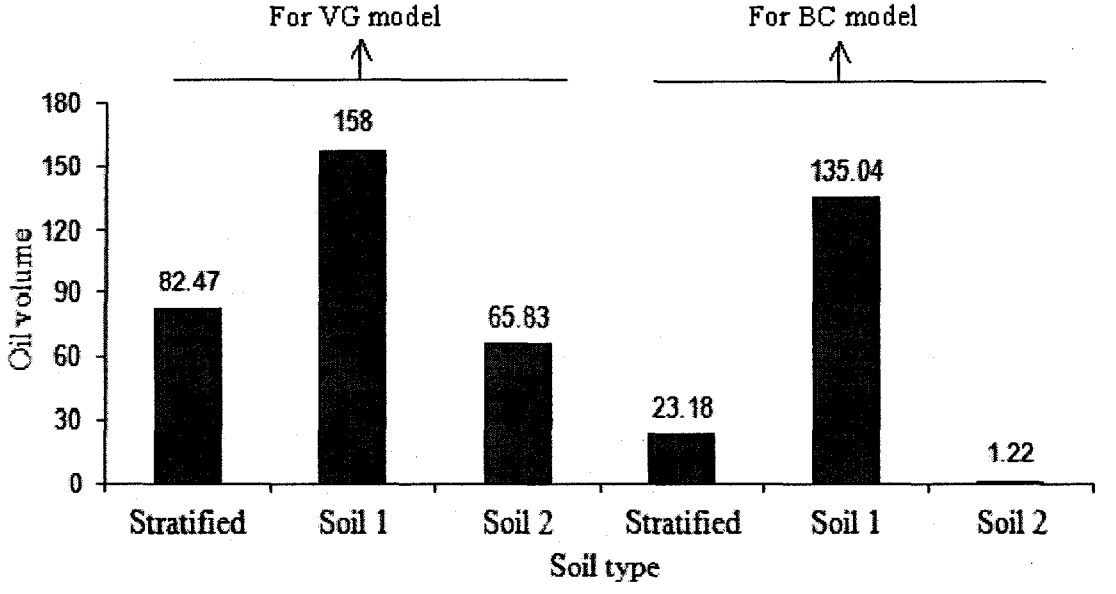

Figure 5.11 Total volume of free phase oil (m^3)

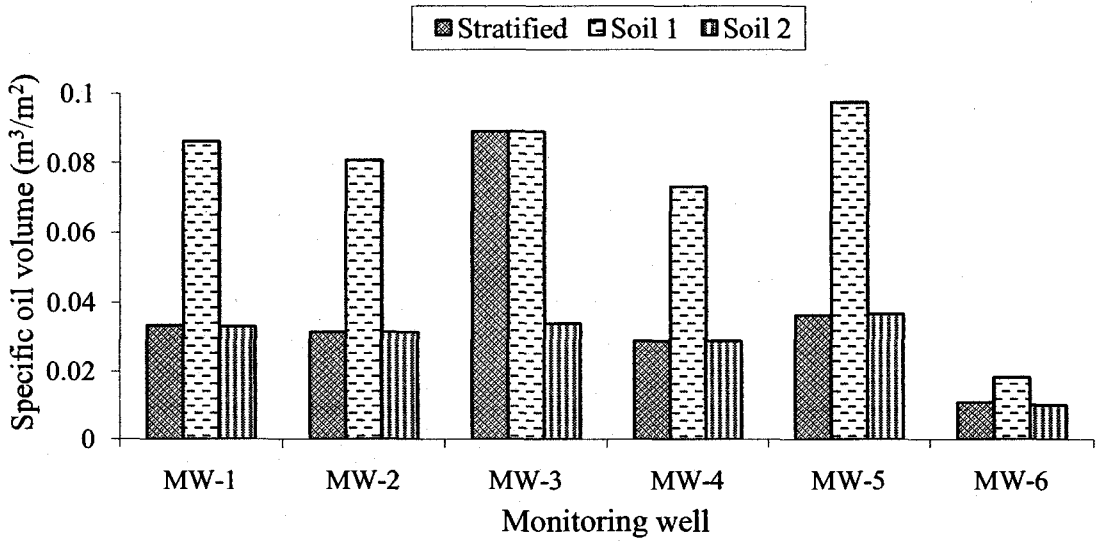

Figure 5.12 Specific oil volume in porous media based on VG model (MW-1 to 6)

Table 5.3 Specific oil volume in porous media based on BC model (MW-1 to 6)

Soil types	Specific oil volume (m^3/m^2)					
	MW-1	MW-2	MW-3	MW-4	MW-5	MW-6
Stratified soils	0.0010	0.0006	0.0740	0.0001	0.0024	0.0
Soil 1	0.0710	0.0653	0.0740	0.0569	0.0830	0.0016
Soil 2	0.0010	0.0006	0.0013	0.0001	0.0024	0.0

In Figures 5.5 and 5.6, it can be seen that for the same apparent oil thickness in monitoring wells (Table 5.2) and same soil types (Table 5.1), the specific oil volume in soils based on the VG model differs from the specific oil volume based on the BC model. This difference is mainly attributed to the assumption in air entry displacement pressure; in other words, air entry pressure is considered in the BC model, but it is assumed to be zero in the VG model. As far as this case is concerned, the specific oil volume based on the BC model is much less than that based on the VG model because both soil 1 and soil 2 have great air entry pressures (Table 5.1). As a result, the total free-phase oil volume based on the BC model is 23.18, whereas the amount of total free-phase oil volume based on the VG model is 82.47, which is greater by 3.5 times. Except for the amount of the specific oil volume in porous media, Figures 11 and 12 show that the distribution of the specific oil volume in porous media based on the VG model (Figure 5.5) is much broader than that based on the BC model (Figure 5.6).

Although there is a difference in the distributions of the specific oil volume for the VG model and the BC model, the specific oil volume distributions in Figures 5.5 and 5.6 reflect the relationship of site contamination and groundwater flow direction

precisely. Along with the groundwater flow direction, site contamination extends from the northwest to the southeast (Figure 5.2); thus, the groundwater flow would significantly influence the contaminant distribution in porous media.

Figures 5.7, 5.8 (soil 1) and Figures 5.9, 5.10 (soil 2) reflect the impact of the soil types on the specific oil volume in homogeneous porous media. They give similar results as Figures 5.5 and 5.6. The specific oil volume based on the VG model is bigger than that based on the BC model, and the bigger the air entry pressure of the soil, the greater the difference in the results for the VG model and BC model.

Figure 5.12 shows the results of the specific oil volume based on the VG model under the conditions of the same apparent oil thickness (in every well) for different soil types. Because the apparent oil thickness in MW-2 and MW-4 occurs in soil 2 completely (Figures 5.3 and 5.4), the computational results for soil layering and homogeneous soil 2 are identical. Similarly, the apparent oil thickness in MW-3 exists only in soil 1 (Figure 5.4), so the same specific oil volume is obtained for soil layer and homogeneous soil 1 (Figure 5.12). Apparent oil thickness in MW-1, MW-5 and MW-6 occurs in both soil 1 and soil 2 (Figure 5.3), but the specific oil volume in porous media for stratified soils is closer to the specific oil volume for soil 2 (upper soil in this case). Actually, the specific oil volume in stratified soils (0.0364 m^3/m^2) for MW-5 is less than the results for any homogeneous soil (0.0976 m^3/m^2 in soil 1 and 0.0368 m^3/m^2 in soil 2, shown in Figure 5.12).

The specific oil volume based on the BC model in porous media for MW-1 to 6 (Table 5.3) has the same trends as that based on the VG model (Figure 5.12). On the

other hand, dissimilar characteristics are present due to air entry pressure. For example, the specific oil volume in stratified soils and in homogeneous soil 2 is much less than that in homogeneous soil 1 (Table 5.3).

Based on the BC model, when the apparent oil thickness in monitoring wells is less than the minimum apparent oil thickness, there will be no free phase oil in porous media; that is, specific oil volume is zero (MW-6 in Table 5.3). Specifically, the minimum apparent oil thickness is 1.563 m for soil 1 and 1.016 m for soil 2, but the apparent oil thickness in MW-6 is 1.1 m. Therefore, the specific oil volume in soil 1 and in stratified oils is zero and it is bigger than the aero in soil 2 (Table 5.3).

5.1.4 Discussions

(1) Specifically, the specific oil volume in stratified soils is the function of the apparent thickness of the free oil in the monitoring wells, the ordering of soils and the distributions of this apparent thickness (i.e. the relation of the interface of soils and the apparent thickness in the monitoring wells). It is different from the specific oil volume in the homogeneous soil that is only the function of the apparent thickness of oil in the monitoring well.

(2) When BC model parameters are used to calculate the specific oil volume of free-phase oil in a two-layer soils system, the apparent oil thickness should be bigger than the minimum apparent oil thickness computed by the upper soil parameters in order to get the non-zero specific oil volume. Unless the height of the apparent oil thickness in lower soil in the monitoring wells is much greater than the minimum

apparent oil thickness computed by the lower soil BC model parameters, the specific oil volume in a two-layer soils system mainly depends on the characteristics of the upper porous medium.

5.2 Development of a user-friendly modeling system

5.2.1 Development of interface system

The developed model in Chapter 3 was programmed into a user-friendly model system in this section. It also provides guidance on how to use the toolkit software utility to evaluate LNAPL volume under a range of conditions. First, an overview of the program menus and structure is given. The reader is then guided through data input, with a discussion of the parameter selection process. Also this chapter provides a sample application of the tool for the real site described in section 5.1.1.

In order to compute the total free-phase oil volume, a program has been developed. The program flowchart is shown in Figure 5.13.

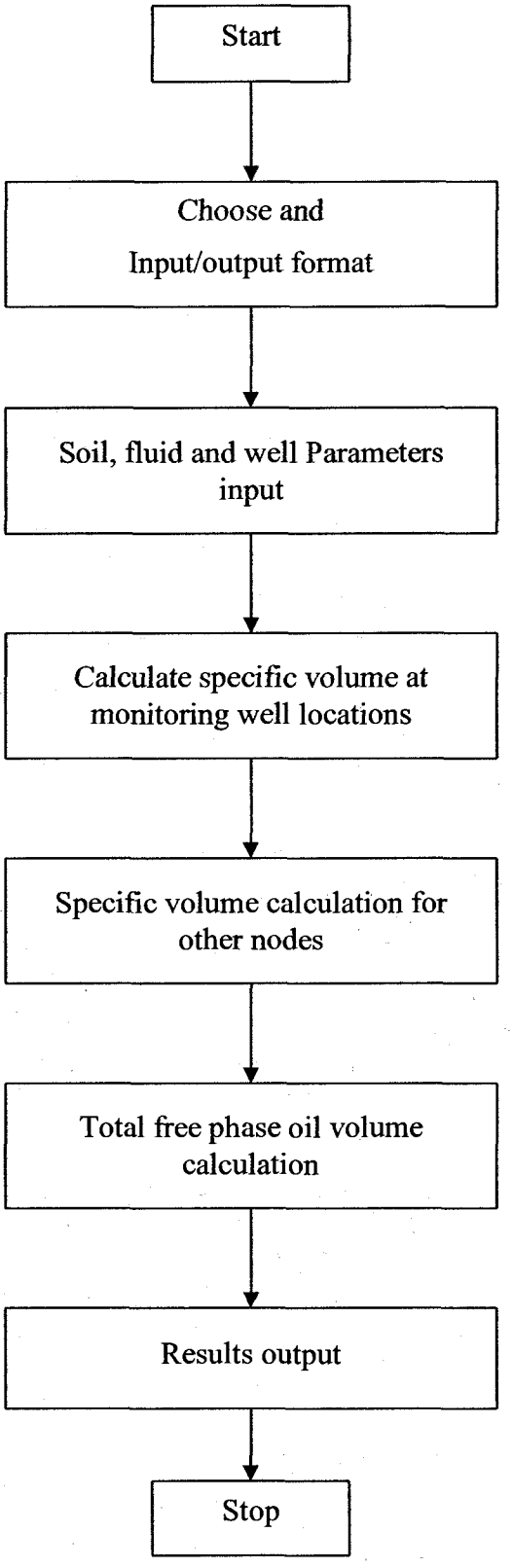

Figure 5.13 Flowchart of the modeling system

5.2.2 System user guide

This software utility is organized as a standard Microsoft Windows program. The user must select and input the appropriate soil, groundwater, and LNAPL physical and chemical properties. This is done through a series of five input tabs in the LNAPL utility, identified as "Soil Properties", "Groundwater Conditions", "Source Area Parameters", and "LNAPL Properties". The petroleum contaminated site in Section 5.1 is used for this user-friendly modeling system.

5.2.2.1 Model and input options

The first step will choose the model. This system includes a BC model and a VG model; users can choose one of them in accordance with the available parameters (Figure 5.14).

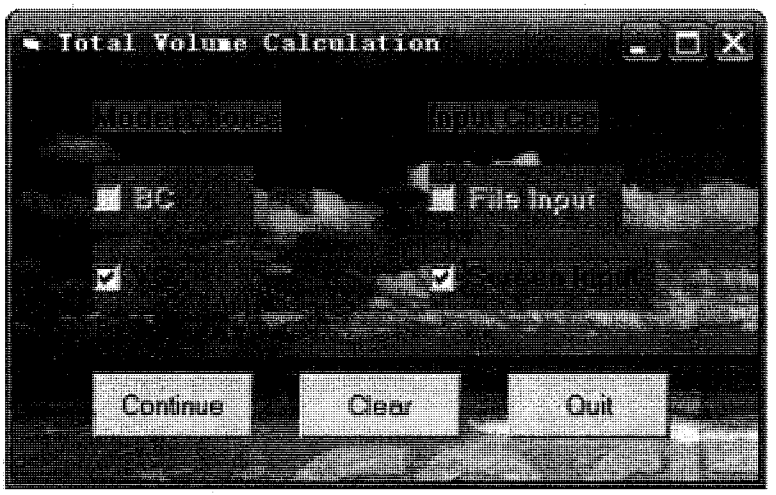

Figure 5.14 Interface of model choice

Also the users can choose an input style-file input or screen input. When users choose the file input, this program will show the file-input option (Figure 5.15). The input file must be in the same folder.

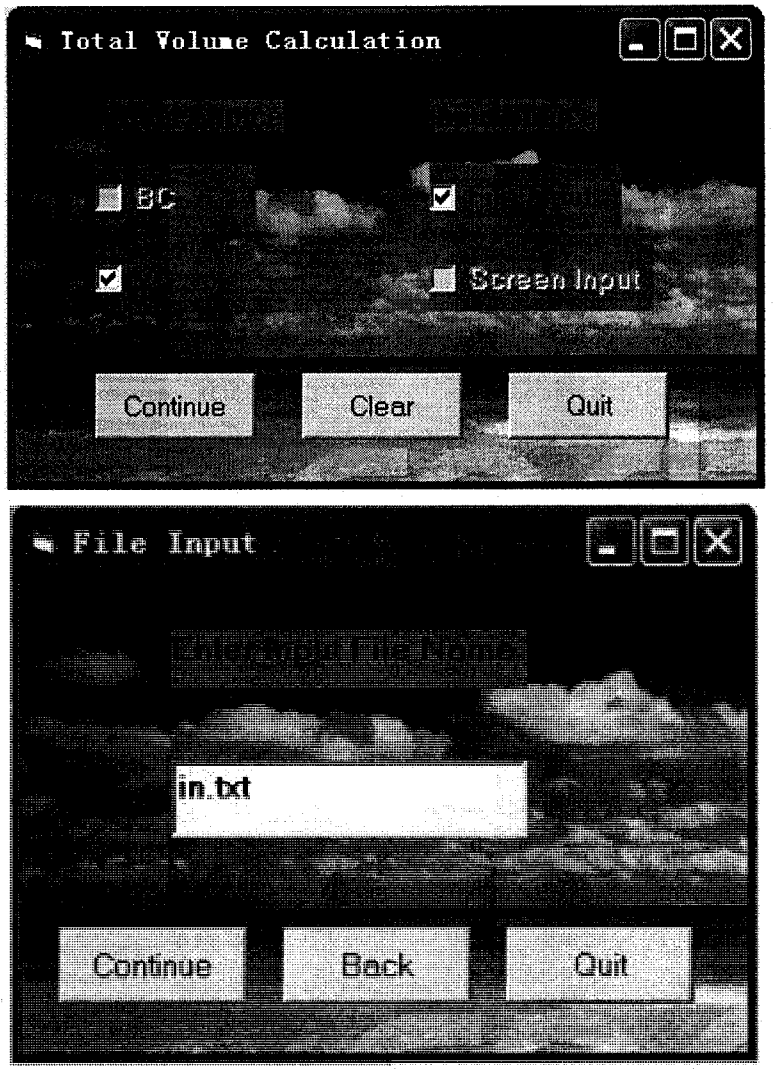

Figure 5.15 Interface of input file

5.2.2.2 Data input

Users familiar with multiphase fluid mechanics and fate and transport principles may not require much guidance, but we still recommend reviewing parameter definitions used here since they may be slightly different from those the user has employed in the past. It should be kept in mind, however, that highly erroneous results can be generated if parameter uncertainty and the sensitivity of the results to the input assumptions and the site conceptual model are not accounted for. Almost certainly a range of site

conditions must be considered to gain a full spectrum of reasonable results. Similarly, the applicability of certain assumptions inherent in the definition of the LNAPL source term and all the other related factors must be carefully thought out.

✓ Soil Properties

The soil parameters may be input either by assuming that the soil is homogeneous, or by subdividing the vertical LNAPL impacted zone into two different layers. The user makes this choice by enterin the soil type numbers (Figure 5.16) to select either the Homogeneous Conditions or the Vertically Layered Conditions option button on the Properties input.

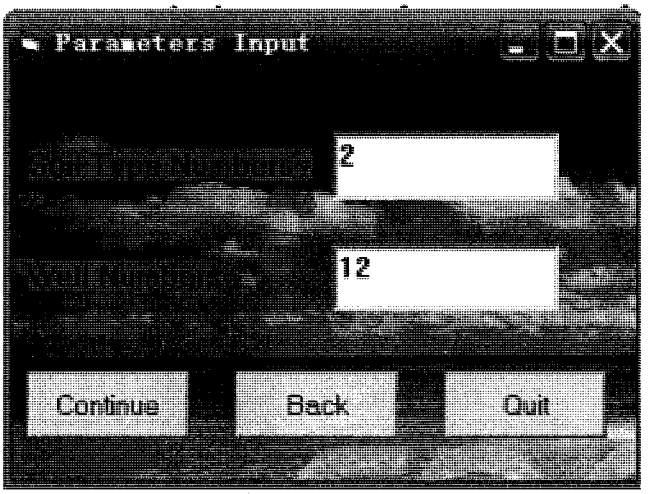

Figure 5.16 Interface of parameters input

If the Vertically Layered Conditions option is selected, values for each of these parameters must be selected for each of the different layers. Users should click "Another soil" to separately input the soil properties (Figure 5.18, 5.18). Figure 5.17 shows the soil properties of the BC model. Figure 5.18 shows the soil properties of a VG model.

Parameters with regards to soils based on the BC model are the following: porosity, residual water saturation in the soil (S_m), and BC model parameters, i.e. λ and h_d. The parameters for soils based on the VG model are the following: porosity, residual water saturation in the soil (S_m), and VG model parameters, i.e. n andα.

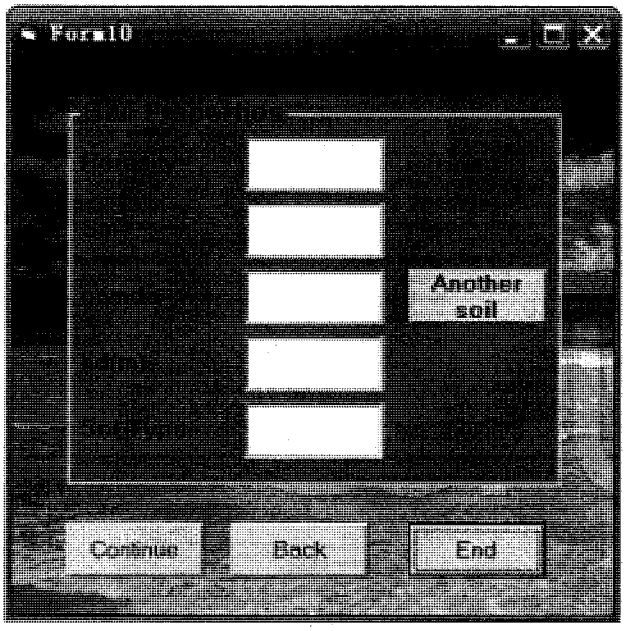

Figure 5.17 Interface of soil parameters input (BC model)

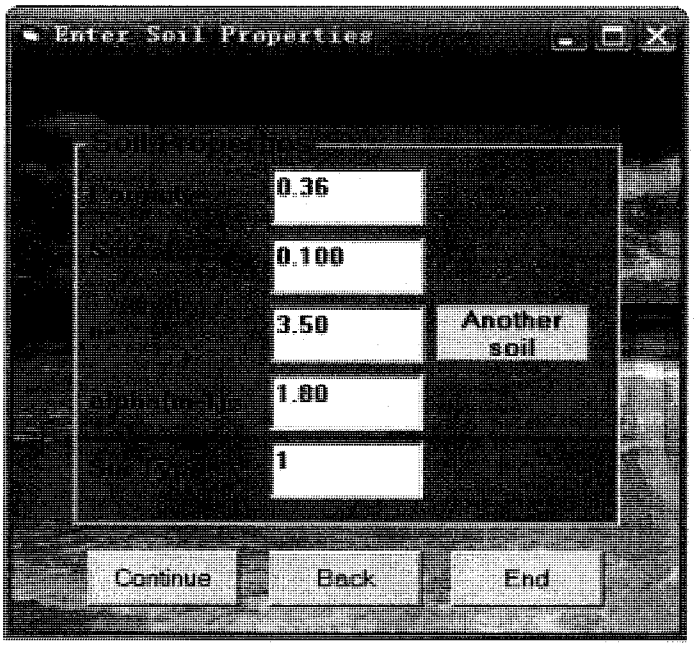

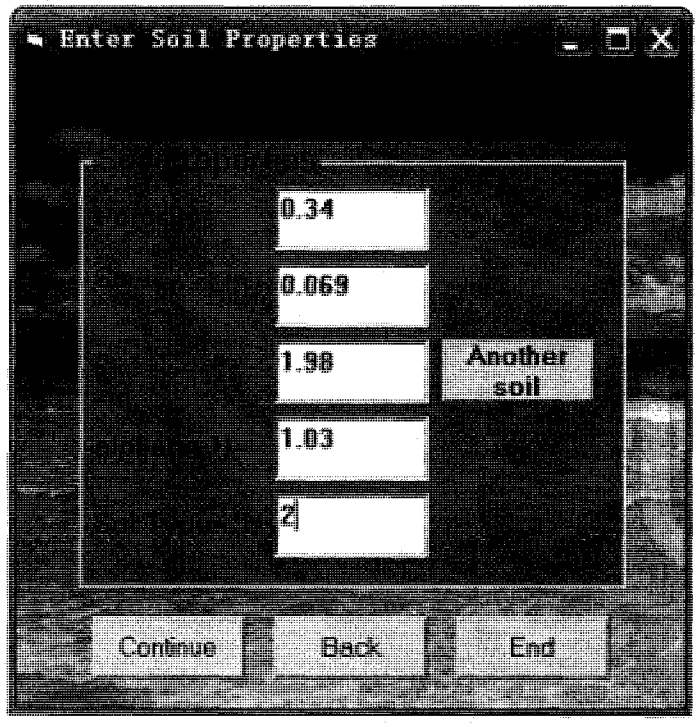

Figure 5.18 Interface of soil parameters input (VG model)

✓ Fluid Properties

Fluid parameters include specific gravity, the air-water scaling factor, and the water-LNAPL scaling factor (Figure 5.19).

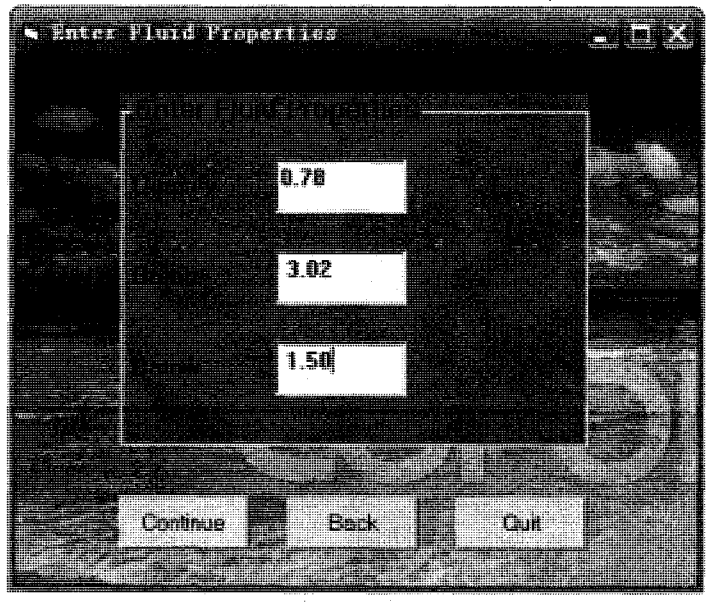

Figure 5.19 Interface of fluid parameters input

✓ Mesh parameters

This section includes site area data and monitoring well data (coordinates, depth of interface of air-oil, depth of interface of oil and water, depth of interface of soils see Figure 5.21), mesh data (number of meshes in x and y directions, maximum length of the site in the x and y directions, see Figure 5.20).

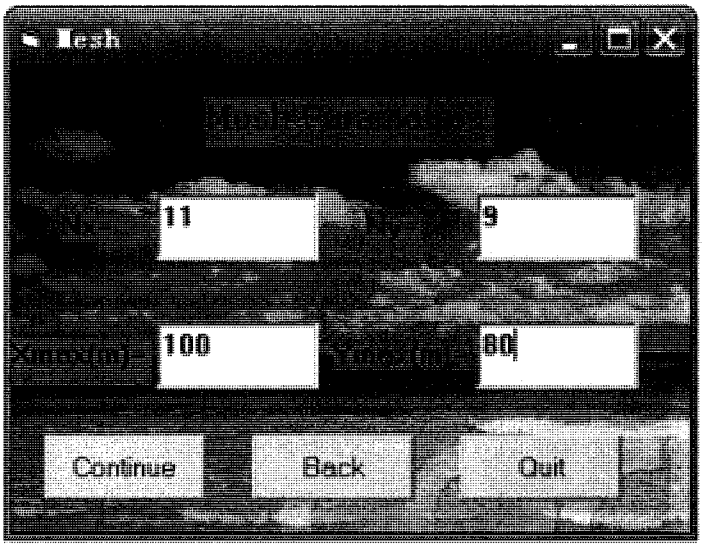

Figure 5.20 Interface of mesh input

The system is developed to calculate the specific volume in the nodes where the monitoring wells are located.

This system is to interpolate the specific volume in other nodes and to compute the total volume. The finite difference method is utilized to interpolate the specific volume.

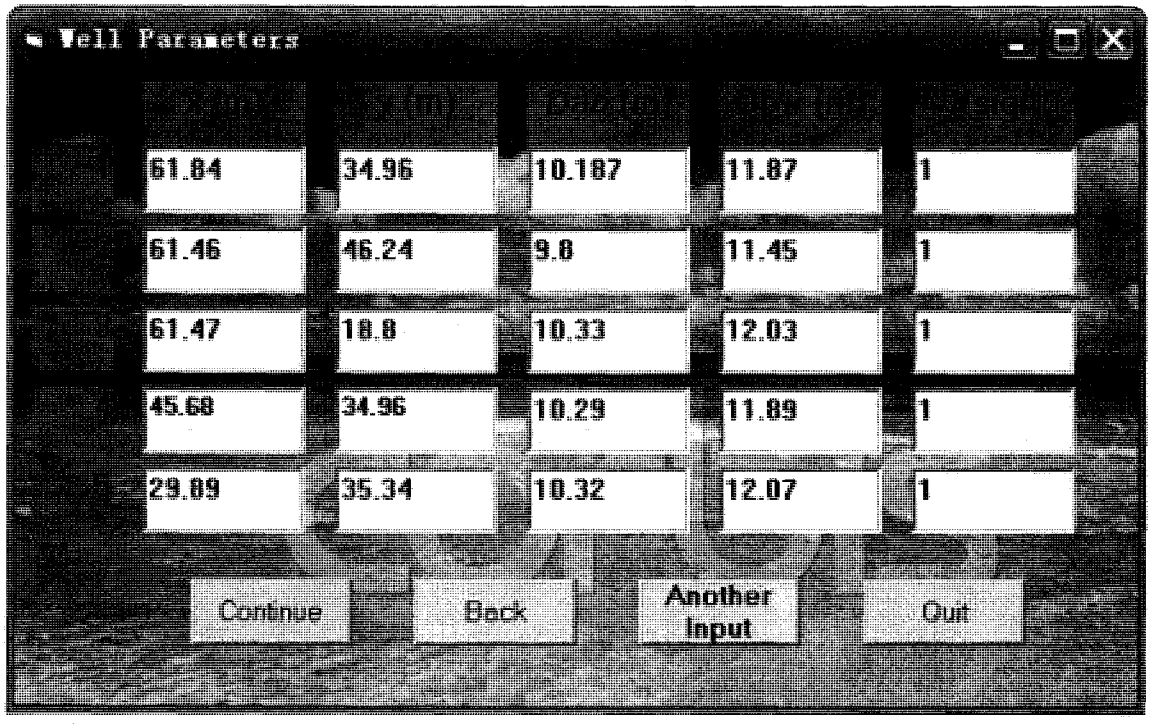

Figure 5.21(a) Interface of well parameters

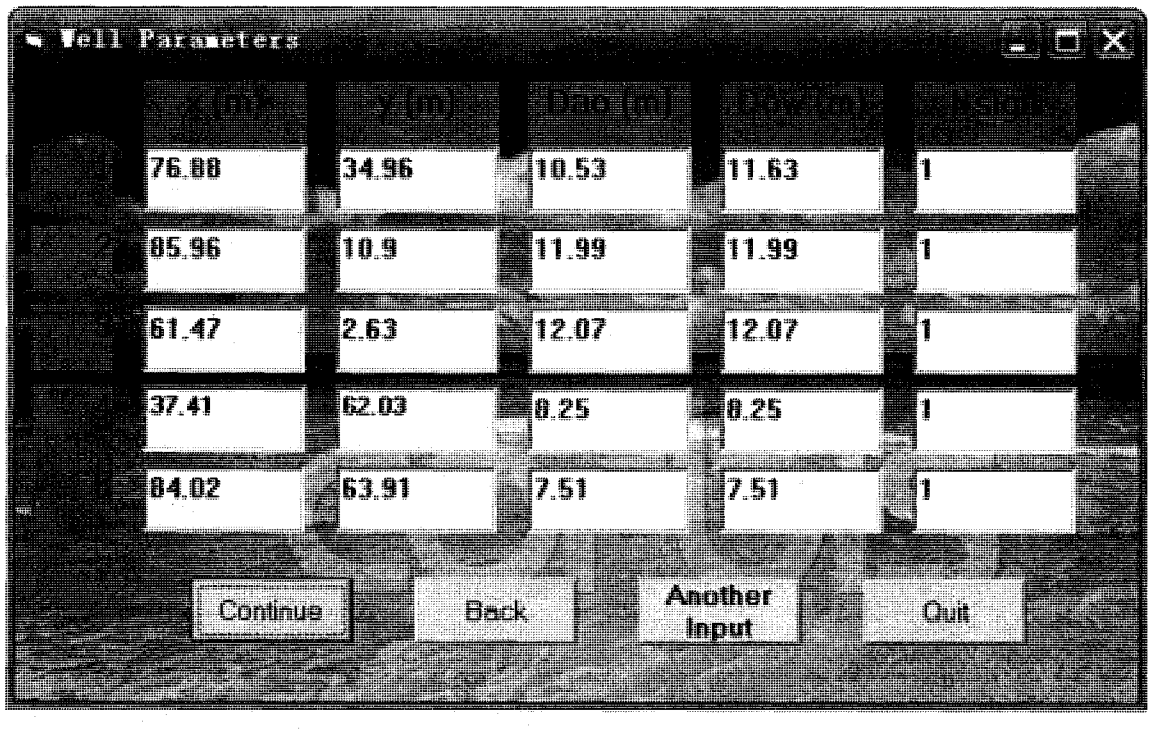

Figure 5.21(b) Interface of well parameters

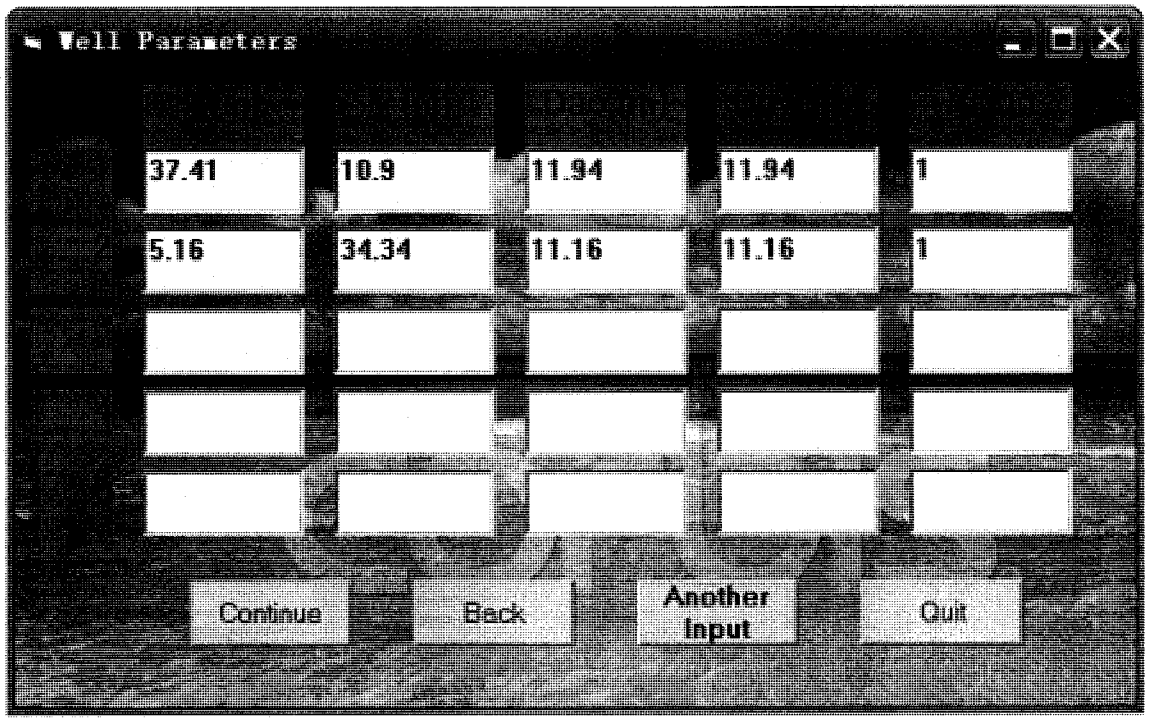

Figure 5.21(c) Interface of well parameters

This system can deal with a maximum of 100 wells and 100*100 coordinate grids.

✓ Output of program

The Output option allows the user to save the result with file and screen output (Figure 5.22, 5.23). The user can use other commercial software to draw a contour map, for example, SURFER.

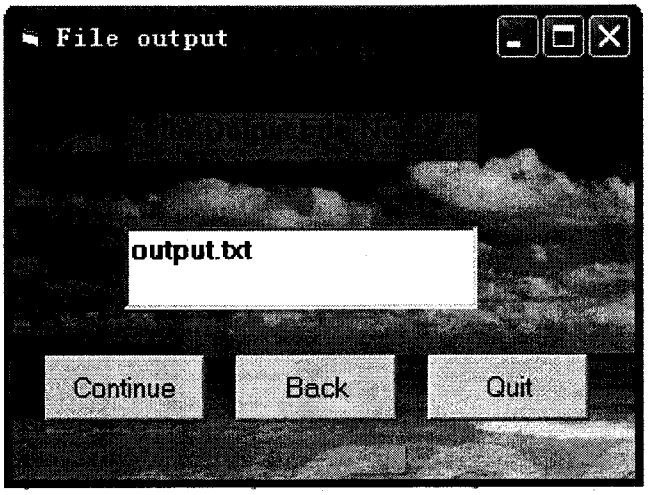

Figure 5.22 Interface of file output option

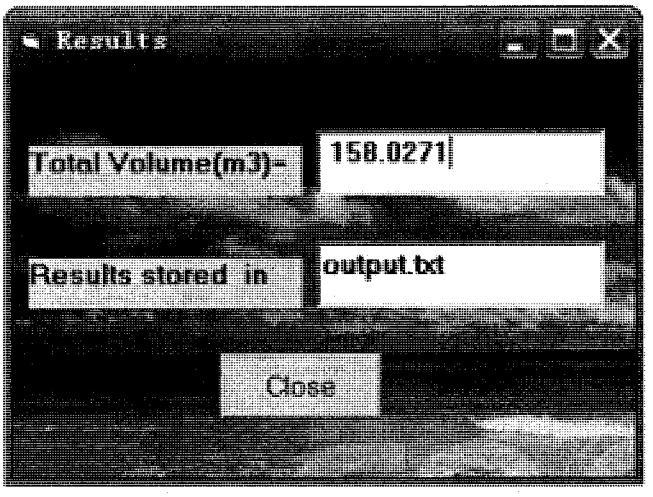

Figure 5.23 Interface of the results

As shown in Figure 5.23, the interface system generates the same result as in the real case study in section 5.1.

Chapter 6

Conclusions, research contributions and future studies

6.1 Conclusions

The following conclusions can be obtained from this study:

(1) The effects of soil layering on the specific oil volume in the porous media have been discussed in this study. It indicates a significant influence of stratified soils on the specific volume of free phase oil and its distribution in the porous media. The developed method for the oil volume in multiple layers porous media is more practical than the solution obtained by assuming that only one kind of soil is present.

(2) Considering the heterogeneity of the sites is very important and the developed system can get accurate results compared with simplified sites

in soil types. Besides soil heterogeneity, the mesh delimitation and interpolation method also affect the total free phase oil volume computed for a site. Nevertheless, the accurate total oil volume estimation of free phase oil is the basis for effective recovery of leaked oil in the sites, and reasonable results have been obtained through applying the developed model to typical site cases.

(3) The developed system is helpful for the estimation of the total free-phase oil volume, and the developed user-friendly interface system facilitates the usage of the model.

6.2 Research contributions

The research contributions of this thesis are summarized in below:

(1) A new modeling approach has been developed in this study to compute the volume of oil spilled into the groundwater system, which is a critical step before any cleanup action being taken.

(2) The developed model improved previous models on considering the heterogeneous characteristics of the nature soil and groundwater system.

(3) A physical pilot scale experiment with different amounts of oil spill was conducted in this thesis study, which has provided a systematic validation of the developed model.

(4) The developed approach has been successfully applied to a real oil spill site with its groundwater being contaminated by the spilled oil. The application has provided technical details to support the site remediation.

(5) Additionally, a user-friendly interface was developed in this study, which will facilitate the use and application of the developed model.

(6) Finally, detailed sensitivity analysis has been conducted to examine various uncertainties associated with the site, spilled oil, and modeling methods.

6.3 Future studies

The following topics are suggested in the future studies:

(1) Advanced methods, such as fuzzy logic and stochastic analysis, can be used to quantify system uncertainties.

(2) The developed method can be linked with pollutants fate and transport simulation to support effective environmental risk assessment and site remediation.

(3) Further, numerical analysis can be incorporated into the developed model to enhance the modeling accuracy.

(4) Also based on the above recommendations, the complete nature heterogeneous soil and groundwater can be considered to obtain accurate calculation of spilled oil volume.

Reference

Abdul, A.S., Kia, S.F. and Gibson, T.L., 1989. Limitations of monitoring wells for the detection and quantification of petroleum products in soils and aquifers, Ground Water Monitoring Review, 9(2): 90-99.

Abriola, L.M., 1983. Mathematical modeling of the multiphase migration of organic compounds in a porous medium, Ph.D. Dissertation, Department of Civil Engineering, Princeton University, Princeton, N.J.

Abriola, L.M. and Pinder, G.F., 1985a. A multiphase approach to the modeling of porous media contamination by organic compounds, 1.Equation development, Water Resour. Res., 21: 11–18.

Abriola, L.M. and Pinder, G.F., 1985b. A multiphase approach to the modeling of porous media contamination by organic compounds, 2. Numerical simulation, Water Resour. Res., 21: 19-26.

AEHS, 1999. Total Petroleum Hydrocarbon Criteria Working Group Series Volume 1: Analysis of Petroleum Hydrocarbons in Environmental Media, edited by Wade Weisman, Amherst Scientific Publishers, Amherst, MA.

AEHS, 1999. Total Petroleum Hydrocarbon Criteria Working Group Series Volume 2: Composition of Petroeum Mixtures, prepared by T.L. Potter and K.E. Simmons, Amherst Scientific Publishers, Amherst, MA.

AEHS, 1999. Total Petroleum Hydrocarbon Criteria Working Group Series Volume 3: Selection of Representative TPH Fractions Based on Fate and Transport Considerations, by J.B. Gustafson, Amherst Scientific Publishers, Amherst, MA.

Ahlfeld, D., Dahmani, A, Hoag, G. and Farrell, M., Ji W., 1994. Field Measurements of Air Sparging in a Connecticut Site: Results and Comments. Proceedings of Petroleum Hydrocarbons and Organic Chemicals in Ground Water: Prevention, Detection and Restoration, Houston.

API (American Petroleum Institute), 1980. The migration of petroleum products in the soil and groundwater, Principles and countermeasures, API Publication 1628, Washington, DC.

API (American Petroleum Institute), 1988. Phase separated hydrocarbon contaminant modeling for corrective action, API Publication 4474, Washington, DC.

API (American Petroleum Institute), 1994. Transport and Fate of Non-BTEX Petroleum Chemicals in Soils and Groundwater, Health and Sciences Department, API Publication 4593, Washington, DC.

API (American Petroleum Institute), 1999. Assessing the Significance of Subsurface Contaminant Vapor Migration to Enclosed Spaces, API Publication 4674, Washington, DC.

API (American Petroleum Institute), 2003. Models for Design of Free-Product Recovery Systems for Petroleum Hydrocarbon Liquids, API Publication 4729, Washington, DC.

API Interactive LNAPL Guide, Version 2.0, 2004. http://www.api.org/ehs/groundwater/lnapl/

ASTM American Society for Testing and Materials, Standard test method for particle-size Analysis of Soils, ASTM D422-63(2002) e1. http://www.astm.org

Ballestero, T.P., Fiedler, F.R. and Kinner, N.E., 1994. An investigation of the relationship between actual and apparent gasoline thickness in a uniform sand aquifer, Ground Water, 32(5): 708-718.

Beahr, A.L. and Corapcioglu, M.Y., 1987. A compositional multiphase model for groundwater contamination by petroleum products, 2. Numerical solution, Water Resour. Res., 23: 201-213

Baehr, A.L., 1987. Selective Transport of Hydrocarbon in the Unsaturated Zone Due to Aqueous and Vapor Phase Partitioning, Water Resour. Res., 23: 1926-1938.

Bear, J., 1972. Dynamics of Fluids in Porous Media. American Elsevier, New York, N.Y.

Beckett, G.D. and Lundegard, P., 1997. Practically Impractical - The limits of LNAPL recovery and relationship to risk. Proceedings of petroleum hydrocarbons and organic chemicals in ground water: prevention, detection and restoration, Houston.

Beckett, G.D., Huntley, D. and Panday, S., 1995. Air Sparging: a Case Study in Characterization, Field Testing, and Modeling Design. Proceedings of the

Petroleum Hydrocarbons and Organic Chemicals in Ground Water: Prevention, Detection and Restoration, Houston.

Beckett, G.D. and Huntley, D., 1998. Soil Properties and Design Factors Influencing Free-phase Hydrocarbon Cleanup, Environmental Science and Technology, 3: 287–293.

Blake, S.B. and Hall, R.A., 1984. Monitoring petroleum spills with wells: some problems and solutions. Proceedings, Fourth National Symposium on Aquifer Restoration and Groundwater Monitoring, National Water Well Association, Columbus, OH, 305-310.

Bradley, H.B., 1987. Petroleum Engineering Handbook. Society of Petroleum Engineers, Richardson, TX.

Brooks, R.H. and Corey, A.T., 1964. Hydraulic properties of porous media, Colo. State Univ., Fort Collins, Colo., Hydrol. Pap.

Brost, E. and Beckett, G.D., 2000. A multiphase screening method to determine fuel immobility in the unsaturated zone, AEHS Conference workshop, San Diego, California.

Buckley, S.E. and Leverett, M.C., 1942. Mechanism of Fluid Displacement in Sands, Trans., AIME, 146: 107–116.

Carsell, R.F. and Parish, R.S., 1988. Developing joint probability distributions of soil water retention characteristics, Water Resour. Res., 24: 755-769.

Charbeneau, R.J., Johns, R.T., Lake, L.W. and McAdams III., M.J., 1999. Free-product recovery of petroleum hydrocarbon liquids, API Publication 4682, Washington, DC.

Chiang, C.Y., Nevin, J.P. and Charbeneau, R.J., 1990. Optimal free hydrocarbon recovery from a single pumping well. Proceedings of Petroleum Hydrocarbons and Organic Chemicals in Ground Water: Prevention, Detection, and Restoration Conference, Houston, TX. National Water Well Association.

Cooley, R.L., 1983. Some New Procedures for Numerical Solution of Variably Saturated Flow Problems, Water Resour. Res., 5: 19-27.

Corapcioglu, M.Y. and Beahr, A.L., 1987. A compositional multiphase model for groundwater contamination by petroleum products, 1. Theoretical considerations. Water Resour. Res., 23: 191-200.

Corey, A.T., 1986. Mechanics of immiscible fluids in porous media, Water Resources Publishers, Littleton, Colo.

De Pastrovich, I.L., Barthel, Y., Chiarelli, A. and Fussell, D.R., 1979. Protection of groundwater from oil pollution, CONCAWE Report No. 3/79, Den Haag, Netherlands.

Domenico, P.A. and Schwartz, F.W., 1990. Physical and chemical hydrogeology, Wiley, New York, NY.

Dragun, J., 1988. The soil chemistry of hazardous materials, Hazardous materials research institute, Silver Spring, MD.

Dupont, R.R., Doucett, W.J., Hinchee, R.J., 1991. Assessment of in-situ bioremediation potential and the applicability of bio-venting at a fuel contaminated site. In: Hinchee, R.E. and Olfenbuttel, eds. In-Situ Bioremedation, Butterworth-Heinemann Pub.

Durnford, D., Brookman, J., Billica, J. and Milligan, J., 1991. LNAPL distribution in a cohesionless soil: a field investigation and cryogenic sampler, Groundwater Monitoring, 11(3): 115–122

Ehrlich, G.G., Schroeder, R.A. and Martin, P., 1985. Microbial populations in a jet-fuel contaminated shallow aquifer at Tustin, California. U.S. Geol. Surv. Open File Rep.

Environmental Protection Agency (EPA), 1995. Risk assessment guidance for superfund, office of emergency and remedial response, EPA Publication EPA/540/R-95/132, Washington, DC.

Farr, A.M., Houghtalen, R.J. and McWhorter, D.B., 1990. Volume estimation of light nonaquous phase liquids in porous media, Ground Water, 28(1): 48-56.

Fetter, C.W. 1994, Applied Hydrogeology, 3rd Edition, MacMillan College Publishing Company, NY.

Fetter, C.W. 1999. Contaminant Hydrogeology , Second Edition, Prentice-Hall Publishing Company, NJ.

Forsyth, P.A., 1990. A finite volume approach to NAPL groundwater contamination, research report, CS-89-46, University of Waterloo, Waterloo, Ontario, Canada.

Frank, R.J. and Huntley, D., 1997. Processes affecting free-phase hydrocarbon removal by vapor extraction. Proceedings of the 1997 Petroleum Hydrocarbons and Organic Chemicals in Ground Water: Prevention, Detection, and Remediation. National Ground Water Association. Houston, TX.

Freeze, R.A. and Cherry, J.A., 1979. Groundwater, Prentice-Hall, Inc., Englewood Cliffs, NJ.

Gillham, R.W., Klute, A. and Heermann, D.F., 1979. Measurement and numerical simulation of hysteretic flow in a heterogeneous porous media, Soil Sci., 43(6):1061-1065.

Hall, R.A., Blake, S.B. and Champlin, S.C., 1984. Determination of hydrocarbon thickness in sediments using borehole data. In: Proceedings of the 4th National Symposium on Aquifer Restoration and Groundwater Monitoring. Natl Water Well Assoc., Columbus, Ohio.

Hampton, D.R. and Miller, P.D.G., 1988. Laboratory investigation of the relationship between actual and apparent product thickness in sands, Environmental Concerns in the Industry, S.M. Testa, ed., Pacific Section, Amer. Assoc. Petrol. Geo., Palm Springs, CA, 31-55.

Heath, R.C., 1989. Basic Ground-Water Hydrology, United States Geological Survey Water-Supply Paper 2220, United States Government Printing Office.

Hillel, D., 1982. Introduction to Soil Physics, Academic Press, New York.

Honapour, M., Koederitz, L. and Harvey, A.H., 1986. Relative Permeability of Petroleum Reservoirs, CRC Press, Inc., Boca Raton, Florida.

Howard, P.H., Boethling, R.S., Jarvis, W.F., Meylan, W.M. and Michalenko, E.M., 1991. Handbook of Environmental Degradation Rates, CRC Press, Inc., Boca Raton, Florida.

Hunt, W.T., Wiegand, J.W. and Trompeter, J.D., 1989. Free gasoline thickness in monitoring wells related to ground water elevation change. In Proc. Conf. on New Field Techniques for Quantifying the Physical and Chemical Properties of Heterogeneous Aquifers, Natl. Ground Water Assoc., Dublin, OH, 671-692.

Huntley, D., 1997. Analytic Determination of Hydrocarbon Transmissibility from Baildown Tests. Conference Proceedings of the 1997 Petroleum Hydrocarbons & Organic Chemicals in Ground Water, Houston, Texas, sponsored by the National Ground Water Association & American Petroleum Institute.

Huntley, D., Hawk, R. and Wallace, J., 1991. An analysis of the history, distribution, and movement of the blob, a hydrocarbon pool underlying downtown San Diego; in, Abbott, P. (ed), Environmental Perils: San Diego Association of Geologists.

Karickhoff, S.W. and Brown, D.S., 1979. Determination of Octanol/Water Distribution Coefficients, Water Solubilities, and Sediment/Water Partition Coefficients for Hydrophobic Organic Pollutants. Series Title: Research Reporting Series 4, Environmental Monitoring ; EPA-600/4-79-032. Environmental Research Laboratory, Office of Research and Development, Athens, GA. U.S. Environmental Protection Agency, Springfield, VA.

Kemblowski, M.W. and Chiang, C.Y., 1990. Hydrocarbon thickness fluctuations in monitoring wells, Ground Water, 28(2): 244-252.

Kramer, W.H., 1982. Ground water pollution from gasoline, Groundwater Monitoring, 2(2): 18-22.

Lenhard, R.J. and Parker, J.C., 1987. Measurement and prediction of saturation-pressure relationships in three-phase porous media systems, Journal of Contaminant Hydrology, 1: 407-424.

Lenhard, R.J., Parker, J.C. and Mishra, S., 1989. On the correspondence between Brooks-Corey and van Genuchten models, Journal of Irrigation and Drainage Engineering, 115(4): 744-751.

Lenhard, R.J. and Parker, J.C., 1990a. Estimation of free hydrocarbon volume from fluid levels in monitoring wells, Ground Water, 28(1): 57-67.

Lenhard, R.J. and Parker, J.C., 1990b. Discussion of estimation of free hydrocarbon volume from fluid levels in monitoring wells, Ground Water, 28(5): 800-801.

Lundy, D.A. 2002. There are better ways to regulate free product, Ground Water Monitoring and Remediation, 22(3): 4-8.

Mace, R.E., Fisher, R.S., Welch, D.M. and Parra, S.P., 1997. Extent, Mass, and Duration of Hydrocarbon Plumes from Leaking Petroleum Storage Tank Sites in Texas, Bureau of Economic Geology, the University of Texas, Austin, TX, Geologic Circular 97-1.

MAGNAS3, 1992. Multiphase analysis of groundwater, non-aqueous phase liquid and soluble component in 3 dimensions, Documentation and user's guide, HydroGeoLogic, Inc., Herndon, Virginia.

Marinelli F. and Durnford, D.S., 1996. LNAPL thickness in monitoring wells considering hysteresis and entrapment, Groundwater, 34: 405-414.

Mercer, J.W. and Cohen, R.M., 1990. A review of immiscible fluids in the subsurface: Properties models, characterization and remediation, J. Conta. Hydrol., 6: 107-163.

Mualem, Y., 1976. A New Model for Predicting the Hydraulic Conductivity of Unsaturated Porous Media, Water Resour. Res., 12: 513–522.

Newell, C., Acree, S.D., Ross, R.R. and Huling, S.G., 1995. Light Non-aqueous Phase Liquids, EPA/540/S-95/500.

Parker, J.C., Lenhard, R.J. and Kuppusamy, T., 1987. A parametric model for constitutive properties governing multiphase flow in porous media, Water Resour. Res., 23: 618-24.

Parker, J.C. and Lenhard, R.J., 1989. Vertical integration of three phase flow equations for analysis of light hydrocarbon plume movement, Transport in Porous Media, 5: 187-206.

Parker, J.C. and Kayal, A., 1990. Technical documentation for the numerical modeling code, ARMOS. Environmental Science and Technology, Blacksburg, Virginia.

Puls, R.W. and Barcelona, M.J., 1996. Ground water issue: low-flow (minimal drawdown) ground-water sampling. Ada, Okla.: National Risk Management Research Laboratory, Subsurface Protection and Remediation Division, Robert S. Kerr Environmental Research Center, 1996. EPA/540/S-95/504

Reid, R.C., Prausnitz, J.M. and Poling, B.E., 1987. The Properties of Gases and Liquids, McGraw -Hill, Inc.

Rice, D.W., Grose, R.D., Michaelsen, J.C., Dooher, B.P., MacQueen, D.H., Cullen, S.J., Kastenberg, W.E., Everette, L.G. and Marino, M.A., 1995. "California Underground Leaking Fuel Tank (LUFT) Historical Case Analyses". Submitted to the California State Water Resources Control Board and the Senate Bill 1764 Advisory Committee.

Schiegg, H.O., 1985. Considerations on water, oil, and air in porous media, Water Science and Technol, 17:467-476.

Schwille, F., 1984. Migration of organic fluids immiscible in water in the unsaturated zone. In: Yaron, B., Dagon, G. and Goldshmid J. (eds.), Pollutants in porous media: the unsaturated zone between soil surface and groundwater, Springer-Verlag, New York.

SERM (Saskatchewan Environment and Resource Management), 1995. Risk based corrective actions for petroleum contaminated sites, Regina, Saskatchewan, Canada.

Shephard, W.D., 1983. Practical geohydrological aspects of ground-water contamination. Proceedings of the National Water Well Association of Ground Water Scientists and Engineers, Third National Symposium on Aquifer Restoration and Ground Water Monitoring, 365–372.

Sleep, B.E., Sehayek, L. and Chien, C.C., 2000. A modeling and experimental study of light Nonaqueous phase liquid (LNAPL) accumulation in wells and LNAPL recovery from wells, Water Resour. Res., 36: 3535-3545.

USEPA. 1990. Laboratory investigation of residual liquid organics from spills, leaks, and disposal of hazardous wastes in groundwater, EPA/600/6-90/004. USEPA, Washington, DC.

van Ganuchten, M.T., 1980. A closed-form equation for predicting the hydraulic conductivity of unsaturated soils, Soil Sci. Soc. Am. J., 44: 892-898.

Weaver, J.W. and Johnson, J.A., 1993. Modeling for assessment and remediation of hydrocarbon spills. In: Proceedings 1993 GASReP Conference on Groundwater and Soil Remediation, Quebec City, Canada.

White, H., Faust, C. and Montroy, M., 1996. How to effectively recover free product at leaking underground storage tank sites, A Guide for state regulators. EPA Bulletin 510-R-96-001.

Wickramanayake, G.B., Gupta, N., Hinchee, N.G. and Nielsen, B.J., 1991. Free petroleum hydrocarbon volume estimates from monitoring well data, Journal of Environmental Engineering, 117(5): 686-691.

Wilson, J.T., Kampbell, D.H. and Armstrong, J., 1993. Natural bioreclamation of alkylbenzenes (BTEX) from a gasoline spill in methanogenic groundwater, Proc II Int Symp on in situ bioremediation, San Diego, CA, April 5-8.

Yaniga, P.M. and Demko, D.J., 1983. Hydrocarbon contamination of carbonate aquifers: assessment and abatement. Proceedings of the National Water Well Association of Ground Water Scientists and Engineers, Third National Symposium on Aquifer Restoration, 60–65.

Appendix A

Model sensitivity analysis

There are a large amount of uncertainties associated with from different types of input data. These parameters to simulation models rang from data include the porosity, VG model parameters, scaling factor, and several parameters used to define fluid characteristics. Sensitivity analysis is conducted in this Chapter to study the above modeling uncertainties.

Model sensitivity analysis

The parameters to be varied for the sensitivity analysis were chosen to demonstrate a range of conditions, all of which could be expected to vary depending on site specific circumstances. Through the model's calculation and considering the parameters' significance, three additional parameters were selected for this study. The porosity, the VG model parameters and the scaling factor are included in the sensitivity analysis.

1. Porosity

A sensitivity analysis was conducted to evaluate the impact of changes in selected variables based on the pilot-scale experiment case. The soil type is sand in the pilot-scale experiment. The ranges of parameters are given in Table A.1 and A.2.

Table A.1 Range of porosity

Soil type	Porosity		
Sand	Minimum	Maximum	Midpoint
	0.242	0.49	0.366

Source: After Carsell and Parish (1988)

The range of Porosity considered in the pilot-scale experiment case is given below (Table A.2).

Table A.2 Porosity in pilot-scale experiment case

			van Genuchten parameter	
Soil types	Porosity	Irreducible water residual saturation S_m	n	α (m^{-1})
Sand	*0.242~0.49	0.01	2.97	17.33
Fluid	Density ratio, ρ_{ro}	0.86		
Properties	Air-oil scaling factor	10.394		
	Oil-water scaling factor	2.275		

* Range used for sensitivity analysis

Based on the input range in Table A.2, three results of oil volume were obtained using the developed model as shown in Table A.3 for 600ml spill case.

Table A.3 The results of the oil volume with different porosity

Porosity	Volume of LNAPL (ml)
0.242 (min)	392
0.334 (mean)	542
0.49 (max)	795

Figure A.1 illustrate that soil porosity significantly influences volume. The minimum or maximum volume occurs and the volume of LNAPL is increasing with porosity increasing. In this case, when porosity is 0.49, the maximum volume emerges.

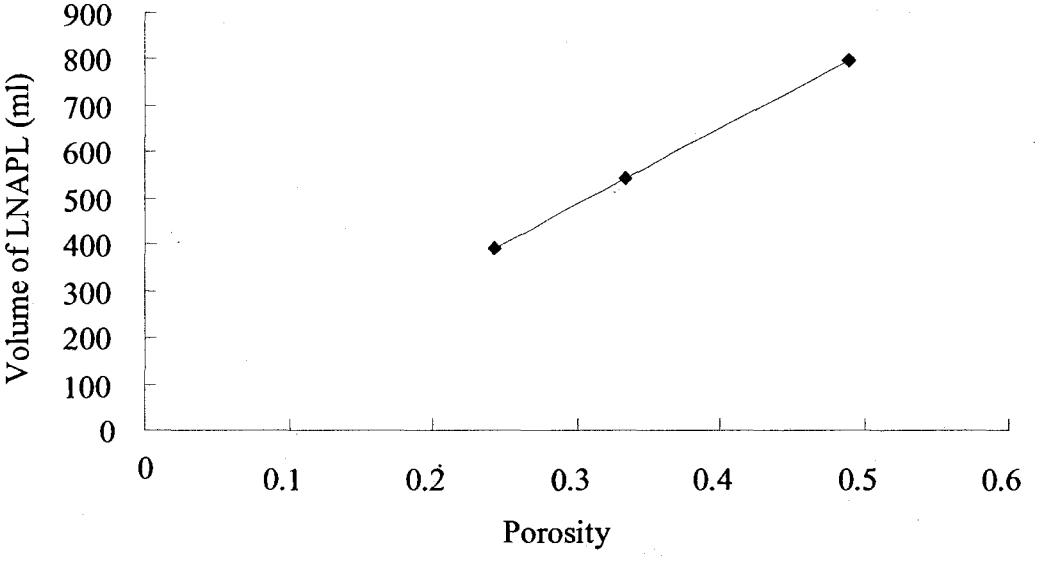

Figure A.1 Comparison LNAPL volumes in variation of porosity

2. VG parameter

The range of VG parameters is given below based on the literature survey (Table A.4).

Table A.4 Range of VG parameters

Soil type	van Genuchten n			van Genuchten α (m^{-1})		
Sand	Minimum	Maximum	Midpoint	Minimum	Maximum	Midpoint
	2.39	2.97	2.68	13.79	17.33	15.56

Source: API Interactive LNAPL Guide and Source: After Carsell and Parish (1988)

The range of the VG parameters is given below (Table A.5) in the pilot-scale experiment for 600ml spill case.

Table A.5 VG parameter based on the pilot-scale experiment case

			van Genuchten parameter	
Soil types	Porosity	Irreducible water residual saturation S_m	n	α (m^{-1})
Sand	0.343	0.01	*2.39~2.97	*13.79~17.33
Fluid	Density ratio, ρ_{ro}		0.86	
Properties	Air-oil scaling factor		10.394	
	Oil-water scaling factor		2.275	

* Range used for sensitivity analysis

The results of oil volume obtained based on the inputs in Table A.5 in the variation of VG-n are given below,

Table A.6 The results of the oil volume with different VG-n

VG-n	Volume of LNAPL (ml)
2.39	501
2.67	532
2.97	542

Figure A.2 illustrate that the VG-n parameter influences the volume. The very small change in the VG-n greatly influences the volume of LNAPL, and higher VG-n values lead to higher oil volume. In this case, when the VG-n is 2.97, the maximum volume emerges (Figure A.2).

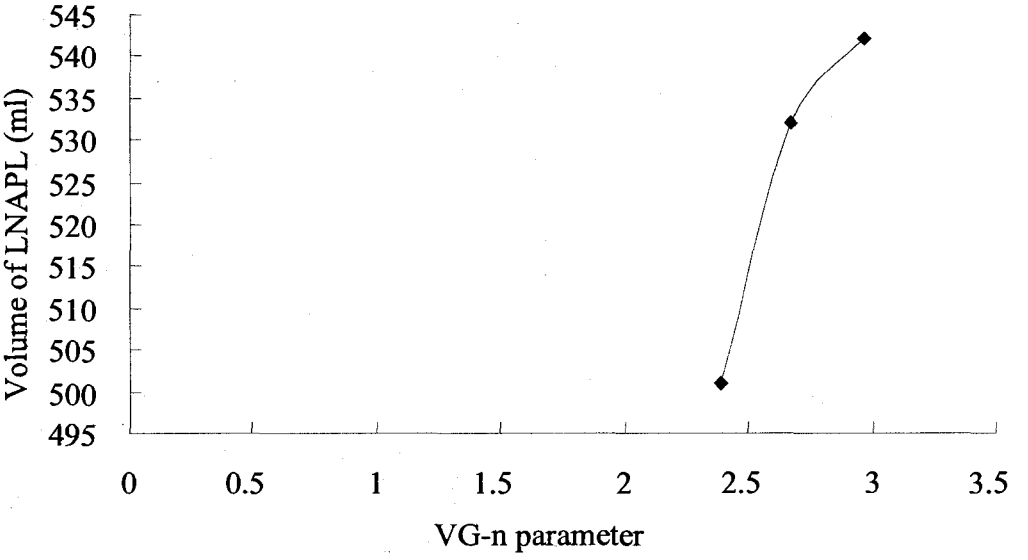

Figure A.2 Comparison LNAPL volumes in variation of VG-n

The results in variation of VG-α are obtained bellow (Table A.7),

Table A.7 The results of the volume in the variation of VG-α

VG-α	Volume of LNAPL (ml)
13.79	472
15.81	508
17.33	542

Figure A.3 illustrate that the VG-α parameter is with the similar effect as the VG-n parameter. It significantly influences the volume. In this case, when the VG-n is 17.33, the maximum volume emerges (Figure A.3).

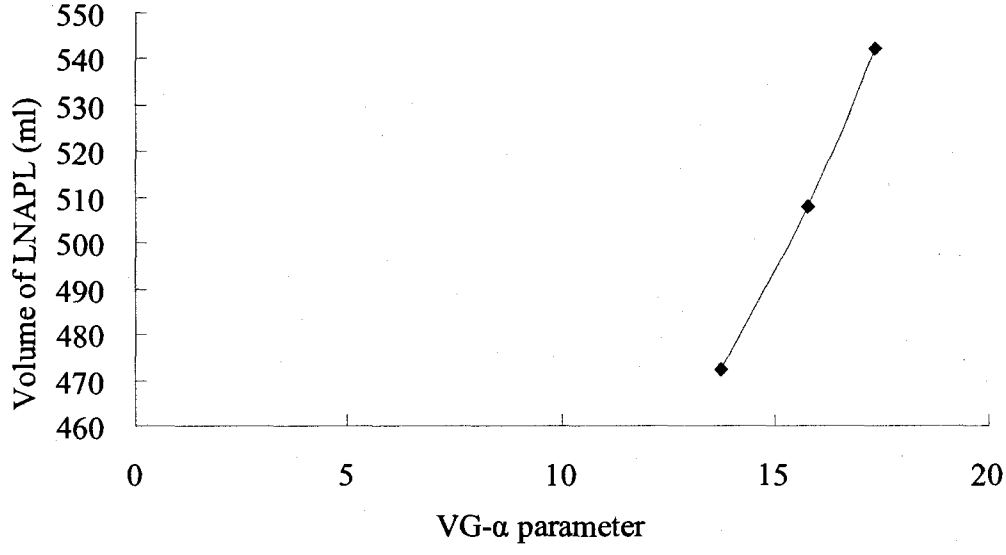

Figure A.3 Comparison LNAPL volumes in variation of VG-α

3. Scaling factor

The model parameters, scaling factor, of oil may also influence the volume of oil in the groundwater system. Scaling factor is reflected to the surface and interfacial tension of oil. The range is found based on literature survey as in Table A.8.

Table A.8 Range of surface and interfacial tension

Temperature (°C)	Surface tension (mN/m or dynes/cm)			Interfacial tension (mN/m or dynes/cm)		
	Minimum	Maximum	Midpoint	Minimum	Maximum	Midpoint
15	21.4	41	32	5.5	8.7	7.1

Source: ESD 96, Lubricating Oil (Industrial, Teresso 150)

The range of the scaling factor is given below (Table A.9) based on the pilot-scale experiment.

Table A.9 Scaling factor in pilot-scale experiment case

			van Genuchten parameter	
Soil types	Porosity	Irreducible water Residual saturation S_m	n	α (m^{-1})
Sand	0.334	0.01	2.97	17.33
Fluid	Density ratio, ρ_{ro}	0.86		
Properties	Air-oil scaling factor	*(10.394, 10.213)		
	Oil-water scaling factor	*(2.275, 2.364)		

* Range used for sensitivity analysis

The results in the variation of the Air-oil Scaling factor are given below (Table A.10),

Table A.10 The results of the oil volume with different air-oil scaling factors

Air-oil scaling factor	Volume of LNAPL (ml)
10.213	535
10.394	542

Figure A.4 illustrate that air-oil scaling factor parameter influences volume but not as significant as porosity, and the air-oil scaling factor parameter is in direct proportion with the volume of LNAPL. In this case, when the VG-n is 10.394, the maximum volume emerges (Figure A.4).

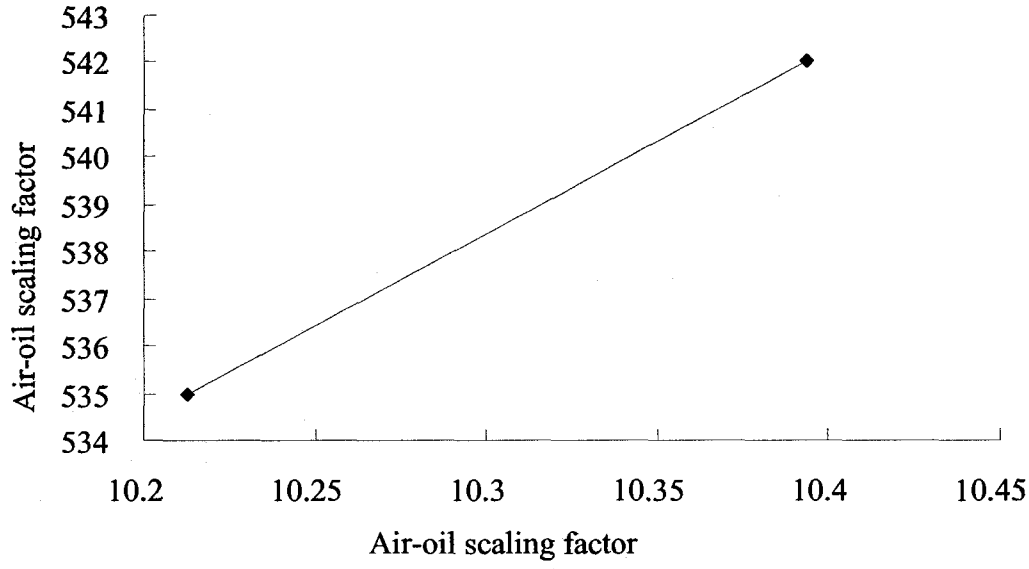

Figure A.4 Comparison LNAPL volumes in variation of air-oil scaling factor

The results in the variation of the oil-water scaling factor is given below (Table A.11),

Table A.11 The results of the oil volume with different oil-water scaling factors

Oil-water scaling factor	Volume of LNAPL (ml)
2.275	542
2.364	479

Figure A.5 illustrate that oil-water scaling factor parameter influences volume but not as significant as porosity. Moreover, the oil-water scaling factor parameter is in inverse proportion with the volume of LNAPL. In this case, when the VG-n is 2.275, the maximum volume emerges (Figure A.5).

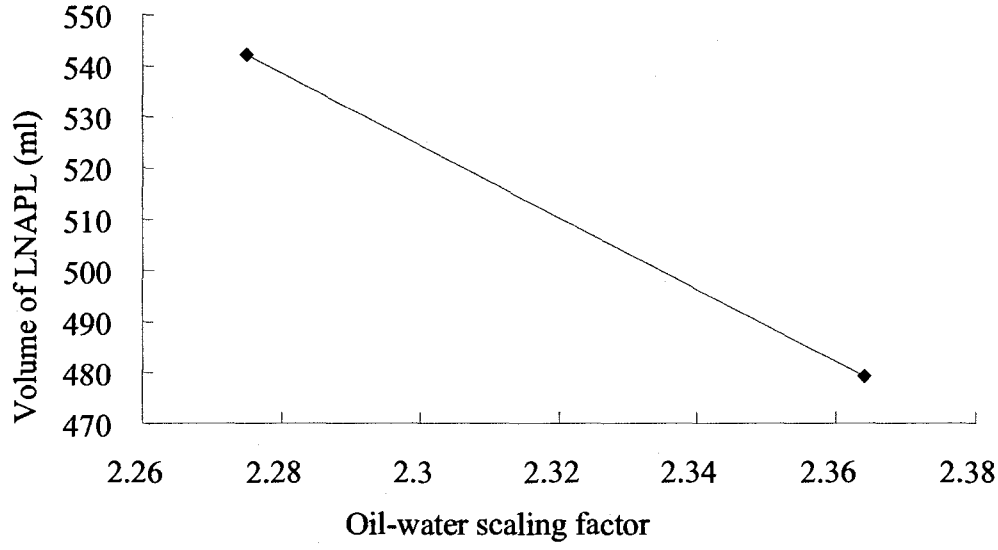

Figure A.5 Comparison of LNAPL volumes with the variation in the oil-water scaling factor

As a result, the volume of the LNAPL will increase with the porosity, the VG parameters and the increase in the air-oil scaling factor. The volume of the LNAPL will decrease with the increase in the oil-water scaling factor. Moreover, the porosity and VG parameters have a great influence on the volume of the LNAPL.

The extensive model sensitivity analyses have helped to examine the model parameters and their values in the model development, validation, and application in this thesis study.

Appendix B

Measurement of porosity and grain size distribution

Soils are made of particles of different types and sizes. The space between particles is called pore space. Pore space determines the amount of water that a given volume of soil can hold. Porosity is the percentage of the total volume of soil that consists of pore space. This is an important measurement in the experiment.

Porosity

The standard technique for measuring effective porosity is as follows (from Fetter, C.W., 1994, porosity measurement is on p. 81.)

Materials:

Balance, backer, measure cylinder, specific gravity bottle;

Procedure:

An alternative method uses density measurements.

Take a sample of known volume, Vt. Dry in an oven at 105 C until the sample weight is constant (this drives off pore water but does not dehydrate minerals).

A material's porosity could be evaluated by measuring its pore volume (V_p) and volume (Vt). The total volume is easily obtained by measuring the total volume of the sample. In principle, the pore volume could be evaluated directly by measuring the volume of needed to completely saturate the sample. In practice, this measurement is very difficult to make. Porosity is usually evaluated indirectly by using the expression $n = 1 - (V_s/V_t) = 1-(\rho_b/\rho_p)$, where n is the porosity, V_s is volume of the solid components, Vt is total volume, ρ_b is the dry bulk density of the sample, and ρ_p is the density of the solid component

The dry bulk density, ρ_b, of a dried soil sample is the mass of the dried sample divided by the volume of the sample.

Then the sample is broken into individual grains and the particle volume is measured by placing all the particles in water and measuring the volume of water displaced by the particles.

The mass of the dried sample, divided by the particle volume gives the particle density, ρ_p, of the sample. The percent porosity is the quantity one minus the bulk density divided by the particle density: $n = 1-(\rho_b/\rho_p)$.

Grain size distribution

The standard grain size analyses allow determining the relative proportions of different grain sizes that make up a given soil mass. The grain size analysis is widely used in soil classification and for determining hydraulic conductivity with a variety of empirically-derived formulas. The data obtained from grain size distribution curves is used in the design of filters for earth dams, the design of well screens, air fields, etc.

Materials:

Balance, Sieves, Soil collection tin

Procedure:

Using a sample of dry sand, the general procedure for completing your analyses is as follows:

In the tin, collect a sample from tank. Fill the tin completely and seal the sample immediately after collecting it to preserve the moisture content.

Record the mass and volume of the tin and sample.

Ovens dry the sample with the lid off on the "low" setting for 24 hours.

Record the mass of the tin and dry sample.

Stack your sieves in order of decreasing sieve size.

Put the sieves on the shaker and pour the dry sample into the top sieve.

Record the mass of each sieve along with the soil it contains.

Analyze the grain size distribution by completing the table and graph on the following Table A.1 and Figure B.1.

Table B.1 Record of masses

Mass of beaker and sample: _____ Mass of empty beaker: _____

Mass of dry sample: _____ Volume of sample: _____

sieve #	grain diameter (mm)	mass of sieve (or tray) (g)	mass of soil and sieve (g)	mass of soil (g)	mass of soil passing (g)	% finer
pan	_					

"Mass of soil passing" is the sum of the masses of soil collected in all the sieves below the sieve of interest.

"% finer" is the percent (by weight) of total soil mass collected in all the sieves below the sieve of interest. (So the pan at the bottom, which contains all the finest material, will have 0% finer.) 4

Create a graph of the grain size distributions by plotting ***% finer by weight*** vs. ***grain diameter***. From the graph, determine the particle diameter corresponding to 10%, 30% and 60% finer (designated as d10, d30, and d60, respectively).

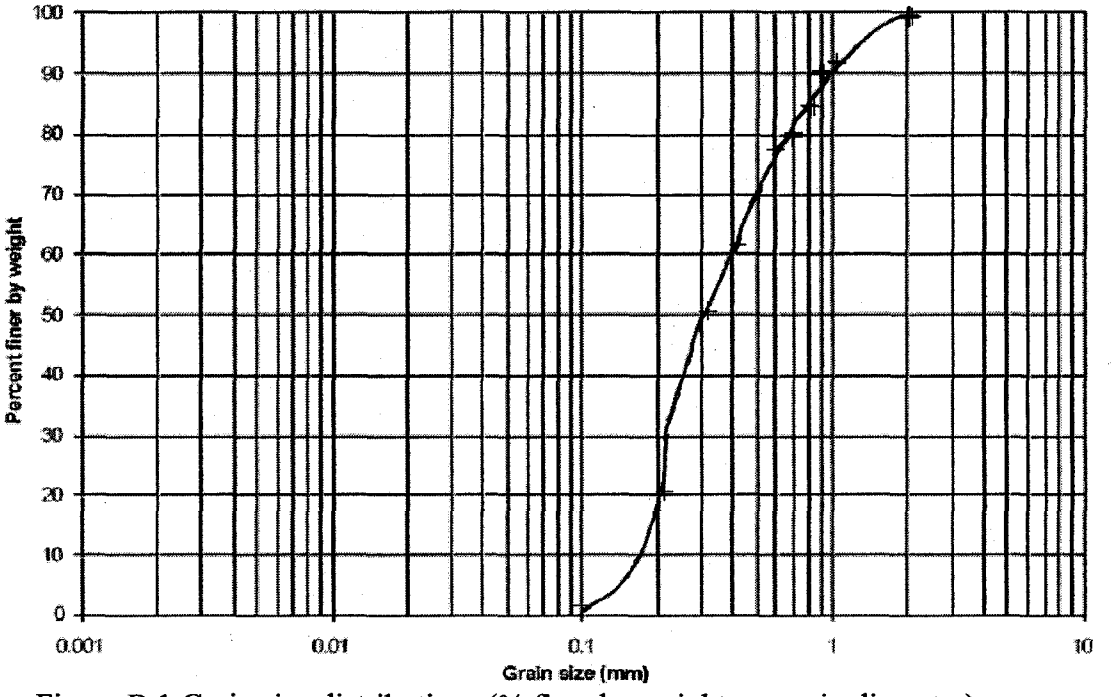

Figure B.1 Grain size distributions (% finer by weight vs. grain diameter)

The information standard methods that used in the experiment adopt the American Society for Testing and Materials (www.astm.org), affectionately known as ASTM. They publish the standard test methods for properties of soil.